

University of Montana

## ScholarWorks at University of Montana

---

Graduate Student Theses, Dissertations, &  
Professional Papers

Graduate School

---

2008

### RESPONSE OF A NEIL1 DEFICIENT MURINE EPITHELIAL CELL LINE TO CHROMATE

Laura G. Little

*The University of Montana*

Follow this and additional works at: <https://scholarworks.umt.edu/etd>

**Let us know how access to this document benefits you.**

---

#### Recommended Citation

Little, Laura G., "RESPONSE OF A NEIL1 DEFICIENT MURINE EPITHELIAL CELL LINE TO CHROMATE" (2008). *Graduate Student Theses, Dissertations, & Professional Papers*. 832.  
<https://scholarworks.umt.edu/etd/832>

This Thesis is brought to you for free and open access by the Graduate School at ScholarWorks at University of Montana. It has been accepted for inclusion in Graduate Student Theses, Dissertations, & Professional Papers by an authorized administrator of ScholarWorks at University of Montana. For more information, please contact [scholarworks@mso.umt.edu](mailto:scholarworks@mso.umt.edu).

RESPONSE OF A NEIL1 DEFICIENT MURINE EPITHELIAL CELL LINE TO  
CHROMATE

By

Laura Grace Little

B.S. Chemistry, University of Nebraska at Kearney, 2005  
B.S. Molecular Biology, University of Nebraska at Kearney, 2005

Thesis

presented in partial fulfillment of the requirements  
for the degree of

Masters of Science  
in Chemistry

The University of Montana  
Missoula, MT

Spring 2008

Approved by:

Dr. David A. Strobel, Dean  
Graduate School

Dr. Kent D. Sugden, Chair  
Chemistry

Dr. Brooke D. Martin  
Chemistry

Dr. Klára Briknarová  
Chemistry

Dr. Keith K. Parker  
Biomedical and Pharmaceutical Sciences

Response of a NEIL1 deficient murine epithelial cell line to chromate.

Chairperson: Dr. Kent D. Sugden

DNA is constantly exposed to oxidants which can lead to nucleobase damage. Chromium is of particular interest as a DNA oxidant because of its abundance in the environment and the ease with which it can be taken into a cell. Chromate, Cr(VI), ions are taken up by a cell through relatively non-selective anion channels which normally regulate uptake of phosphate and sulfate ions. Once in the cell, chromate ions are reduced by intracellular reductants such as ascorbate and glutathione to Cr(III). Highly reactive Cr(V) and Cr(IV) species are created during this transition which are able to directly oxidize DNA, particularly guanine residues due to their low reduction potential relative to the other three bases, adenine, thymine, and cytosine. 7,8-dihydro-8-oxo-2'-deoxyguanosine (8-oxoG) has previously been viewed as the primary marker of oxidative stress but the reduction potential of 8-oxoG is even lower than that of the parent guanine residue making it a prime target for further oxidative events. Spiroiminodihydantoin (Sp) is one product of these further oxidative events.

The NEIL1 base excision repair (BER) glycosylase has been shown to recognize and cleave the oxidative DNA lesion Sp. NEIL1 belongs to a family of three mammalian DNA glycosylases *Neil1*, *Neil2*, and *Neil3*. NEIL1 and NEIL2 are both able to recognize and cleave the oxidative lesion Sp in single stranded DNA in vitro. In duplex DNA, only NEIL1 is able to recognize and cleave the Sp lesion.

A *Neil1*<sup>-/-</sup> mouse model was recently developed and displayed a range of metabolic disorders that could be linked to oxidative DNA damage. These altered phenotypes included obesity, fatty liver, kidney vacuolization, hyperleptinemia, hyperinsulinemia, and increased mitochondrial DNA damage and deletions. Using kidney epithelial cells from the *Neil1*<sup>-/-</sup> mouse model, we have shown that a NEIL1 glycosylase deficiency alters toxicity, cell cycle arrest and apoptosis patterns following exposure to chromate.

## **Acknowledgements**

I would like to thank Kent and Brooke for all of their help and support.

This is dedicated to my husband Nolan.

## Table of Contents

<b>Authorization to submit thesis</b>	<b>i</b>
<b>Abstract</b>	<b>ii</b>
<b>Acknowledgements</b>	<b>iii</b>
<b>Table of Contents</b>	<b>iv</b>
<b>List of Abbreviations</b>	<b>vi</b>
<b>List of Tables</b>	<b>vii</b>
<b>List of Figures</b>	<b>viii</b>
<b>Chapter 1: Introduction</b>	<b>1</b>
1.1 Chromium – An Occupational and Environmental Health Hazard	1
1.2 Chromium – Oxidative DNA Damage	2
1.3 Base Excision Repair	8
<b>References</b>	<b>12</b>
<b>Chapter 2: Chromium Uptake and Toxicity in NEIL1 Deficient Murine Cell Lines</b>	<b>19</b>
2.1 Introduction	19
2.2 Materials and Methods	22
2.2.1 Murine Cell Growth Conditions	22
2.2.2 DNA Extraction	22
2.2.3 Genotyping NEIL1 Cell Lines	23
2.2.4 Sp Oligonucleotide Synthesis	24
2.2.5 <sup>32</sup> P Labeling and Annealing of Oligonucleotides	24
2.2.6 Nuclear Extract Preparation	25
2.2.7 Sp Cleavage Assay	25
2.3 Results	26
2.3.1 Genotype Analysis	26
2.3.2 Sp Cleavage Assay	27
2.4 Discussion	30
2.4.1 Genotype Confirmation	30
2.4.2 Sp Cleavage in a NEIL1 Deficient Cell Line	30
2.5 Conclusions	33
<b>References</b>	<b>34</b>
<b>Chapter 3: The Effects of a NEIL1 Deficiency on Chromate Sensitivity and Cell Cycle Regulation</b>	<b>37</b>
3.1 Introduction	37
3.2 Materials and Methods	42

3.2.1	Chromium Uptake Analysis	42
3.2.2	Cell Quantification and Plating	42
3.3.3	Toxicity Assay	43
3.2.4	Cell Cycle Analysis	43
3.2.5	BrdU TUNEL Assay	44
3.2.6	PARP-1 Assay	44
3.2.7	Statistical Analysis	44
3.3	Results	45
3.3.1	Chromate Toxicity	45
3.3.2	Chromium Uptake Analysis	47
3.3.3	Cell Cycle Progression Following Chromate Exposure	48
3.3.4	Quantification of Free 3'-OH Ends	51
3.3.5	PARP-1 Activity	53
3.4	Discussion	55
3.4.1	Replication Coupled Base Excision Repair	55
3.4.2	Implications of NEIL1 Deficient Epithelial Cell Data	58
3.5	Conclusions	60
	<b>References</b>	<b>62</b>
<b>Chapter 4:</b>	<b>Lesion and Mutation Accumulation in NEIL1 Cell Lines</b>	<b>68</b>
4.1	Introduction	68
4.2	Materials and Methods	71
4.2.1	MCF7 Cell Line Growth Conditions	71
4.2.2	Cell Treatment	72
4.2.3	Genomic DNA Extraction	72
4.2.4	DNA Hydrolysis	73
4.2.5	8-oxoG Quantification	73
4.2.6	<i>Hprt</i> Mutation Analysis	74
4.3	Results	75
4.3.1	8-oxoG Quantification	75
4.3.2	<i>Hprt</i> Mutation Assay	80
4.4	Discussion	84
4.4.1	Formation and Detection of Further Oxidized Lesions	84
4.4.2	Implications of the <i>Hprt</i> Mutation Assay	87
4.5	Conclusions	90
	<b>References</b>	<b>91</b>

## List of Abbreviations

6-TG:	6-thioguanine
8-oxoG:	8-oxo-7,8-dihydro-2'-deoxyguanosine
9-1-1:	Rad9-Rad1-Hus1 complex
A:	adenine
AP site:	apurinic/aprimidinic site
Apaf1:	apoptotic protease activating factor 1
APE1:	apurinic/aprimidinic endonuclease 1
Bax:	Bcl-2 associated X protein
Bcl2:	B-cell lymphoma 2 protein
BER:	base excision repair
bp:	base pair
BrdUTP:	5-bromo-2'-deoxyuridine 5'-phosphate
C:	cytosine
E2:	17 $\beta$ -estradiol
ECD:	electrochemical detection
ESI-MS:	electrospray ionization mass spectrometry
FEN1:	flap endonuclease 1
G:	guanine
Gh:	guanidinohydantoin
HPLC:	high performance liquid chromatography
HPRT:	hypoxanthine-guanine phosphoribosyl transferase
ICP-AES:	inductively coupled plasma-atomic emission spectroscopy
LP-BER:	long patch base excision repair
MMR:	mismatch repair
MYH:	MutY homolog
NEIL1:	Nei-like BER glycosylase 1
NEIL2:	Nei-like BER glycosylase 2
NEIL3:	Nei-like BER glycosylase 3
NER:	nucleotide excision repair
NTH1:	endonuclease III-like BER glycosylase 1
OGG1:	8-oxo-7,8-dihydro-2'-deoxyguanosine BER glycosylase 1
PARP-1:	poly (ADP-ribose) polymerase 1
PCNA:	proliferating cell nuclear antigen
PI:	propidium iodide
PNK:	polynucleotide kinase
SN-BER:	single nucleotide base excision repair
Sp:	spiroiminodihydantoin
T:	thymine
TdT:	terminal deoxynucleotidyl transferase
TUNEL:	transferase dUTP nick end labeling
UDG:	uracil DNA glycosylase
VDAC:	voltage-dependent anion channel
WRN:	Werner syndrome protein

## List of Tables

<b>Table 1.1:</b>	Active superfund sites in Montana involving chromium contamination.	2
<b>Table 1.2:</b>	Reduction potentials for nucleosides and DNA sequences.	4
<b>Table 1.3:</b>	BER glycosylases known to repair Cr(VI) induced nucleobase lesions.	10

## List of Figures

<b>Figure 1.1:</b>	Phosphate and chromate ions at physiological pH.	3
<b>Figure 1.2:</b>	Single electron oxidation of a guanine residue to give the 8-oxoG lesion.	5
<b>Figure 1.3:</b>	The Fenton-like reactions that have been proposed for chromium metabolism within a cell.	5
<b>Figure 1.4:</b>	Some of the further oxidized guanine lesions that have been proposed to form in oxidatively damaged DNA.	7
<b>Figure 1.5:</b>	Single electron reduction of 8-oxoG to give the Sp lesion.	8
<b>Figure 1.6:</b>	General reaction mechanism of a DNA glycosylase with $\beta$ -lyase activity.	9
<b>Figure 1.7:</b>	Sp accumulation in Nei deficient <i>E. coli</i> over their wild type counterpart.	11
<b>Figure 2.1a:</b>	The NEIL1 glycosylase cleaves Sp across from all four of the natural DNA bases.	20
<b>Figure 2.1b:</b>	The NEIL2 glycosylase is unable to cleave the Sp lesion in duplex DNA paired with any of the four natural DNA base.	20
<b>Figure 2.2:</b>	$\beta\delta$ -elimination scheme that is carried out by the NEIL1 and NEIL2 glycosylases.	21
<b>Figure 2.3a:</b>	<i>NeiI</i> gene showing primer locations in both the wild type and interrupted form of the gene.	26
<b>Figure 2.3b:</b>	Genotyping	27
<b>Figure 2.4a:</b>	HPLC trace of the oligonucleotide containing a single 8-oxoG lesion.	28
<b>Figure 2.4b:</b>	HPLC trace of the oligonucleotide containing a single 8-oxoG lesion after oxidation by Cr(V) – Salen.	29
<b>Figure 2.5:</b>	Sp and 8-oxoG cleavage assay products.	29
<b>Figure 2.6:</b>	The spiroiminodihydantoin lesion.	33
<b>Figure 3.1:</b>	The eukaryotic cell cycle.	38

<b>Figure 3.2:</b>	The cell cycle checkpoints for monitoring the integrity of DNA and other cell components.	39
<b>Figure 3.3:</b>	The intrinsic apoptotic pathway.	41
<b>Figure 3.4:</b>	Toxicity curve for chromate exposure of the NEIL1 cell lines.	46
<b>Figure 3.5:</b>	Extended toxicity curve for chromate exposure of the NEIL1 cell lines.	47
<b>Figure 3.6:</b>	Chromium uptake reported on a pg of chromium/cell basis.	48
<b>Figure 3.7a:</b>	Percentages of NEIL1 cells in the G0/G1 phase of the cell cycle following chromate exposure.	50
<b>Figure 3.7b:</b>	Percentages of NEIL1 cells in the S phase of the cell cycle following chromate exposure.	50
<b>Figure 3.7c:</b>	Percentages of NEIL1 cells in the G2/M phase of the cell cycle following chromate exposure.	51
<b>Figure 3.8:</b>	Graphical representation of the number of free 3'-hydroxyl ends in genomic DNA of NEIL1 cell lines following exposure to chromate.	53
<b>Figure 3.9:</b>	PARP-1 activity measured as poly (ADP-ribose) deposition on immobilized histones.	55
<b>Figure 4.1a:</b>	Watson-Crick base pairing between guanine and cytosine and between 8-oxoG and cytosine.	69
<b>Figure 4.1b:</b>	An 8-oxoG lesion can be paired with a cytosine or an adenine residue during DNA replication.	69
<b>Figure 4.2:</b>	8-oxoG, Sp, and Gh/Ia lesion structures.	70
<b>Figure 4.3:</b>	HPLC traces from a guanine standard and a digested DNA sample.	76
<b>Figure 4.4:</b>	Ultraviolet absorbance spectrum of guanine.	76
<b>Figure 4.5:</b>	ECD trace of an 8-oxoG standard.	77
<b>Figure 4.6:</b>	8-oxoG lesions relative to the total number of guanine residues present in hydrolyzed DNA samples from NEIL1 epithelial cell lines exposed to chromate for 4 hours.	78

<b>Figure 4.7:</b>	8-oxoG lesions relative to the total number of guanine residues present in hydrolyzed DNA samples from MCF7 cells exposed to chromate for 4 hours and/or E2 for 48 hours.	79
<b>Figure 4.8:</b>	Plating efficiency represented as raw colony numbers and percentage of control colonies.	81
<b>Figure 4.9a:</b>	Difference in colony formation patterns between the NEIL1 <sup>+/+</sup> and NEIL1 <sup>-/-</sup> cell lines following exposure to chromate and growth in media supplemented with 6-TG.	82
<b>Figure 4.9b:</b>	Difference in cell growth patterns in media supplemented with 6-TG for NEIL1 <sup>-/-</sup> cells dosed with low chromate concentrations and those dosed with high chromate concentrations.	83
<b>Figure 4.10:</b>	Colony growth trends in NEIL1 <sup>-/-</sup> cells dosed with low chromate concentrations and maintained in media supplemented with 6-TG.	84
<b>Figure 4.11a:</b>	Sp isomers from a single stranded oligonucleotide oxidized with Cr(V)-Salen.	86
<b>Figure 4.11b:</b>	The Sp isomer peaks from (a) both represent ions with a mass to charge ratio of 184.	86
<b>Figure 4.12:</b>	Mass profile of the Sp nucleoside and the free base.	87

## CHAPTER 1

### Introduction

#### 1.1 Chromium – An Occupational and Environmental Health Hazard

Hexavalent chromium – Cr(VI) - is a well established human carcinogen. The first evidence showing that hexavalent chromium may be a carcinogen was a high incidence of nasal tumors reported in the late 19<sup>th</sup> century in chrome pigment workers in Scotland.<sup>1</sup> Cr(VI) has also been shown to cause lung cancer. In the 20<sup>th</sup> century chromate workers in Germany, the United Kingdom, and the United States showed an increased risk for the development of lung cancer.<sup>2-5</sup> Industries in which workers are still exposed to Cr(VI) today include chrome plating, stainless steel welding, leather tanning, and chrome pigment and dye production.<sup>6</sup> Occupational hazards of hexavalent chromium are made clear by the enhanced incidence of cancer due to workplace exposure but environmental exposure from years of industrial dumping of chrome waste is also a major factor to be considered in the overall risk to human health posed by Cr(VI).

Chromium exists at an average level of 100 mg/kg in the earth's crust. The majority of that chromium exists in the trivalent – Cr(III) – form.<sup>7</sup> What little Cr(VI) that is present exists mainly as chromate ( $\text{CrO}_4^{2-}$ ) and is much more mobile than Cr(III) compounds due to its significantly higher solubility.<sup>7</sup> Industrial use of chromate chemicals that contributes to environmental contamination includes its use in cooling towers to prevent rust accumulation, waste from the manufacture and use of chromate compounds, and the mist of chromic acid produced in the chrome-plating industry.<sup>8</sup> This chromate waste can travel over significant distances if introduced into a water source. Some of the chromate may be reduced to Cr(III), most of which will precipitate as  $\text{Cr}(\text{OH})_3 \cdot 3\text{H}_2\text{O}$  but the portion that remains in the hexavalent form will be carried downstream.<sup>7,9</sup> People that work with chromate compounds and those that encounter chromate compounds in the environment run a higher risk of developing cancer than the general population. The mode of action for the carcinogenicity observed with chromate needs to be more clearly understood in order to reduce the risks associated with human interaction with chromate compounds.

Chromium, especially hexavalent chromium, is of great interest not only because of its toxic effects on humans but also because of the high risk of exposure to hexavalent chromium that still exists for the general public. In 1992 the drinking water standard for total chromium was lowered to 0.1 ppm due to the emergence of new information about amounts of chromium being released into the environment.<sup>10</sup> Between the years 1987 and 1993, there were 2,876,055 pounds of chromium released into bodies of water in the United States and 196,880,624 pounds released on land. There are currently four locations in Montana alone that are active superfund sites containing chromium (Table 1.1).<sup>10</sup> The contamination stems from the mining, smelting, and wood treatment industries. There are 719 superfund sites nationwide with chromium listed as at least one of the contaminants present.<sup>11</sup> Not only is the Environmental Protection Agency still concerned about chromium exposure, so too is the Occupational Safety and Health Administration (OSHA). In February of 2006, OSHA settled on a new standard for occupational exposure to hexavalent chromium. The standard was lowered from 52 to 5  $\mu\text{g}/\text{m}^3$  of air as an 8 hour time-weighted average for hexavalent chromium.<sup>12</sup>

**Table 1.1** – Active superfund sites in Montana containing chromium.<sup>10</sup>

<b>City</b>	<b>Site Name</b>	<b>Date of Listing</b>
Anaconda	Anaconda Co. Smelter	Sept. 8, 1983
Butte	Montana Pole and Treating	July 22, 1987
Butte	Silver Bow Creek/Butte Area	Sept. 8, 1983
Libby	Libby Ground Water Contamination	Sept. 8, 1983

## **1.2 Chromium – Oxidative DNA Damage**

There are a several theories that have been proposed to explain the genotoxicity of chromium. These include the formation of DNA adducts, single strand breaks, DNA-

protein crosslinks, and oxidized nucleobases.<sup>13</sup> All of these theories concerning the genotoxicity of chromium recognize Cr(VI) and not Cr(III) as the genotoxic chromium species. This is because Cr(VI) ions, unlike Cr(III) ions, are taken up by the cell through relatively non-selective anion channels<sup>14</sup> which normally regulate the uptake of phosphate and sulfate ions required for the synthesis of proteins and DNA. Cr(III) ions are able to cross the cell membrane but rely solely on diffusion and are therefore taken up approximately three orders of magnitude more slowly than Cr(VI) ions.<sup>15</sup> Chromate, phosphate and sulfate ions are all of a similar size and share the same charge and tetrahedral geometry (Figure 1.1).<sup>1</sup> Once in the cell, Cr(VI) is quickly reduced by a variety of intracellular reductants including ascorbic acid and reduced thiols such as cysteine and glutathione. Ascorbic acid is the most kinetically favored of these reductants and is therefore generally regarded as the major intracellular reductant of Cr(VI).<sup>16</sup> The rapid reduction of Cr(VI) to Cr(V), Cr(IV), and finally to Cr(III) creates a concentration gradient across the cell membrane that favors the continual uptake of Cr(VI) from the extracellular matrix.



**Figure 1.1** – Phosphate and chromate ions at physiological pH.

Cr(VI) can gain access to the cell but it is not Cr(VI) that causes damage to nucleic acids. The reduced forms of Cr(VI) – Cr(V), Cr(IV), and Cr(III) are the species which interact with DNA.<sup>17</sup> Cr(V) species have been shown to directly oxidize the nucleobases.<sup>18</sup> The highly reactive Cr(V) species can abstract an electron from the conjugated ring system of DNA.<sup>19</sup> Guanine residues are preferentially attacked because of their low one-electron reduction potential relative to that of the other three bases (Table

1.2).<sup>20-22</sup> That reduction potential becomes even lower for the 5' guanine residue when a run of guanine residues is present in a DNA sequence (Table 1.2). The most widely recognized lesion formed by a one electron abstraction from a guanine residue is 7,8-dihydro-8-oxo-2'-deoxyguanosine (8-oxoG) (Figure 1.2).<sup>20</sup> When an electron is abstracted from the C8 position of a guanine, a radical cation is formed. Water then acts as a nucleophile and attacks the charged C8 position. The C8 hydrogen leaves along with a second electron giving an 8-oxoG residue.<sup>19</sup>

An alternate explanation for Cr(VI) induced oxidative DNA damage that has also been extensively investigated involves the formation of reactive oxygen species (ROS). Through Fenton-like reactions (Figure 1.3) with H<sub>2</sub>O<sub>2</sub>, both Cr(III)<sup>20</sup> and Cr(VI)<sup>21,22</sup> have been shown to be capable of producing hydroxyl radicals which can then attack the electron rich aromatic rings of the nucleobases. This pathway is favorable in the presence of high concentrations of H<sub>2</sub>O<sub>2</sub> ([0.5 mM – 27 mM])<sup>20-22</sup> which have been used for *in vitro* studies. Under normal physiological conditions, the concentration of H<sub>2</sub>O<sub>2</sub> in a cell is much lower than 1 mM (in the  $\mu$ M range)<sup>23</sup> indicating that oxidation of nucleic acids by ROS is likely to play a very small role in the overall oxidative damage that has been observed in cells exposed to Cr(VI).

**Table 1.2** – Reduction potentials for nucleosides and DNA sequences.<sup>24,26,27</sup> The 5' guanine in a run of guanine residues has a lower reduction potential than a single guanine and the 8-oxoG has a lower reduction potential than the parent guanine residue.

<i>Nucleoside</i>	<i>E° (V vs NHE)</i>	<i>DNA Sequence</i>	<i>E° (V vs NHE)</i>
Guanine (G)	1.29	<u>G</u> GG	0.64
Adenine (A)	1.42	<u>G</u> G	0.82
Cytosine (C)	1.6	<u>G</u> A	1.00
Thymine (T)	1.7	<u>G</u> C	1.15
8-oxoG	0.74	<u>G</u> T	1.16

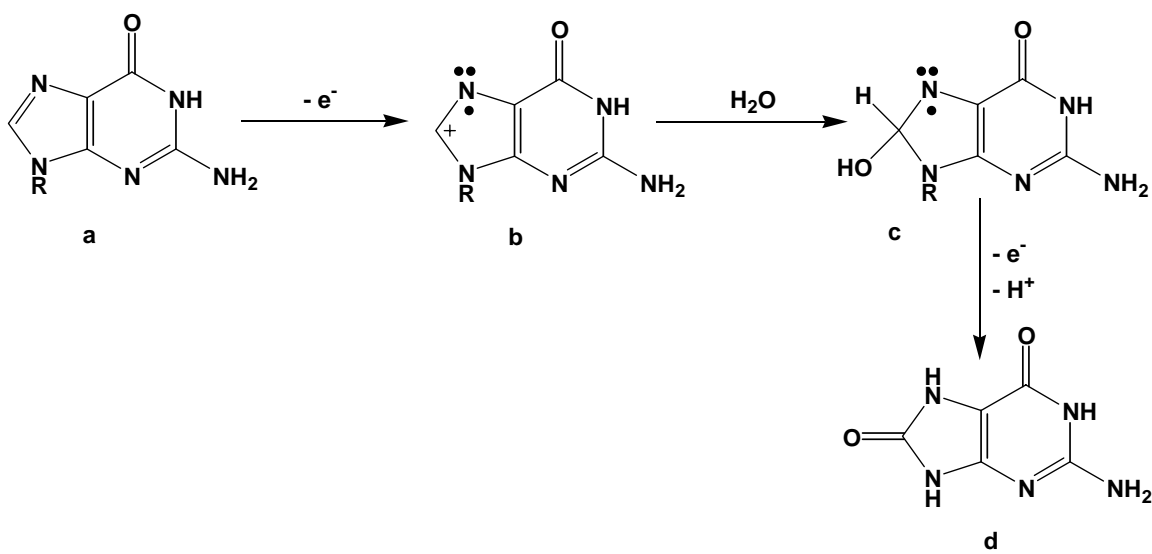


**Figure 1.2** – Single electron oxidation of a guanine residue to give the 8-oxoG lesion.<sup>19</sup>

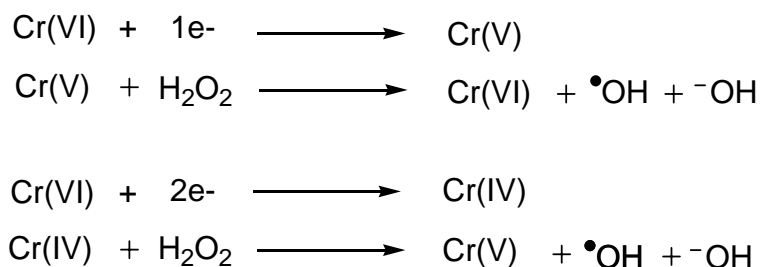


**Figure 1.3** – The Fenton-like reactions that have been proposed for chromium metabolism within a cell. Hydroxyl radicals formed in these reactions could directly abstract an electron from DNA.

8-oxoG has previously been viewed as the primary marker of oxidative stress.<sup>28</sup> The 8-oxoG lesion, if allowed to persist in the genome, is mutagenic as it can cause a mispairing with adenine during DNA replication causing G:C→T:A transversion mutations.<sup>29</sup> However, the one-electron reduction potential of 8-oxoG is even lower than that of the parent guanine residue making it a prime target for further oxidative events (Table 1.2). It would be highly unlikely for an electron to be directly abstracted from the

same DNA base twice but further oxidized products of 8-oxoG have been observed both *in vitro* and in cellular systems.<sup>30,31</sup> Charge transfer is one mechanism that has been proposed to explain how two oxidative events can occur at the same base in a DNA sequence. This mechanism proposes that an electron hole will be translated through the DNA to a sink – a nucleoside with a lower reduction potential than that of the neighboring nucleosides.<sup>26</sup> The stacked bases create an array of overlapping  $\pi$ -orbitals that facilitate charge transfer through a DNA sequence.<sup>32</sup> 8-oxoG lesions can act as a sink for charge transfer because of their lower reduction potential relative to that of the four undamaged nucleosides. When an 8-oxoG lesion is present within approximately 10-20 base pairs (greatly dependent on the DNA sequence)<sup>32</sup> of the site of an electron abstraction from a nucleobase, the resultant charge can be transferred to an 8-oxoG residue resulting in a secondary oxidative event at the same base.

The low reduction potential of 8-oxoG along with its ability to act as a sink for charge transfer in a DNA sequence indicates that 8-oxoG is not likely to be the end product of an oxidative attack on the nucleobases. One of the secondary lesions that has been shown to form both *in vitro* and in cellular systems is spiroiminodihydroantoin (Sp).<sup>30,31</sup> Sp, like 8-oxoG, can produce G:C→T:A transversion mutations but at a higher level. In addition to the G:C→T:A transversion mutations, Sp can also produce G:C→C:G transversion mutations and polymerase arrest both *in vitro* and in cellular systems.<sup>33-35</sup> The formation of Sp helps to explain the high level of mutations observed in Cr(VI) treated systems that cannot be accounted for by the formation of 8-oxoG lesions alone.

There are a host of further oxidized lesions that have been proposed to form following oxidation of DNA. Some of the more common examples are shown in figure 1.4. Sp is a further oxidized lesion of particular interest because it has been observed to form in cellular systems,<sup>31</sup> it has an increased mutagenic potential over that of 8-oxoG, and it has been shown to accumulate in much larger quantities than 8-oxoG in an *Escherichia coli* repair deficient model exposed to Cr(VI).<sup>31</sup> Accumulation of Sp in a cellular system is possible because while water may not be the strongest nucleophile present in a cell it is the most abundant and can thus attack the radical cation formed when an electron is abstracted from an 8-oxoG residue (Figure 1.5).<sup>30</sup> Further more, Sp

forms ideally at 37°C and at pH 7.4<sup>30</sup> which are both biologically relevant parameters. Because it is more favorable for further oxidized lesions such as Sp to be the end product of an oxidative event at a nucleobase, these lesions may serve as more relevant biomarkers for oxidative stress in a cellular system.

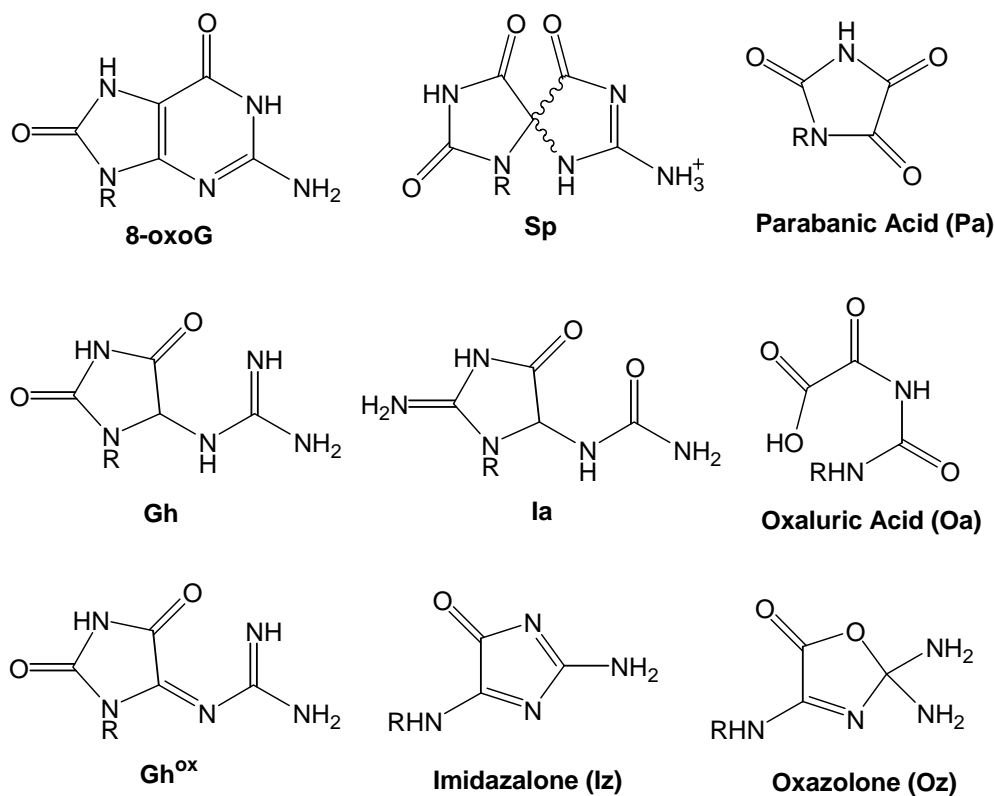


**Figure 1.4** – A sample of some of the further oxidized guanine lesions that have been proposed to form in oxidatively damaged DNA.

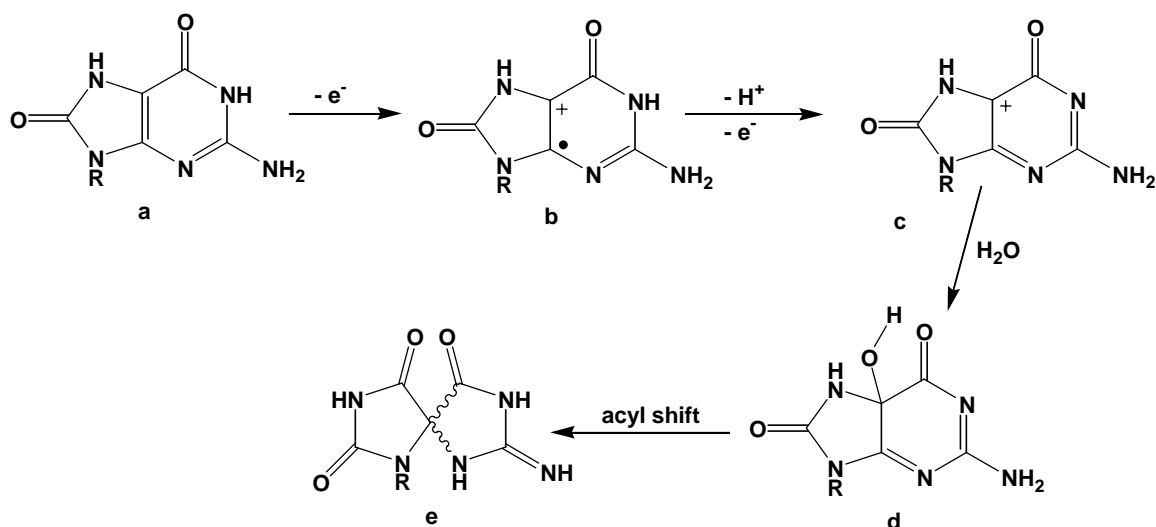


**Figure 1.5** – Single electron reduction of 8-oxoG to give the Sp lesion.<sup>30</sup>

### 1.3 Base Excision Repair

Cells have three types of repair systems in place to deal with damaged or mismatched DNA bases which are conserved from prokaryotes to mammals.<sup>36</sup> They include base excision repair, nucleotide excision repair, and mismatch repair.<sup>37</sup> Base excision repair (BER) is the direct removal of a single nucleobase that is damaged or mismatched.<sup>37</sup> Nucleotide excision repair (NER) is the direct removal of a short sequence of DNA (~25-30 bases) containing a damaged or mismatched base(s).<sup>37</sup> Mismatch repair (MMR) is the direct removal of a large sequence of DNA (up to a few kilodaltons in size) that contains a mismatched base(s) following DNA replication.<sup>37</sup> Cells primarily use the BER pathway to remove oxidative DNA base lesions.<sup>38</sup> The BER pathway involves a DNA glycosylase that recognizes an individual damaged base. The damaged base is then flipped out of the DNA strand and cleaved at the glycosidic bond forming an apurinic/aprimidinic (AP) site.<sup>38</sup> The DNA glycosylase binds to the 1' carbon of the deoxyribose subunit allowing the damaged nucleobase to leave and a Schiff base to be formed between the abasic site and the BER enzyme.<sup>38</sup> Many DNA glycosylases do not further process the AP site but some glycosylases involved in repair of oxidized DNA

base lesions possess lyase activity allowing them to further degrade the AP site.<sup>39</sup> Further degradation leads to release of the DNA glycosylase and the formation of a 5'-phosphomonoester and a 3'-unsaturated deoxyribose phosphate residue, also referred to as the  $\beta$ -elimination product (Figure 1.6 c).<sup>39</sup>

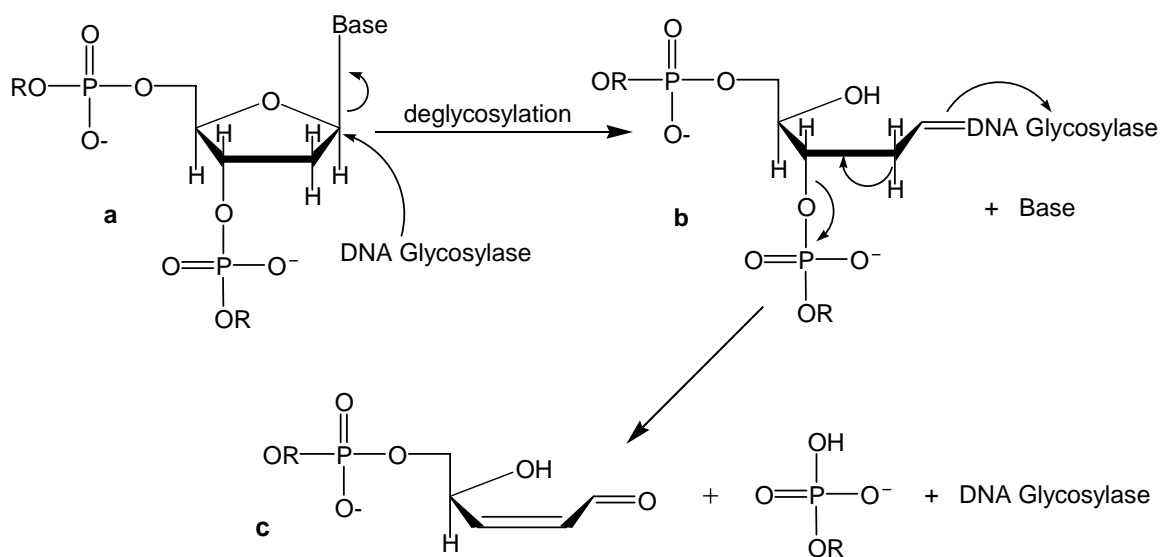


**Figure 1.6** – General reaction mechanism of a DNA glycosylase with  $\beta$ -lyase activity. Structure c is the  $\beta$ -elimination product.

Cells have a variety of genes that encode for DNA glycosylases that repair specific oxidative damage to the nucleobases. 8-oxoG is a major product of a single electron oxidative event at a guanine residue<sup>24</sup> and is formed frequently in cellular DNA.<sup>25</sup> Therefore, cellular systems are well-equipped to deal with 8-oxoG formation. Table 1.3 outlines the various bacterial BER enzymes responsible for the removal of 8-oxoG lesions and their mammalian homologues. The bacterial glycosylases include MutM which excises 8-oxoG lesions formed within a DNA sequence<sup>40,41</sup> and MutY which excises an adenine paired with an 8-oxoG residue<sup>42</sup> which will occur following a round of replication. MutT degrades 8-oxoGTP to the monophosphate before it can be incorporated into the genome.<sup>43</sup> OGG1 is the mammalian glycosylase which is

homologous to the bacterial glycosylase MutM.<sup>44</sup> 8-oxoG was considered to be the major DNA base lesion caused by oxidative stress until just recently and OGG1 was considered to be the major repair enzyme for oxidative DNA damage in mammalian systems. Studies conducted with OGG1 deficient mice have shown that 8-oxoG lesions accumulate in genomic DNA at a rate of nearly 10-100 fold as compared to OGG1 proficient mice.<sup>45,46</sup> Despite the fact that such high levels of 8-oxoG were observed to accumulate in OGG1 deficient mice, the spontaneous mutation rate in those mice was relatively low and no tumor formation was detected.<sup>45</sup> However, there are many oxidants that are known to induce tumor formation so based on studies conducted with OGG1 deficient mice, it can be reasoned that 8-oxoG is not likely the major oxidative base lesion leading to cancer initiation in cells exposed to oxidants. Further oxidative nucleobase lesions produce higher mutation rates than 8-oxoG<sup>33-35</sup> and therefore have the potential to play a more significant role in cancer initiation than 8-oxoG.

**Table 1.3** – BER glycosylases known to repair Cr(VI) induced nucleobase lesions.<sup>47</sup> Some of these glycosylases are known to repair additional lesions not listed here but those additional lesions are not associated with Cr(VI) induced genetic damage.

<b>BER Glycosylase</b>	<b>Nucleobase Lesion Substrates</b>	<b>Mammalian Homolog</b>
MutM (Fpg)	8oxoG:C, Sp:C, Gh:C, 8oxoG:G, Sp:G, Gh:G	OGG1
MutY	8oxoG:A, G:A	MYH
MutT	8oxo dGTP, 8oxo dATP	NTH1
Nei	Sp:A, Gh:A, 8oxoG:C, Sp:C, Gh:C, 8oxoG:G, Sp:G, Gh:G	NEIL1, NEIL2, NEIL3

With the discovery of further oxidized DNA lesions such as Sp came the discovery of DNA glycosylases that recognize and cleave those further oxidized DNA lesions. Endonuclease VIII (Nei) is a bacterial glycosylase that has been shown to repair

further oxidized DNA lesions including Sp.<sup>48,49</sup> *Nei* deficient *E. coli* have been shown to accumulate Sp lesions but not 8-oxoG lesions following chromate exposure (Figure 1.7).<sup>31</sup> This indicated that the *Nei* repair enzyme is directed specifically at further oxidized lesions. Recently, three mammalian homologues of the *Nei* gene were identified and labeled *Neil1*, *Neil2*, and *Neil3* (*Nei*-Like).<sup>50,51</sup> NEIL1 and NEIL2 have been shown to recognize the further oxidized DNA lesion Sp and NEIL1 was shown to cleave Sp in both single and double stranded oligonucleotides.<sup>49</sup> We expected that NEIL1 deficient mammalian cells would accumulate Sp lesions and be less resistant to Cr(VI) as was observed in the *Nei* deficient *E. coli* studies. However, as this thesis will demonstrate, NEIL1 plays a much more complex role in mammalian cells that just BER creating a different outcome than initially hypothesized.

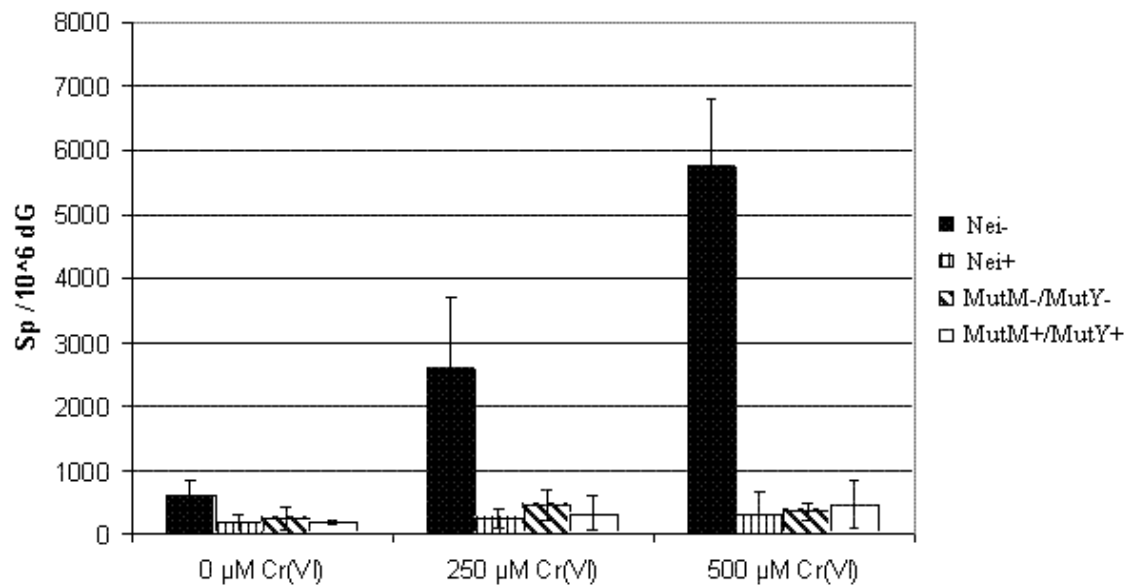


**Figure 1.7** – Sp accumulation in *Nei* deficient *E. coli* over their wild type counterpart but not in *MutM/MutY* deficient *E. coli* over their wild type counterpart. Taken from [31].

## References

1. Newman, D. (1890) A Case of Adeno-carcinoma of the Left Inferior Turbinated Body, and Perforation of the Nasal Septum, in the Person of a Worker in Chrome Pigments. *Glasgow Medical Journal* 33, 469-70.
2. Baetjer, A.M. (1950) Pulmonary carcinoma in chromate workers II. Incidence on basis of hospital records. *Arch. Indust. Hyg. Occup. Med.* 2, 505-516.
3. Bidstrup, P.L. (1951) Carcinoma of the lung in chromate workers. *Br. J. Ind. Med.* 8, 302-305.
4. Bidstrup, P.L., Case, R.A.M. (1956) Carcinoma in the lung of workmen in the bichromate-producing industry in Great Britain. *Br. J. Ind. Med.* 13, 260-264.
5. Pfeil, R. (1935) Lungentumoren als Berufskrankung in Chromatbetrieben. *Dtsch. Med. Wochensh* 61, 1197-1202.
6. Stern, R.M. (1982) Chromium compounds: production and occupational exposure. In: Langard, S. ed. *Biological and Environmental Aspects of Chromium*. Elsevier Biomedical Press, 5-47.
7. Katz, S.A., Salem, H. (1994) *The biological and environmental chemistry of chromium*. VCH Publishers: New York, 5.
8. *Toxicological Review of Hexavalent Chromium*, U.S. Environmental Protection Agency, Washington, DC, 1998.
9. Spiccia, L., Marty, W. (1986) Fate of active chromium hydroxide  $\text{Cr}(\text{OH})_3 \cdot 3\text{H}_2\text{O}$ , in aqueous suspension. A study of chemical changes involving aging. *Inorg. Chem.* 25, 266-271.

10. National Priorities List Basic Site Query Results. 9 Nov. 2006. U.S. Environmental Protection Agency. 9 Nov. 2006. <[oaspub.epa.gov/oerrpage/basicqry](http://oaspub.epa.gov/oerrpage/basicqry)>.
11. Consumer Factsheet on: Chromium. 21 Feb. 2006. EPA Ground Water and Drinking Water. 9 Nov. 2006. <[www.epa.gov/safewater/contaminants/dw\\_contamfs/chromium.html](http://www.epa.gov/safewater/contaminants/dw_contamfs/chromium.html)>.
12. Corporate-Wide Settlement Agreements. 25 Oct. 2006. Occupational Safety and Health Administration. 9 Nov. 2006. <[www.osha.gov/pls/oshaweb/owadisp.show\\_document?p\\_table=CWSA&p\\_id=883](http://www.osha.gov/pls/oshaweb/owadisp.show_document?p_table=CWSA&p_id=883)>.
13. O'Brien, T.J., Ceryak, S., Patierno, S.R. (2003) Complexities of chromium carcinogenesis: role of cellular response, repair and recovery mechanisms. *Mut. Res.* 533, 3-36.
14. Arslan, P., Beltrame, M., Tomasi, A. (1987) Intracellular chromium reduction. *Biochim. Biophys. Acta.* 931, 10-15.
15. Kortenkamp, A., Beyersmann, D., O'Brien, P. (1987) Uptake of chromium (III) complexes by erythrocytes. *Toxicol. Environ. Chem.* 14, 23-32.
16. Standeven AM, Wetterhahn KE. (1991) Ascorbate is the principle reductant of chromium(VI) in rat liver and kidney ultrafiltrates. *Carcinogenesis* 12, 1733-1737.
17. Taspakos, M.J., Wetterhahn, K.E. (1983) The interaction of chromium with nucleic acids. *Chem. Biol. Interact.* 46, 265-277.
18. Bose, R.N., Fonkeng, B.S., Moghaddas, S., Stroup, D. (1998) Mechanisms of DNA damage by chromium(V)-DNA carcinogens. *Nucleic Acids Res.* 26, 1588-1596.

19. Burrows, C.J., Muller, J.G. (1998) Oxidative nucleobase modifications leading to strand scission. *Chem. Rev.* 98, 1109-1151.
20. Tsou, T.C., Yang, J.L. (1996) Formation of reactive oxygen species and DNA strand breakage during interaction of chromium(III) and hydrogen peroxide in vitro: evidence for a chromium(III)-mediated Fenton-like reaction. *Chem. Biol. Interact.* 102, 133-153.
21. Aiyar, J., Berkovits, H.J., Floyd, R.A., Wetterhahn, K.E. (1990) Reaction of chromium(VI) with hydrogen peroxide in the presence of glutathione: reactive intermediates and resulting DNA damage. *Chem. Res. Toxicol.* 3, 595-603.
22. Aiyar, J., Berkovits, H.J., Floyd, R.A., Wetterhahn, K.E. (1991) Reaction of chromium(VI) with glutathione or with hydrogen peroxide: identification of reactive intermediates and their role in chromium(VI)-induced DNA damage. *Environ. Health Perspect.* 92, 53-62.
23. Mueller, S., Riedel, H.D., Stremmel, W. (1997) Determination of catalase activity at physiological hydrogen peroxide concentrations. *Anal. Biochem.* 245, 55-60.
24. Steenken, S., Jovanovic, S. (1997) How easily oxidizable is DNA? One-electron reduction potentials of adenosine and guanosine radicals in aqueous solution. *J. Am. Chem. Soc.* 119, 617-618.
25. ESCODD (2002) Comparative analysis of baseline 8-oxo-7,8-dihydroguanine in mammalian cell DNA, by different methods in different laboratories: an approach to consensus. *Carcinogenesis* 23, 2129-2133.
26. Steenken, S., Jovanovic, S.V., Bietti, M., Bernhard, K. (2000) The trap depth (in DNA) of 8-oxo-7,8-dihydro-2'-deoxyguanosine as derived from electron-transfer equilibria in aqueous solution. *J. Am. Chem. Soc.* 122, 2373-2374.

27. Saito, I., Takayama, M., Sugiyama, H., Nakatani, K. (1995) Photoinduced DNA cleavage via electron transfer: demonstration that guanine residues located 5' to guanine are the most electron-donating sites. *J. Am. Chem. Soc.* 117, 6406-6407.
28. Helbock, H.J., Beckman, K.B., Ames, B.N. (1999) 8-hydroxydeoxyguanosine and 8-hydroxyguanine as biomarkers of oxidative DNA damage. *Methods Enzymol.* 300, 155-156.
29. Shibutani, S., Takeshita, A., Grollman, A.P. (1991) Insertion of specific bases during DNA synthesis past the oxidation-damaged base 8-oxodG. *Nature* 349, 431-434.
30. Luo, W., Muller, J.G., Rachlin, E.M., Burrows, C.J. (2000) Characterization of spiroiminodihydantoin as a product of one electron oxidation of 8-oxo-7,8-dihydroguanosine. *Org. Lett.* 2, 613-616.
31. Hailer, M.K., Slade, P.G., Martin, B.D., Sugden, K.D. (2005) Nei deficient *Escherichia coli* are sensitive to chromate and accumulate the oxidized guanine lesion spiroiminodihydantoin. *Chem. Res. Toxicol.* 18, 1378-1383.
32. Delaney, S., Barton, J.K. (2003) Long range DNA charge transport. *J. Org. Chem.* 68, 6475-6483.
33. Duarte, V., Muller, J.G., Burrows, C.J. (1999) Insertion of dGMP and dAMP during in vitro DNA synthesis opposite an oxidized form of 7,8-dihydro-8-oxoguanine. *Nucleic Acids Res.* 27, 496-502.
34. Henderson, P.T., Delaney, J.C., Muller, J.G., Neeley, W.L., Tannenbaum, S.R., Burrows, C.J., Essigmann, J.M. (2003) The hydantoin lesions formed from oxidation of 7,8-dihydro-8-oxoguanine are potent sources of replication errors in vivo. *Biochemistry* 42, 9257-9262.

35. Korniyushyna, O., Berges, A.M., Muller, J.G., Burrows, C.J. (2002) In vitro nucleotide misinsertion opposite the oxidized guanosine lesions spiroiminodihydantoin and guanidinohydantoin and DNA synthesis past the lesions using *Escherichia coli* DNA polymerase I (Klenow fragment). *Biochemistry* 41, 15304-15314.
36. David, S.S., Williams, S.D. (1998) Chemistry of glycosylases and endonucleases involved in base-excision repair. *Chem. Rev.* 98, 1221-1261.
37. Lewin, B. (2004) Genes VIII. Pearson Education, Inc. Upper Saddle River, NJ. pp. 447-452.
38. Sancar, A., Lindsey-Boltz, L.A., Ünsal-Kaçmaz, K., Linn, S. (2004) Molecular mechanisms of mammalian DNA repair and the DNA damage checkpoints. *Annu. Rev. Biochem.* 73, 39-85.
39. McCullough, A.K., Dodson, M.L., Llyod, R.S. (1999) Initiation of base excision repair: glycosylase mechanisms and structures. *Annu. Rev. Biochem.* 68, 255-85.
40. Chung, M.H., Kasai, H., Jones, D.S., Inoue, H., Ishikawa, H., Ohtsuka, E., Nishimura, S. (1991) An endonuclease activity of *Escherichia coli* that specifically removes 8-hydroxy-guanine residues from DNA. *Mut. Res.* 254, 1-12.
41. Tchou, J., Kasai, H., Shibutani, S., Chung, M.H., Laval, J., Grollman, A.P., Nishimura, S. (1991) 8-oxoguanine (8-hydroxyguanine) DNA glycosylase and its substrate specificity. *Proc. Natl. Acad. Sci. USA* 88, 4690-4694.
42. Michaels, M.L., Cruz, C., Grollman, A.P., Miller, J.H. (1992) Evidence that MutY and MutM combine to prevent mutations by an oxidatively damaged form of guanine in DNA. *Proc. Natl. Acad. Sci. USA* 89, 7022-7025.

43. Tajiri, T., Maki, H., Sekiguchi, M. (1995) Functional cooperation of MutT, MutM, and MutY proteins in preventing mutations by spontaneous oxidation of guanine nucleotide in *Escherichia coli*. *Mut. Res.* 336, 257-267.
44. Aburantani, H., Hippou, Y., Ishida, T., Takashima, R., Matsuba, C., Kodama, M.T., Yasui, A., Yamamoto, K., Asano, M., Fukasawa, K., Yoshinari, T., Inoue, H., Ohtsuka, E., Nishimura, S. (1997) Cloning and characterization of mammalian 8-hydroxyguanine-specific DNA glycosylase/apurinic, apyrimidinic lyase, a functional mutM homologue. *Cancer Res.* 57, 2151-2156.
45. Minowa, O., Arai, T., Hirano, M., Monden, Y., Nakai, S., Fukuda, M., Itoh, M., Takano, H., Hippou, Y., Abutantani, H., Masumura, K., Nohmi, T., Nishimura, S., Noda, T. (2000) Mmg/Ogg1 gene inactivation results in accumulation of 8-hydroxyguanine in mice. *Proc. Natl. Acad. Sci. USA* 97, 4156-4161.
46. Arai, T., Kelly, V.P., Minowa, O., Noda, T., Nishimura, S. (2002) High accumulation of oxidative DNA damage, 8-hydroxyguanine, in *Mmh/Ogg1* deficient mice by chronic oxidative stress. *Carcinogenesis* 23, 2005-2010.
47. Hazra, T.K., Muller, J.G., Manuel, R.C., Burrows, C.J., Llyod, R.S., Mitra, S. (2001) Repair of hydantoins, one electron oxidation product of 8-oxoguanine, by DNA glycosylases of *Escherichia coli*. *Nucleic Acids Research* 29, 1967-1974.
48. Jiang, D., Hatahet, Z., Melamede, R.J., Kow, Y.W., Wallace, S.S. (1997) Characterization of *Escherichia coli* endonuclease VIII. *J. Biol. Chem.* 272, 32230-32239.
49. Hailer, M.K., Slade, P.G., Martin, B.D., Rosenquist, T.A., Sugden, K.D. (2005) Recognition of the oxidized lesions spiroiminodihydantoin and guanidinohydantoin in DNA by the mammalian base excision repair glycosylases NEIL1 and NEIL2. *DNA Repair* 4, 41-50.

50. Takao, M., Kanno, S., Kobayashi, K., Zhang, Q., Yonei, S., van der Horst, G., Yasui, A. A back-up glycosylase in Nth1 knock-out mice is a functional Nei (endonuclease VIII) homologue. *J. Biol. Chem.* 277, 42205-42213.
  
51. Hazra, T.K., Kow, Y.W., Hatahet, Z., Imhoff, B., Boldogh, I., Mokkalpati, S.K., Mitra, S., Izumi, T. (2002) Identification and characterization of a novel human DNA glycosylase for repair of cytosine derived lesions. *J. Biol. Chem.* 277, 30417-30420.

## CHAPTER 2

### Characterization of a NEIL1 Deficient Cell Line

#### 2.1 Introduction

The NEIL1 BER glycosylase was first described in the literature in 2002.<sup>1-4</sup> The *Neil1* gene maps to the 15q22 chromosome location in humans.<sup>5</sup> Deletions in the 15q chromosome arm are observed in more than 70% of human small cell lung carcinomas.<sup>5</sup> Substrates for NEIL1 include DNA base lesions such as formamido-pyrimidines (FapyG and FapyA), thymine glycol, and 5-hydroxyuracil.<sup>1-3,6</sup> These lesions are associated with oxidative base damage so it was thought that NEIL1 may also be capable of cleaving some of the oxidative base lesions which form following exposure of DNA to chromate. Of particular interest were the hydantoin lesions as they had previously been shown to form directly from 8-oxoG lesions in synthetic oligonucleotide systems exposed to single electron oxidants.<sup>7-9,16</sup> The specific activity of NEIL1 and NEIL2 in excising spiroiminodihydantoin (Sp), guanidinohydantoin (Gh), and 8-oxoG lesions has been studied using purified NEIL1 and NEIL2 enzymes.<sup>10</sup> These studies have shown that NEIL1 but not NEIL2 will cleave Sp lesions from duplex DNA (Figure 2.1a).<sup>10</sup> NEIL2 was capable of cleaving Sp from single-stranded oligonucleotides and could recognize but not cleave Sp in duplex DNA (Figure 2.1b).<sup>10</sup> Both enzymes showed little or no affinity for the 8-oxoG lesion.<sup>10</sup>

The NEIL glycosylases harbor intrinsic lyase activity that allows them to complete  $\beta\delta$ -elimination (Figure 2.2) at an apurinic/apyrimidinic (AP) site unlike OGG1.<sup>11</sup> OGG1 also possesses intrinsic lyase activity that would allow it to carry out  $\beta$ -elimination at an AP site following glycosidic bond cleavage.<sup>12</sup> However, this lyase activity is weak and OGG1 is typically out competed for the AP site by apurinic/apyrimidinic endonuclease (APE).<sup>11</sup> The  $\beta\delta$ -elimination product formed by further processing of the AP site by NEIL1 or NEIL2 has both a 5' and 3' phosphate termini.<sup>13</sup> APE will not recognize a free 3' phosphate suggesting that the NEIL1 and NEIL2 cleavage products must be processed differently than through the typical APE-dependent pathway. In fact, it has been shown that the 3' phosphate can be removed by DNA 5'-kinase/3'-phosphatase – polynucleotide

kinase (PNK)<sup>14</sup> - providing the alternative pathway needed to complete processing of the damaged site prior to reinsertion of a new base by a DNA polymerase.

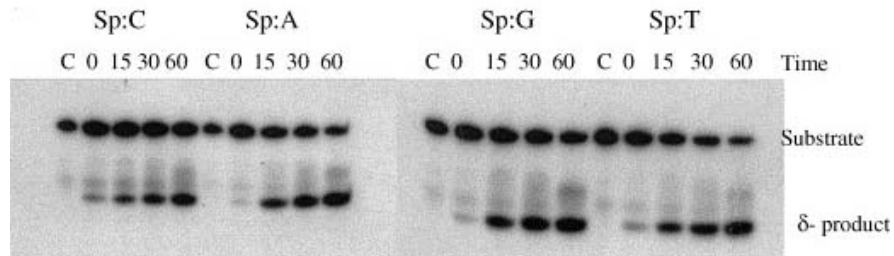


**Figure 2.1a** – The NEIL1 glycosylase cleaves Sp paired with any of the four natural DNA bases. A  $\delta$ -elimination product was observed in a duplex DNA system. Taken from [10].

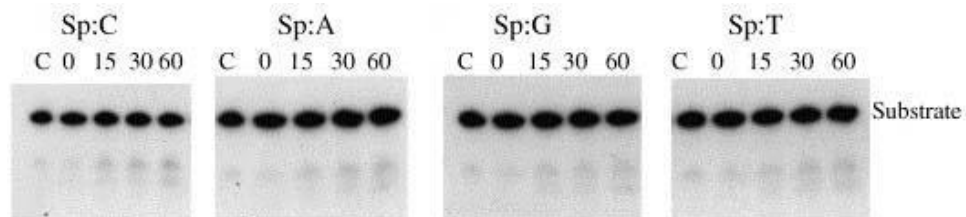


**Figure 2.1b** – The NEIL2 glycosylase is unable to cleave the Sp lesion in duplex DNA regardless of which natural DNA base it is paired. Taken from [10].

Armed with the knowledge that NEIL1 and NEIL2 are capable of cleaving secondary oxidative lesions from chromate damaged DNA, a system was developed to monitor intracellular lesion accumulation. OGG1 is the mammalian homolog of MutM and NEIL1 and NEIL2 are mammalian homologues of Nei. A MutM<sup>-</sup>/MutY<sup>-</sup> double knock-out and Nei deficient *E. coli* cell lines were exposed to chromate and their DNA was monitored for accumulation of 8-oxoG and Sp lesions.<sup>15</sup> The Nei deficient cell line was shown to have elevated sensitivity to chromate and to accumulate Sp lesions but not 8-oxoG lesions as was observed in the MutM<sup>-</sup>/MutY<sup>-</sup> double knock-out.<sup>15</sup>

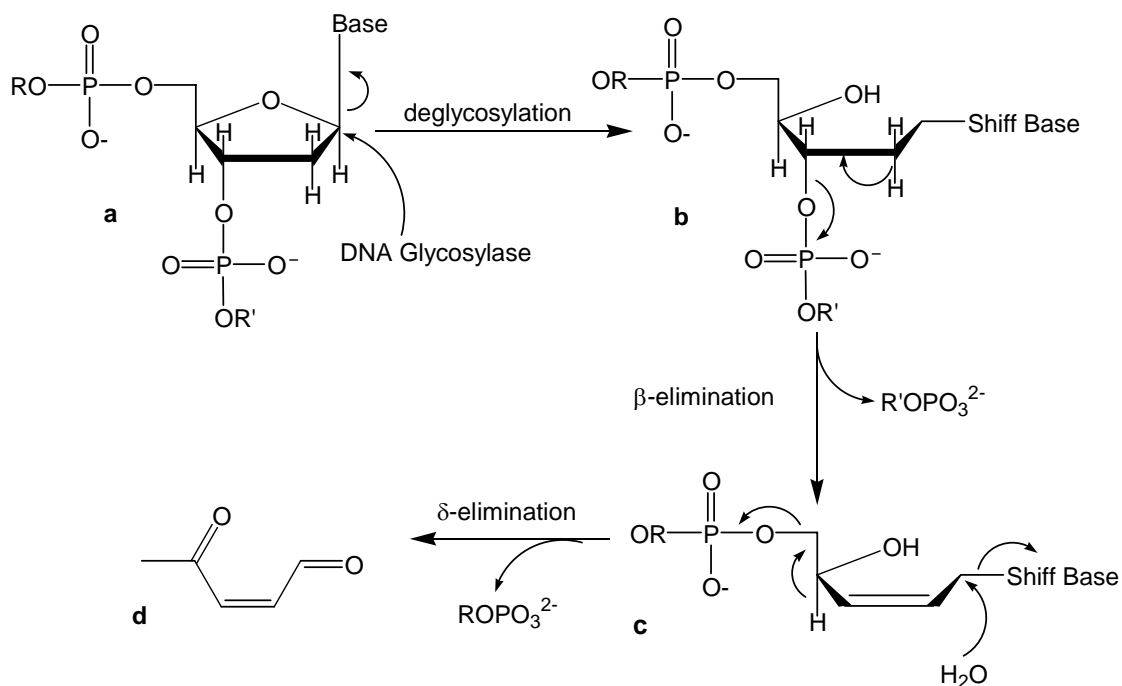


**Figure 2.2** –  $\beta\delta$ -elimination scheme that is carried out by the NEIL1 and NEIL2 glycosylases.<sup>13</sup>

A *Neil1*<sup>-/-</sup> mouse was engineered using a null-gene knock out plasmid which was inserted into the *Neil1*-coding region.<sup>16</sup> The *Neil1*<sup>-/-</sup> mice developed a number of metabolically related problems including obesity, fatty liver disease, kidney vacuolization, hyperleptinemia, hyperinsulinemia and increased mitochondrial DNA damage.<sup>16</sup> All of these conditions can be linked to genetic damage initiated by reactive oxygen species (ROS) and therefore indicated that cells from a *Neil1*<sup>-/-</sup> mouse line should be more sensitive to oxidative stress than their wild type counterparts. Kidney epithelial cells from both the wild type and *Neil1*<sup>-/-</sup> mouse lines have been generously donated allowing us to analyze the effects of chromate exposure in a NEIL1 deficient mammalian system.

To begin our studies with the NEIL1 cell lines, we first analyzed the cells for the presence or absence of an uninterrupted *Neil1* gene and then for their ability to excise 8-oxoG and Sp lesions from duplex DNA. We expected to observe cleavage of the 8-oxoG lesion by both the wild type and *Neil1*<sup>-/-</sup> cell lines as the *mOGG1* gene was unmodified in both cell lines. Without the presence of a functional *Neil1* gene however, we predicted that the *Neil1*<sup>-/-</sup> cell line would be unable to cleave Sp lesions. Our results however demonstrated that Sp can still be cleaved by cellular extracts devoid of functional NEIL1 enzyme indicating that NEIL1 may not be solely responsible for excision of Sp lesions in a cellular environment.

## **2.2 Materials and Methods**

**2.2.1 Murine Cell Growth Conditions** *Neil1*<sup>+/+</sup>, *Neil1*<sup>+/-</sup>, and *Neil1*<sup>-/-</sup> murine kidney epithelial cells were obtained from Dr. Steven Llyod at the Oregon Health and Science University (Portland, OR). All three cell lines were grown in DMEM containing 4.5 g/L D-glucose, L-glutamine, and 110 mg/L sodium pyruvate (Gibco) which was supplemented with 15% fetal calf serum (HyClone) and 1% 100X antibiotic-antimycotic (Gibco). Cells were maintained at 37° C under an atmosphere of 5% CO<sub>2</sub> to maintain a constant pH.

**2.2.2 DNA Extraction** Media was removed and discarded from flasks in which cells had formed a complete monolayer. The cells were rinsed with 1X PBS (Sigma) and harvested by treatment with Trypsin-EDTA (Gibco). The cell samples were pelleted at 300 x g and the supernatant was discarded. Samples were placed in 15 mL conical tubes which were placed on ice followed by the addition of 1 mL of 4° C DNA extraction buffer (0.1 M Tris-HCl, 0.1 M NH<sub>4</sub>Cl, pH 8.0) to each sample. Cell pellets were mixed thoroughly but gently and then sonicated for 5 min. in a Branson 3200 sonicating water bath. Cell samples were pelleted at 2400 x g (4° C) for 5 min. and the supernatant was discarded. Pellets were resuspended in 300 µL of DNA extraction buffer containing 33 U of RNase T1 (Sigma) and 200 µg of RNase A (Sigma). After 1 hour of incubation at 37° C, 300 µL of DNA extraction buffer containing 300 µg of Proteinase K

(Invitrogen) and 1% SDS (Gibco) was added. The samples were again mixed thoroughly but gently and allowed to incubate for an additional 1 hour at 37° C. 750 µL of concentrated, buffered phenol (pH 7.9, Sigma) was then added and each sample was thoroughly mixed before being centrifuged at 2400 x g for 5 min. The top layer was removed and placed into a fresh 1.5 mL tube, mixed with 250 µL of a 25:24:1 phenol : chloroform : isoamyl alcohol solution (pH 7.9, EMD), and centrifuged at 12000 x g for 5 min. Again the top layer was removed and placed into a fresh 1.5 mL tube, mixed with 250 µL of a 24:1 chloroform : isoamyl alcohol solution (Sigma), and centrifuged at 12000 x g for 5 min. The top layer was mixed with 30 µL of 10 M ammonium acetate (pH 5.0) and 1 mL of -20° C 100% ethanol in a fresh 1.5 mL tube. Samples were mixed and allowed to precipitate at -20° C overnight before being pelleted at 12000 x g (4° C) for 15 min. The supernatant was discarded, the pellet was washed with 1 mL of 70% ethanol, and re-centrifuged at 12000 x g (4° C) for 10 min. Residual ethanol was dried and the pellet was resuspended in 100 µL of deionized water. Absorbance at 260 nm (OD<sub>260</sub>) was obtained in order to determine the DNA content of each sample.

**2.2.3 Genotyping NEIL1 Cell Lines** A PCR reaction was run for a DNA sample from each cell line using the same forward *Neill* primer and a two different reverse primers specific for either the wild type *Neill* gene or the interrupted form. The forward primer used for both genotypes was derived from *Neill* intron 1 to *Neill* exon 2, 5'-CAC CAG TGA GCA AGA CAG CCA T-3'. A reverse primer for the *Neill*<sup>+/+</sup> genotype was developed from codons 6-12 in the *Neill* gene which were interrupted in the *Neill*<sup>-/-</sup> genotype, 5'-GTG GCT GGC CAG GTG CAG CTC-3'. A reverse primer for the *Neill*<sup>-/-</sup> genotype was developed from the neomycin open reading frame (ORF) that was used to interrupt the *Neill* gene, 5'-CCA GCT CAT TCC TCC CAC TCA-3' (Figure 2.3a). Template DNA (500 ng) was reacted with 2.5 U of Taq DNA polymerase (Novagen) in a solution of 16 nM forward *Neill* primer (Integrated DNA Technologies), 0.2 mM dNTP mixture (New England Biolabs), 1.5 mM MgCl<sub>2</sub> buffer (Novagen), and 16 nM of either the wild type or knock-out *Neill* reverse primer (Integrated DNA Technologies). The reaction underwent 35 rounds of PCR amplification in a PTC-200 Peltier Thermocycler. Amplified DNA samples were loaded onto a 1.2% agarose gel

containing 0.5 µg/mL ethidium bromide. Samples were loaded in a 30% glycerol buffer supplemented with 0.25% xylene cyanol (Sigma) and 0.25% bromophenol blue (Aldrich). The gel was run in a Tris-Borate buffer (0.045M Tris-Base, 0.045 M Borate, 0.001 M EDTA) at 90 V for 1.5 hours. PCR product bands were visualized using a Fujifilm FLA-3000 phosphoimager.

**2.2.4 Sp Oligonucleotide Synthesis** A 22 base pair (bp) oligonucleotide containing a single 8-oxoG lesion (5'-ACC AGC AGC <sup>8-oxo</sup>GGC CGC ACC AGT G-3') was purchased from TriLink Biotech. This oligonucleotide was oxidized using Cr(V) – Salen which was synthesized by reacting Cr(III) – Salen with iodosylbenzene in a 1:2 molar ratio respectively in dry acetonitrile for 15 min. at room temperature.<sup>17</sup> Each oxidation reaction consisted of 0.1 mM 8-oxoG oligonucleotide, 10 mM phosphate buffer at pH 7.4, and 0.8 mM Cr(V) – Salen. The reaction was allowed to proceed for 40 min. at 37° C. Upon completion of the reaction, the resulting Sp oligonucleotide was isolated on a Dionex NucleoPac PA-100 4 mm x 250 mm anion exchange column. A linear gradient was employed over 18 minutes from 90% mobile phase A (10% aqueous acetonitrile) and 10% mobile phase B (1.5 M ammonium acetate, pH 6.0 in 10% aqueous acetonitrile) to 100% mobile phase B. Sp containing oligonucleotide fractions were collected, combined and concentrated.

**2.2.5 <sup>32</sup>P Labeling and Annealing of Oligonucleotides** Oligonucleotide concentrations were obtained by measuring an OD<sub>260</sub> for the synthesized Sp oligonucleotide and the 8-oxoG oligonucleotide. A control oligonucleotide with a normal guanine residue present in place of the 8-oxoG lesion and a complement oligonucleotide were purchased from Integrated DNA Technologies and the concentration of each was determined in the same way. Equivalent molar concentrations of the Sp, 8-oxoG, and control oligonucleotides were 5' labeled with <sup>32</sup>P-γ-ATP (GE Health Care). Each reaction consisted of 10 U of polynucleotide kinase (Promega) 10 µCi <sup>32</sup>P-γ-ATP and 1X polynucleotide kinase buffer (Promega). Excess <sup>32</sup>P-γ-ATP was removed using a P6 Micro Bio-Spin Chromatography Column from BioRad. A 20% excess of the complement oligonucleotide was added to each of the three labeled oligonucleotide

solutions. These were then annealed by heating to 95° C for 5 min. before being cooled slowly (~1° C/5 min.) to room temperature. Once annealed, the solutions were stored at 4° C and used as a stock solution for up to a week.

**2.2.6 Nuclear Extract Preparation** Both NEIL1 deficient and wild type epithelial cells were harvested by gently scraping them from 75 cm<sup>2</sup> flasks with a cell scraper after being rinsed with ice cold 1X PBS containing phosphatase inhibitors. Nuclear extracts were then isolated using the Nuclear Extract Kit from Active Motif. A 20 µL aliquot of nuclear extracts from each cell line was retained to determine protein concentrations. The Bicinchoninic Acid Protein Assay Reagent Kit (Pierce) was used to determine protein concentrations. The remainder of the nuclear extracts were stored at -80° C in 25 µL aliquots.

**2.2.7 Sp Cleavage Assay** Nuclear extracts were thawed immediately prior to use in the cleavage assay. Reaction buffer for the cleavage assay was composed of 20 mM Tris-HCl (GibcoBRL) pH 8.0, 1 mM ethylenediaminetetraacetic acid (EDTA, Sigma), 1 mM Dithiothreitol (DTT, Fisher), and 100 µg/mL DNase free Bovine Serum Albumin (New England Biolabs). 500 nM concentrations of each annealed oligonucleotide were reacted with 40 µg of nuclear extracts at 37° C. 500 nM concentrations of each annealed oligonucleotide were also reacted with 0.8 U of purified hOGG1 (New England Biolabs) as a control for 8-oxoG cleavage. 5 µL aliquots of the reaction solutions were removed at 0, 60, 90 and 120 min. Each aliquot was immediately quenched by adding 5 µL of a formamide denaturing loading dye (1 mL formamide (Fisher), and 1 mg/mL bromophenol blue (Aldrich)) that had been preheated to 95° C. These were allowed to denature at 95° C for 5 min. and were then placed on ice for 3 min. immediately prior to being loaded onto a pre-poured 15% TBE, 7 M urea pre-poured gel (Invitrogen). The gel was run in a Tris-Borate-EDTA buffer (45 mM Tris Base (Aldrich), 45 mM Boric Acid (EMD Biosciences), and 0.001 M EDTA (Sigma)) for 40 min. at 180 V. Gels were visualized on a Fujifilm FLA-3000 phosphoimager.

## 2.3 Results

**2.3.1 Genotype Analysis** Primer sequences for the *Neill*<sup>+/+</sup> and the *Neill*<sup>-/-</sup> genotypes were provided by Dr. Stephen Llyod (Figure 2.3a). The expected PCR fragment lengths were 268 bp for the *Neill*<sup>+/+</sup> genotype, 448 bp for the *Neill*<sup>-/-</sup> genotype and both a 268 bp fragment and a 448 bp fragment for the *Neill*<sup>+/-</sup> genotype. A representative gel is shown in figure 2.3b.

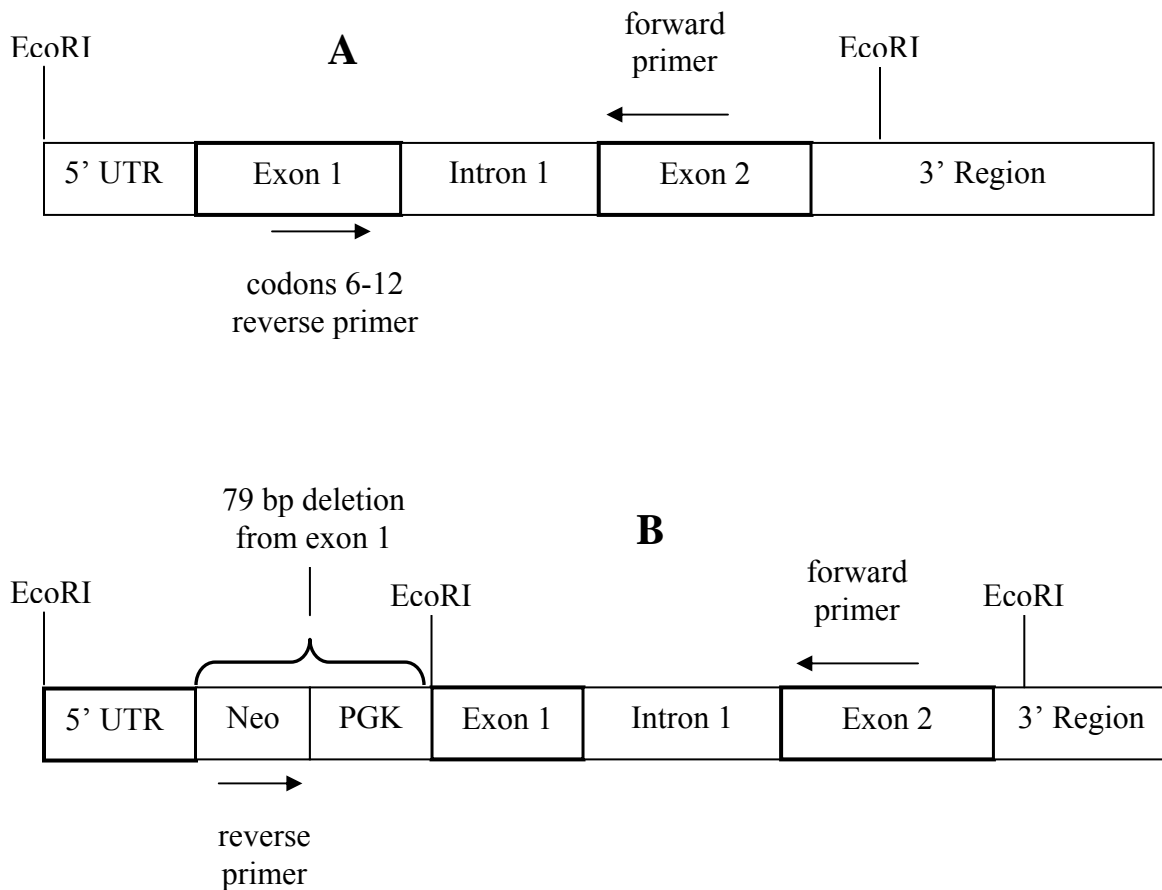


**Figure 2.3a** – *Neill* gene showing primer locations in both the wild type and interrupted form of the gene. The reverse primers are derived from exon 1. Codons 6-12 make up the wild type reverse primer (A). The knock out reverse primer is derived from the neomycin resistance gene that is inserted into the 5' region of exon 1 in the *Neill*<sup>-/-</sup> gene (B). This insertion causes a 79 bp deletion from the 5' end of exon 1 and includes the neomycin open reading frame (Neo) and a phosphoglycerate kinase promoter (PGK).<sup>16</sup>

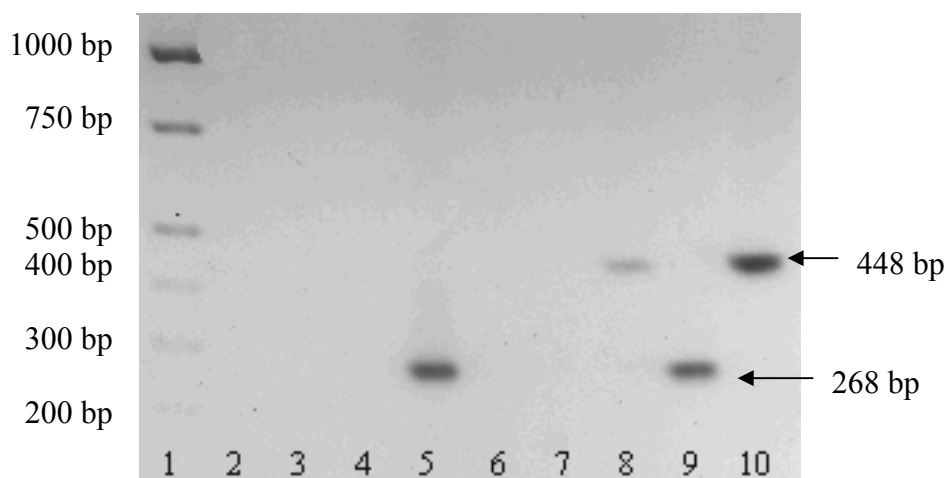


**Figure 2.3b** –PCR products corresponding to the three murine kidney epithelial cell lines. Lanes 3-10 all include the forward *Neill* primer. Lanes: 1 - molecular weight marker, 2 - empty, 3 - no template with *Neill*<sup>+/+</sup> reverse primer, 4 - no template with *Neill*<sup>-/-</sup> reverse primer, 5 - *Neill*<sup>+/+</sup> template with *Neill*<sup>+/+</sup> reverse primer (268 bp product), 6 - *Neill*<sup>+/+</sup> template with *Neill*<sup>-/-</sup> reverse primer, 7 - *Neill*<sup>-/-</sup> template with *Neill*<sup>+/+</sup> reverse primer, 8 - *Neill*<sup>-/-</sup> template with *Neill*<sup>-/-</sup> reverse primer (448 bp product), 9 - *Neill*<sup>+/+</sup> template with *Neill*<sup>+/+</sup> reverse primer (268 bp product), 10 - *Neill*<sup>+/+</sup> template with *Neill*<sup>-/-</sup> reverse primer (448 bp product).

**2.3.2 Sp Cleavage Assay** The original 8-oxoG 22-mer was purified on a Dionex NucleoPac PA-100 4 mm x 250 mm anion exchange column under the same separation conditions mentioned previously for the oxidized Sp 22-mer. The 8-oxoG 22-mer eluted after 11.7 min. (Figure 2.4a). This peak was collected and concentrated before being oxidized with Cr(V) – Salen to form the Sp 22-mer. Figure 2.4b is the HPLC trace from the product of the oxidized 8-oxoG 22-mer. The oxidation reaction was not cleaned-up prior to separation by HPLC resulting in a significant peak at 1.3 min. representing residual reaction components in the buffer front. Two small peaks with retention times of 9.8 and 10.2 min. represent a small amount of Gh/Ia 22-mer. Residual 8-oxoG 22-mer eluted at 11.5 min. while the two peaks representing the Sp 22-mer eluted at 13.1 and 13.5 min. When synthesized in single-stranded DNA, Sp will form two isomers (Figure 2.4b). The identity of these three sets of peaks has been confirmed in previous studies using ESI-MS analysis.<sup>18</sup>

Purified hOGG1 enzyme, as well as 40  $\mu\text{g}$  of nuclear extracts from both the *NeiI*<sup>+/+</sup> and *NeiI*<sup>-/-</sup> cell lines, were reacted with a control 22-mer, an 8-oxoG containing 22-mer, and an Sp containing 22-mer. The hOGG1 enzyme was unable to cleave the control substrate or the Sp substrate but showed very efficient cleavage of the 8-oxoG substrate (Figure 2.5-1). Both the *NeiI*<sup>+/+</sup> and *NeiI*<sup>-/-</sup> nuclear extracts were unable to cleave the control substrate but cleaved both the 8-oxoG and the Sp substrate (Figure 2.5-2,3). A single 12 bp product was observed in all of the reactions for which cleavage occurred.

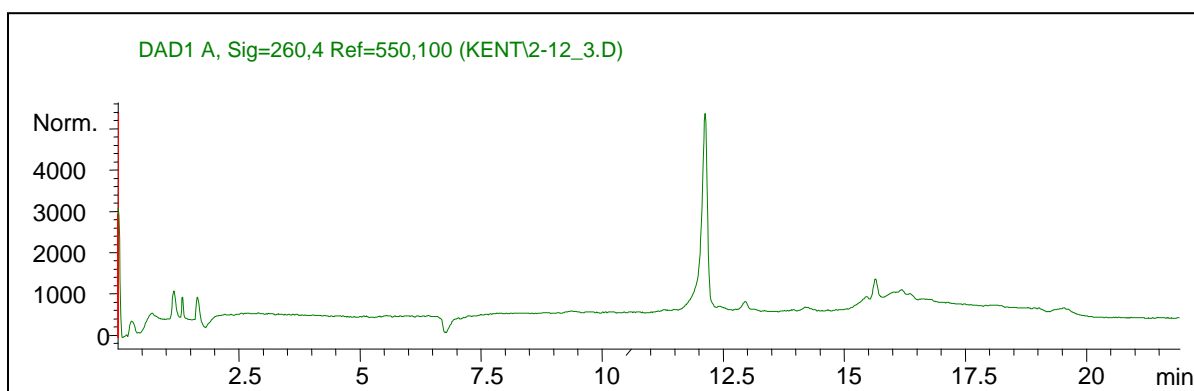


**Figure 2.4a** – HPLC trace of the oligonucleotide containing a single 8-oxoG lesion. Retention time was 11.7 minutes.

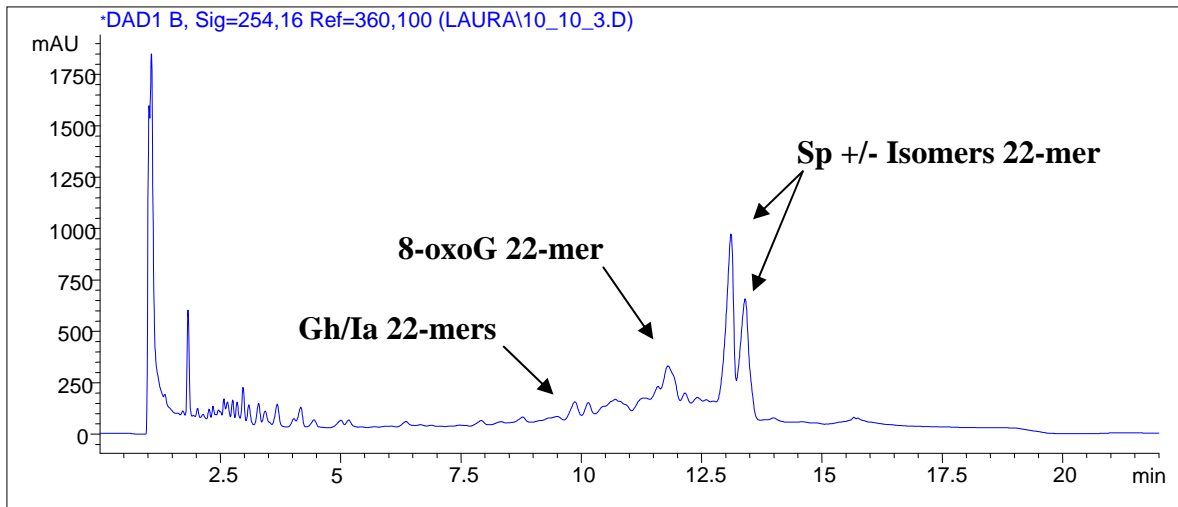


**Figure 2.4b** – HPLC trace of the oligonucleotide containing a single 8-oxoG lesion after oxidation by Cr(V) – Salen. Residual 8-oxoG 22-mer elutes at 11.5 minutes. The two peaks that elute at 13.1 and 13.5 minutes represent the two 22-mer oligonucleotides containing each of the two Sp isomers.

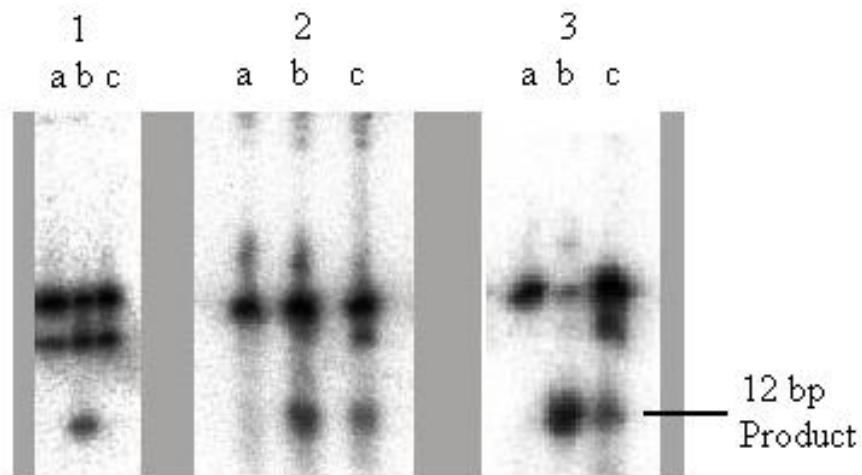


**Figure 2.5** – Gel 1 shows the reaction between purified hOGG1 and a 22 bp substrate. Gel 1: a) lesion-free substrate, b) 8-oxoG substrate, c) Sp substrate. Gel 2 shows the reaction between *Neill*<sup>+/+</sup> nuclear extracts and a 22 bp substrate. Gel 2: a) lesion-free substrate, b) 8-oxoG substrate, c) Sp substrate. Gel 3 shows the reaction between *Neill*<sup>-/-</sup> nuclear extracts and a 22 bp substrate. Gel 3: a) lesion-free substrate, b) 8-oxoG substrate, c) Sp substrate. Double bands in the substrate region occurred due to incomplete denaturation of oligonucleotides prior to electrophoretic separation.

## 2.4 Discussion

**2.4.1 Genotype Confirmation** The genotype of each of the kidney epithelial cell lines was confirmed upon receipt of the cells. The *Neil1*<sup>+/+</sup> cell line produced only a 268 bp PCR amplified product confirming that it did indeed have two unaltered copies of the *Neil1* gene. The *Neil1*<sup>+/-</sup> cell line produced both a 268 bp and a 448 bp PCR amplified product indicating that it possessed one uninterrupted copy of the *Neil1* gene and one interrupted *Neil1* gene copy. Finally, the *Neil1*<sup>-/-</sup> cell line produced only the 448 bp PCR amplified product confirming that both copies of the *Neil1* gene had been successfully interrupted with the neomycin open reading frame. Many of our subsequent studies were conducted without use of the heterozygous cell line.

**2.4.2 Sp Cleavage in a NEIL1 Deficient Cell Line** A control reaction between a lesion-free DNA substrate and hOGG1 enzyme or the NEIL1 proficient and deficient nuclear extracts ensured that there was no spontaneous DNA cleavage occurring due to reaction conditions. A second control reaction using the 8-oxoG DNA substrate showed that all three systems were able to excise the 8-oxoG lesion in duplex DNA. This was the expected result as 8-oxoG is the primary target lesion for hOGG1 and because the *mOGG1* gene was unaltered in both the wild type and *Neil1*<sup>-/-</sup> cell lines. Based on studies conducted with purified NEIL1 enzyme showing that only NEIL1 and not NEIL2 could excise Sp lesions in duplex DNA, we hypothesized that a NEIL1 deficient cell line may not be capable of cleaving Sp lesions from duplex DNA. Our results, however, demonstrated that the NEIL1 deficient as well as the NEIL1 proficient nuclear extracts were able to cleave the Sp lesion from duplex DNA. The signal intensity of the cleaved 12 bp Sp product looks similar between Gel 2 and 3 in figure 2.5. However, the intensity of the 12 bp Sp product relative to that of the 12 bp 8-oxoG product on Gel 3 is much lower than that of the same comparison made on Gel 2. This indicates that while the NEIL1 deficient nuclear extracts may be cleaving the Sp lesion, they are not cleaving Sp as efficiently as the NEIL1 proficient nuclear extracts. There are several possible explanations for the Sp cleavage seen in the NEIL1 deficient nuclear extract reactions. It

is likely that all three of the following explanations contribute to this observed Sp cleavage.

First, there may be a small amount of 8-oxoG substrate present in the Sp substrate lane. It is possible that the shoulder on the 8-oxoG 22-mer peak runs into the Sp peaks as they are separated by HPLC (Figure 2.4b). This proposal is based on the fact that in some of the cleavage gels, a faint 12 bp product band was visible in the Sp substrate lane for the purified hOGG1 reaction. While some OGG1 homologues such as yeast OGG1 and OGG2 are capable of cleaving the Sp lesion in duplex DNA, the human form – hOGG1 – does not recognize the Sp lesion<sup>19</sup> and hOGG1 is unable to excise Sp from duplex DNA paired with any of the four natural bases.<sup>18</sup> This fact suggests it is unlikely that the faint cleavage product seen in the Sp substrate lane for the hOGG1 reaction is actually a 12 bp DNA fragment containing the Sp lesion. There is also a small possibility that there may be some Gh/Ia substrate present as well. This is much more unlikely than having 8-oxoG substrate contamination as the Gh/Ia substrate elutes prior to both the 8-oxoG and Sp substrate when separated by HPLC (Figure 2.4b). This type of contamination, however, would not account for the faint cleavage product observed in the Sp substrate lane for the hOGG1 reaction as hOGG1 also has little or no affinity for the Gh/Ia lesion in duplex DNA.<sup>18</sup> Thus, it is most likely that the small amount of product observed in the hOGG1 reaction with the Sp substrate is a small amount of 8-oxoG substrate contaminating that reaction lane. The amount of cleavage product observed in the NEIL1 deficient nuclear extract reaction with the Sp substrate was much more extensive than that observed for the hOGG1 reaction with that same substrate based on relative product intensities. This indicates that 8-oxoG substrate contamination does not account for all of the observed Sp cleavage by the NEIL1 deficient nuclear extracts.

Secondly, the NEIL2 enzyme may be capable of excising the Sp lesion *in vivo*. NEIL2 was not capable of excising Sp from duplex DNA,<sup>10</sup> however, purified NEIL2 was capable of excising Sp from a single-stranded oligonucleotide and was able to recognize the Sp lesion in duplex DNA as demonstrated by a protein trapping assay.<sup>10</sup> It is reasonable to then suggest that the NEIL2 enzyme may be capable of excising the Sp lesion when functioning in a complete cellular system probably by recruiting downstream proteins of the BER apparatus. Unlike the *in vitro* NEIL1 and NEIL2 cleavage set-up, the

nuclear extracts used in our cleavage assay contain a wide variety of proteins capable of aiding in the BER process. For example, the OGG1 enzyme has the ability to carry out  $\beta$ -elimination at an AP site but it is much less efficient at this step than APE1.<sup>20,21</sup>

Therefore, in a cellular system, OGG1 will be displaced by APE1 which will then remove the sugar residue preparing the AP site for insertion of a new base.<sup>20</sup> Not much is yet known about NEIL1 and NEIL2 enzymatic functioning in a whole cell environment but it is likely that there are a variety of cellular proteins (for example DNA 5'-kinase/3'-phosphatase) that may be able to assist NEIL1 and/or NEIL2 making it possible for these BER enzymes to excise lesions *in vivo* that they are incapable of cleaving without the aid of accessory proteins.

Thirdly, Mismatch Repair (MMR) may also be playing a role in excising the Sp lesion *in vivo*. Typically MMR recognizes mismatched base pairs because they create a distortion in the DNA backbone. This distortion is usually quite small as it just involves a few misplaced hydrogen bonds between base pairs. The 8-oxoG lesion is not repaired by MMR because it does not create enough of a distortion in the DNA backbone to be recognized by MMR proteins as it simply shifts the N7 from a hydrogen bond acceptor to a hydrogen bond donor position. The Sp lesion however, may be able to recruit both BER and MMR proteins. Sp is small enough for BER enzymes to recognize and cleave it from duplex DNA. However, unlike 8-oxoG, Sp creates a more significant distortion in the DNA backbone (Figure 2.6) since Sp does not maintain a planar conformation like the natural DNA bases and 8-oxoG. This distortion is similar in magnitude to that seen with ternary Cr-DNA adducts and MMR has been shown to recognize DNA bending caused by ternary Cr-DNA adducts<sup>22</sup> which do not create a large enough distortion to recruit Nucleotide Excision Repair (NER) proteins but are too bulky for BER enzymes. Sp is probably not so bulky as to cause a DNA helix distortion large enough to recruit NER proteins but it may be enough of a distortion to recruit MMR proteins in addition to BER enzymes.

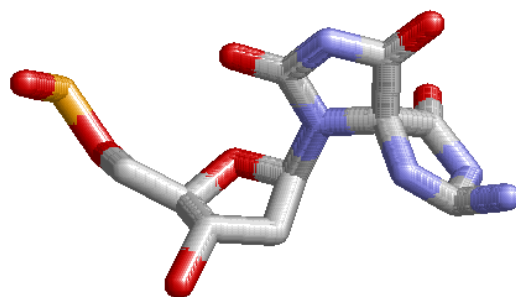


**Figure 2.6** – The spiroiminodihydroantoin lesion is composed of two imidazole rings which sit at a  $90^\circ$  angle to one another distorting the  $\pi$ -stacking structure of normal B-form DNA.

## 2.5 Conclusions

We were able to confirm that the NEIL1 deficient cell line did not carry a functional copy of the *Neil1* gene. Based on that finding and the results of studies carried out with purified NEIL1 and NEIL2 glycosylases, we anticipated that the NEIL1 deficient murine epithelial cells would be unable to excise the Sp lesion from duplex DNA. This did not turn out to be true although the efficiency of Sp excision from duplex DNA is reduced in the NEIL1 deficient cells as compared to their wild type counterpart. Therefore, we expected that the *Neil1*<sup>-/-</sup> cell line would be more sensitive to chromate than the *Neil1*<sup>+/+</sup> cell line. Since there was some Sp cleavage occurring in the *Neil1*<sup>-/-</sup> cell line, we did not expect that the difference in sensitivity to chromate would be as pronounced as that seen in *Nei* deficient *E. coli*.

## References

1. Morland, I., Rolseth, V., Luna, L, Rognes, T., Bjoras, M, Seeberg, E. (2002) Human DNA glycosylases of the bacterial Fpg/MutM superfamily: an alternative pathway for the repair of 8-oxoguanine and other oxidation products in DNA. *Nucleic Acids Res.* 30, 4926-4936.
2. Hazra, T.K., Izumi, T., Boldogh, I., Imhoff, B., Kow, Y.W., Jaruga, P., Dizdaroglu, M., Mitra, S. (2002) Identification and characterization of a human DNA glycosylase for repair of modified bases in oxidatively damaged DNA. *Proc. Natl. Acad. Sci. USA* 99, 3523-3528.
3. Bandaru, V., Sunkara, S., Wallace, S.S., Bond, J.P. (2002) A novel human DNA glycosylase that removes oxidative DNA damage and is homologous to *Escherichia coli* endonuclease VIII. *DNA Repair* 1, 517-529.
4. Takao, M., Kanno, S., Kobayashi, K., Zhang, Q., Yonei, S., van der Horst, G., Yasui, A. A back-up glycosylase in Nth1 knock-out mice is a functional Nei (endonuclease VIII) homologue. *J. Biol. Chem.* 277, 42205-42213.
5. Stanton, S.E., Shin, S.W., Johnson, B.E., Meyerson, M. (2000) Recurrent allelic deletion of chromosome arms 15q and 16q in human small cell lung carcinomas. *Genes Chromosomes Cancer* 27, 323-331.
6. Rosenquist, T.A., Zaika, E., Fernandes, A.S., Zharkov, D.O., Miller, H., Grollman, A.P. (2003) The novel DNA glycosylase NEIL1, protects mammalian cells from radiation-mediated cell death. *DNA Repair* 2, 581-891.
7. Duarte, V., Muller, J.G., Burrows, C.J. (1999) Insertion of dGMP and dAMP during in vitro DNA synthesis opposite an oxidized form of 7,8-dihydro-8-oxoguanine. *Nucleic Acids Res.* 27, 496-502.

8. Luo, W., Muller, J.G., Rachlin, E.M., Burrows, C.J. (2000) Characterization of spiroiminodihydantoin as a product of one-electron oxidation of 8-oxo-7,8-dihydroguanosine. *Org. Lett.* 2, 613-616.
9. Luo, W., Muller, J.G., Rachlin, E.M., Burrows, C.J. (2001) Characterization of hydantoin products from one-electron oxidation of 8-oxo-7,8-dihydroguanosine in a nucleoside model. *Chem. Res. Toxicol.* 14, 927-938.
10. Hailer, M.K., Slade, P.G., Martin, B.D., Rosenquist, T.A., Sugden, K.D. (2005) Recognition of the oxidized lesions spiroiminodihydantoin and guanidinohydantoin in DNA by the mammalian base excision repair glycosylases NEIL1 and NEIL2. *DNA Repair* 4, 41-50.
11. Mokkalapati, S.K. Wiederhold, L., Hazra, T.K., Mitra, S. (2004) Stimulation of DNA glycosylase activity of OGG1 by NEIL1: functional collaboration between two human DNA glycosylases. *Biochemistry* 43, 11596-11604.
12. McCullough, A.K., Dodson, M.L., Llyod, R.S. (1999) Initiation of base excision repair: glycosylase mechanisms and structures. *Annu. Rev. Biochem.* 68, 255-85.
13. Burrows, C.J., Muller, J.G. (1998) Oxidative nucleobase modifications leading to strand scission. *Chem. Rev.* 98, 1109-1151.
14. Wiederhold, L., Leppard, J.B., Kedar, P., Karimi-Busheri, F., Rasouli-Nia, A., Weinfeld, M., Tomkinson, A., Izumi, T., Prasad, R., Wilson, S.H., Mitra, S., Hazra, T.K. (2004) AP-endonuclease-independent DNA base excision repair in human cells. *Mol. Cell* 15, 209-220.
15. Hailer, M.K., Slade, P.G., Martin, B.D., Sugden, K.D. (2005) Nei deficient *Escherichia coli* are sensitive to chromate and accumulate the oxidized guanine lesion spiroiminodihydantoin. *Chem. Res. Toxicol.* 18, 1378-1383.

16. Vartanian, V., Lowell, B., Minko, I.G., Wood, T.G., Ceci, J.D., George, S., Ballinger, S.W., Corless, C.L., McCullough, A.K., Llyod, R.S. (2006) The metabolic syndrome resulting from a knockout of the NEIL1 DNA glycosylase. *Proc. Natl. Acad. Sci. USA* 103, 1864-1869.
17. Srinivasan, K., Kochi, J.K. (1985) Synthesis and molecular structure of oxochromium(V) cations. *Inorg. Chem.* 24, 4671-4675
18. Sugden, K.D., Campo, K.C., Martin, B.D. (2001) Direct oxidation of guanine and 7,8-dihydro-8-oxoguanine in DNA by a high-valent chromium complex: a possible mechanism for chromate genotoxicity. *Chem. Res. Toxicol.* 14, 1315-1322.
19. Leipold, M.D., Workman, H., Muller, J.G., Burrows, C.J., David, S.S. (2003) Recognition and removal of oxidized guanines in duplex DNA by the base excision repair enzymes hOGG1, yOGG1, and yOGG2. *Biochemistry* 42, 11373-11381.
20. Hill, J.W., Hazra, T.K., Izumi, T., Mitra, S. (2001) Stimulation of human 8-oxoguanine-DNA glycosylase by AP-endonuclease: potential coordination of the initial steps in base excision repair. *Nucleic Acids Res.* 29, 430-438.
21. Vidal, A.E., Hickson, I.D., Boiteux, S., Radicella, J.P. (2001) Mechanism of stimulation of the DNA glycosylase activity of hOGG1 by the major human AP endonuclease: bypass of the AP lyase activity step. *Nucleic Acids Res.* 29, 1285-1292.
22. Strauss-Soukup JK, Vaghefi MM, Hogrefe RI, Maher III LJ. (1997) Effects of neutralization pattern and stereochemistry on DNA bending by methylphosphonate substitutions. *Biochemistry* 36, 8692-8698.

## CHAPTER 3

### The Effects of a NEIL1 Deficiency on Chromate Sensitivity and Cell Cycle Regulation

#### 3.1 Introduction

The eukaryotic cell cycle is composed of four distinct phases - G1, S, G2, and M (Figure 3.1). The G1 and G2 phases are growth periods for the cell. During these phases, the overall mass of the cell will increase as the majority of cellular proteins are synthesized as well as organelles such as membranes, endoplasmic reticulum, mitochondria, and ribosomes. Much of this growth prepares the cell to undergo a round of division since duplicates of most cellular components must be synthesized prior to replication. Between the two growth phases is the S phase, or DNA synthesis phase. It is at this time that all of the genomic DNA will be replicated. The final stage of the cell cycle is mitosis (M phase) – cell division. Mitosis is further broken down in to four segments; prophase, metaphase, anaphase, and telophase. A rapidly replicating mammalian cell will complete one full cell cycle every 24 hours.<sup>1</sup> Roughly 12 hours are spent in G1, 6 hours in S, 6 hours in G2, and 30 minutes in mitosis.<sup>1</sup>

The time spent in each phase of the cell cycle varies greatly between different types of cells in multicellular organisms. A 24-hour cell cycle is common for skin cells or intestinal cells that are regenerated frequently.<sup>1</sup> At the other extreme, neurons leave the cell cycle permanently so will never divide during their life time. Neurons exit the cell cycle during the G1 phase and enter a sub-phase referred to as G0 (Figure 3.1).<sup>1</sup> Other cells will also arrest at the G0 sub-phase but many can be stimulated to re-enter the main cell cycle, such as liver cells that only need to be regenerated about once per year or following damage to the liver tissue. This type of arrest is normal for cells that do not need to replicate frequently. Some cells may also enter an arrest phase during the G2 period of growth as demonstrated by certain epidermal cells.<sup>1</sup> Another reason that cells may enter a cell cycle arrest sub-phase, is due to the accumulation of DNA damage. Four checkpoints throughout the cell cycle lead to temporary or permanent cell cycle arrest or

death.<sup>2</sup> Three of these checkpoints are dedicated to monitoring DNA damage (Figure 3.2).<sup>2</sup>

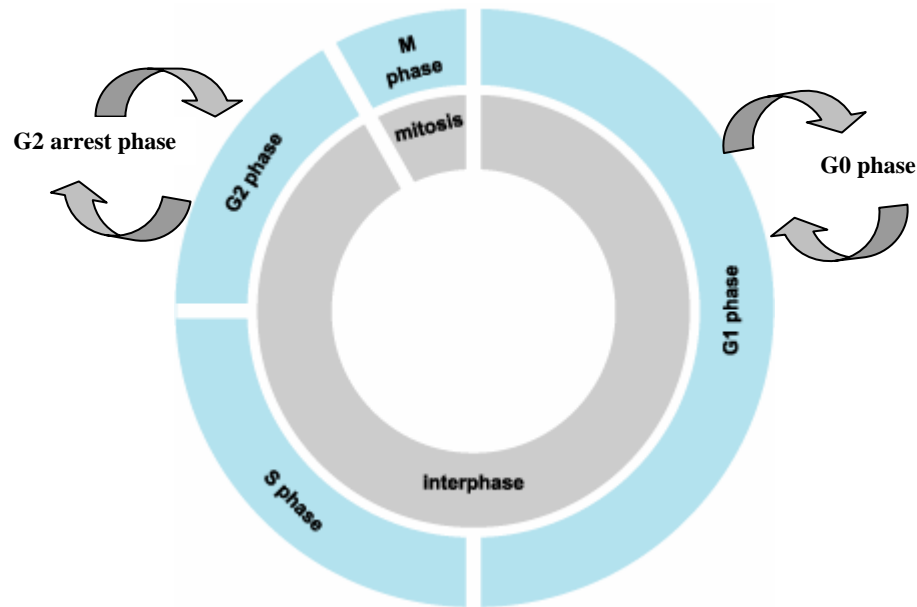


**Figure 3.1** – The eukaryotic cell cycle. A growth period composed of the G1, S, and G2 phases is collectively referred to as interphase. Mitosis, or the phase of cell division, completes the cycle. Cells can enter two arrest phases, G0 and G2 arrest as a way to temporarily or permanently exit the cell cycle.

In the G1 phase, DNA is scanned to ensure that no damage was incurred during the previous round of mitosis and that one copy of each chromosome was distributed to the daughter nuclei. However, the DNA may also be damaged during G1 by an exogenous factor such as chromate. The cell can then enter the G0 arrest phase while any genetic damage is repaired. If repair is successful, arrested cells can then re-enter the cell cycle and proceed into S phase. Following S phase, the DNA will again be monitored for damage and to ensure that all DNA was properly replicated. If there is damage, the cell will again be arrested but this time in the G2 arrest phase while the damage is repaired so that the cell can then progress into mitosis.

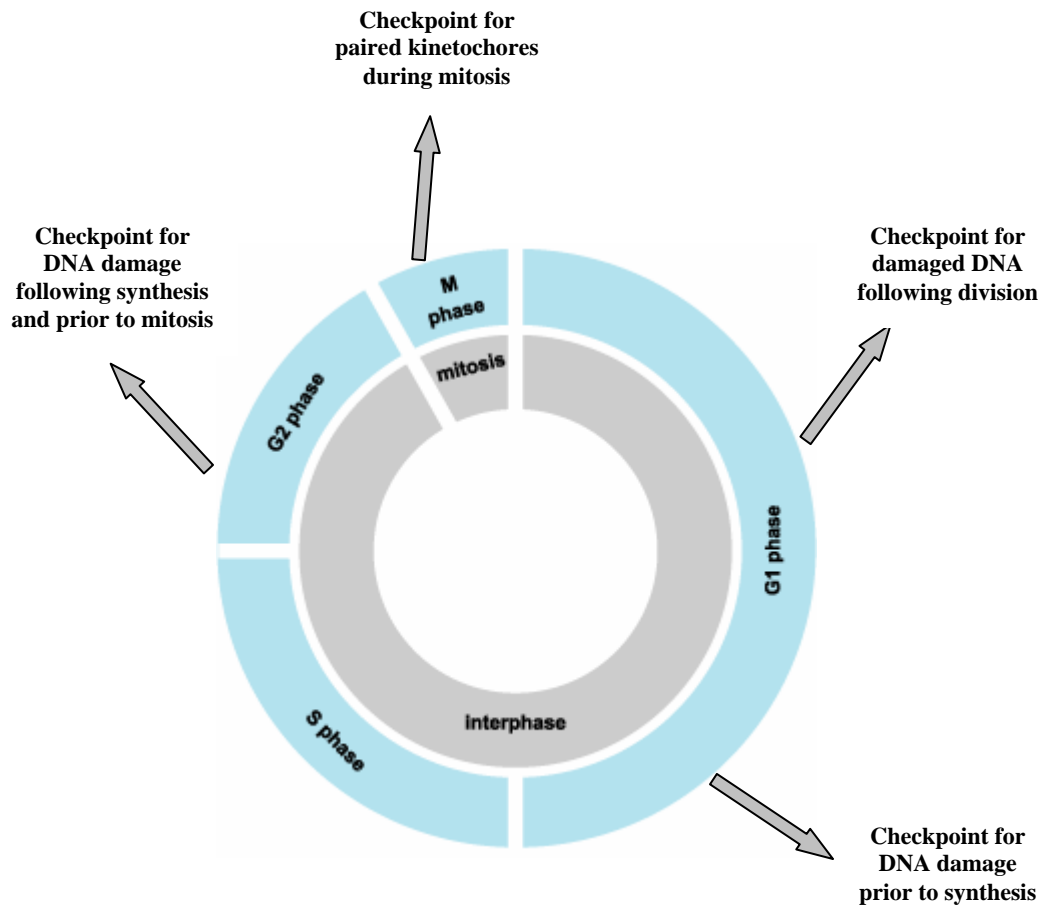


**Figure 3.2** – The cell cycle maintains checkpoints to monitor the integrity of DNA and other cell components. If damage to cellular components is detected at these checkpoints, the cell will either go into arrest followed by entering a survival mode where the damage will be repaired or it will self-destruct via necrosis or apoptosis.

A cell is only capable of repairing so much genetic damage. With a mutagen such as chromate, normal cells can survive following exposure to low concentrations of Cr(VI) since they are equipped to repair the oxidative DNA lesions that will be formed. The cells should go into a period of arrest, repair the damage and then reenter the cell cycle. Exposure to very high concentrations of Cr(VI) may cause a cell to enter a necrotic pathway. Necrosis is an unorganized form of cell death that will occur when a cell is

physically disrupted or incurs severe metabolic damage.<sup>3</sup> This pathway can be viewed as a last resort as it can induce necrosis in many neighboring cells as well. As a necrotic cell dies, its contents are rapidly released into the extracellular matrix and much of that material can be toxic when not compartmentalized within a cell.<sup>3</sup> A third, and more common scenario is the apoptotic pathway. When cells are exposed to intermediate but toxic concentrations of chromate, they can reach a point where they have too much DNA damage to be effectively repaired but have not been poisoned so badly that they will enter a necrotic pathway. At what point the damage becomes so great that a cell will be diverted from a survival pathway into an apoptotic pathway is unknown.<sup>4</sup> Instead, these cells will undergo cell degradation in a tightly regulated cascade of events collectively referred to as apoptosis.<sup>3</sup>

There are two apoptotic pathways, extrinsic and intrinsic.<sup>5</sup> Both pathways are regulated by the action of caspases (cysteine proteases)<sup>5</sup> and converge once the apoptotic cascade reaches the point of activation of the executioner caspases-2, 3, and 7.<sup>6,7</sup> An internal signal such as DNA damage induced by Cr(VI), activates the intrinsic apoptotic pathway.<sup>5</sup> The intrinsic pathway differs from the extrinsic in that the first signals for apoptosis are generated at the mitochondria rather than at the cell membrane. p53, a tumor suppressor protein, monitors DNA for damage.<sup>8</sup> Once that damage reaches a certain level, p53 will activate B-cell lymphoma 2 protein (Bcl-2) to form a dimer with Bcl-2 associated X protein (Bax).<sup>9-11</sup> The Bax protein will travel to the mitochondria, associate with Bcl-2, insert itself into the outer membrane, and form a pore that allows cations to freely flow into the negatively charged intermembrane space of the mitochondria.<sup>3,12</sup> This shift in voltage causes voltage-dependent anion channels (VDACs) present in the outer mitochondrial membrane to open allowing cytochrome c to escape into the cytoplasm.<sup>3,13</sup> Cytochrome c will then bind to apoptotic protease activating factor 1 (Apaf1) to cleave caspase 9.<sup>14</sup> This cascade of events (Figure 3.3) activates numerous proteases and nucleases which will begin the orderly degradation of cellular proteins and DNA.

Apoptosis helps to protect cells exposed to chromate from accumulating mutations that could eventually lead to the initiation of cancer. Based on the information obtained from the cleavage assays described in chapter 2, we hypothesized that a NEIL1

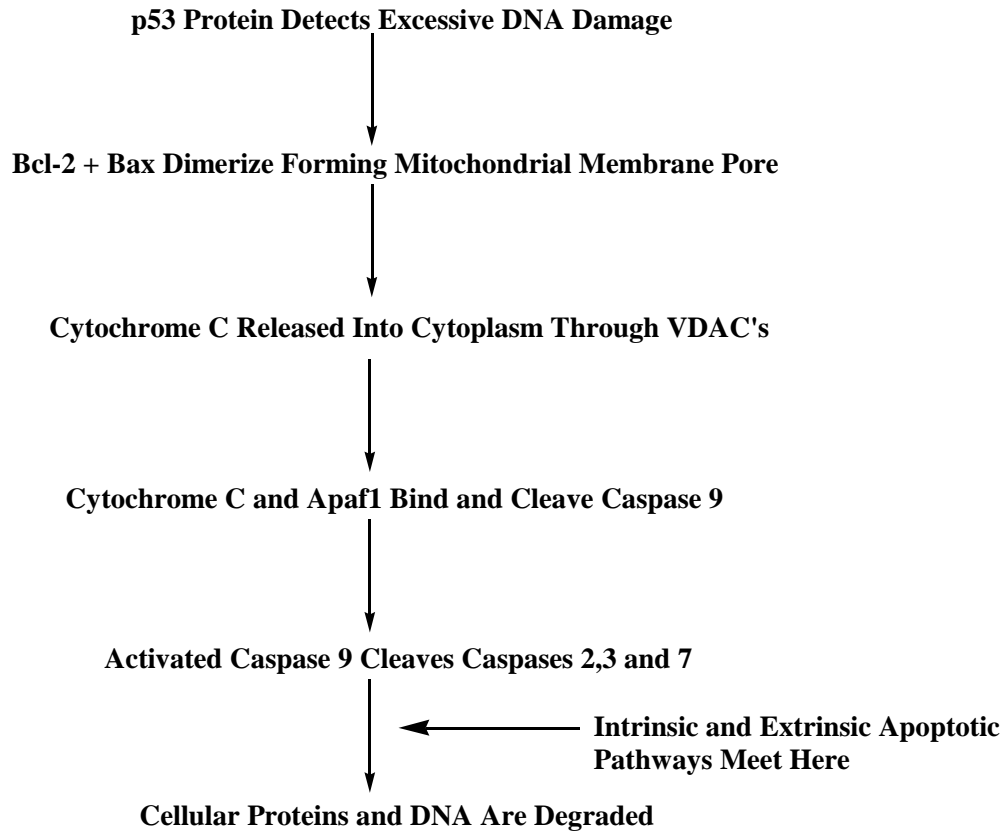


**Figure 3.3** – The intrinsic apoptotic pathway. The p53 protein detects excessive DNA damage and initiates a cascade of events that lead to release of cytochrome C from the mitochondria followed by activation of caspase 9. Activated caspase 9 will then cleave and activate caspases 2,3, and 7 leading to the degradation of cellular proteins and DNA. The intrinsic and extrinsic pathways are initiated by different mechanisms but the two pathways join at the point where caspases 2,3, and 7 are activated.

deficient murine epithelial cell line would accumulate more chromate-specific genetic damage and thus be more sensitive to chromate than a NEIL1 proficient murine epithelial cell line. However, since the NEIL1 deficient cells were still capable of excising some chromate-induced Sp lesions from duplex DNA, we thought that the sensitivity difference between these two mammalian cell lines would not be as pronounced as had previously been observed in Nei deficient versus Nei proficient *E. coli*.<sup>15</sup> Instead, the NEIL1 deficient cell line was less sensitive to chromate than its wild type counterpart. The only

difference between the two cell lines used in this study was the inactivation of a single BER glycosylase, NEIL1, and yet we found striking cell cycle progression differences between the two cell lines following exposure to chromate. The NEIL1 deficient cell line also demonstrated apoptosis resistance. As apoptosis resistance is a hallmark of cancer, this may provide evidence to explain why deletions in the 15q chromosome arm (the location of the *Neil1* gene) are observed in more than 70% of human small cell lung carcinomas.<sup>16</sup> This information taken together suggests that NEIL1, unlike other BER glycosylases including OGG1, plays a more dynamic role in maintaining control of the cell cycle engine than would be seen if this protein were solely involved in excising oxidized nucleobase lesions.

## **3.2 Materials and Methods**

**3.2.1 Chromium Uptake Analysis** Chromate-treated cells that had formed a complete monolayer were harvested as described previously using Trypsin-EDTA and lyophilized prior to digestion. For each freeze-dried sample, 1 mL of trace metal grade nitric acid (Fisher) was added and allowed to react for two hours. This was followed by the addition of 200  $\mu$ L of 30% hydrogen peroxide (J.T. Baker). Samples were then allowed to digest for 48 hours uncovered in a ventilation hood. Being careful not to disturb the salts which settled to the bottom of each tube, the liquid was transferred to a second 15 mL conical tube and brought up to a volume of 7 mL with nanopure water. Each sample was then analyzed for chromium content using an ICP-AES (IRIS Thermo Jarrell Ash).

**3.2.2 Cell Quantification and Plating** *Neil1*<sup>+/+</sup>, *Neil1*<sup>+/-</sup>, and *Neil1*<sup>-/-</sup> epithelial cells were harvested using Trypsin-EDTA. Cells were placed in 15 mL conical tubes and pelleted at 300 x g. Each sample was resuspended in 10 mL of complete media. A 20  $\mu$ L aliquot of each cell suspension was placed on a hemocytometer for counting. Cell samples were then diluted to a final concentration of 10,000 cells/mL. Once diluted, cells were distributed in 96-well plates (200  $\mu$ L/well or 2,000 cells/well).

**3.2.3 Toxicity Assay** Plated cells were allowed to grow for 48 hours at 37° C and 5% CO<sub>2</sub> before being treated with K<sub>2</sub>Cr<sub>2</sub>O<sub>7</sub> (J.T. Baker). Chromate solutions were made up as a 5X stock using filtered sterilized water. Media was removed from the 96-well plates. Each stock solution was diluted to the final 1X concentration using complete media before being added to the 96-well plates. The final concentrations of chromate used for the toxicity assay were 0, 1, 5, 10, 15, 20, 25, 30, 40, and 50 μM. The plates were maintained for 24 hours under the conditions listed above.

Chromate solutions were removed and each plate was then rinsed with 1X phosphate buffered saline (PBS). CellTiter-Blue (Promega) was mixed with complete media to form a 10% CellTiter-Blue solution. 200 μL of this solution was added to each well in the 96-well plate. Plates were allowed to incubate in the CellTiter-Blue solution for 22 hours at which time fluorescence at 585 nm (excitation at 555 nm and cut-off at 570 nm) was measured using the SpectraMax M2<sup>e</sup> Molecular Devices fluorescent plate reader.

**3.2.4 Cell Cycle Analysis** *Nei11<sup>+/+</sup>*, *Nei11<sup>+/-</sup>*, and *Nei11<sup>-/-</sup>* cells in the log phase of growth were exposed to chromate (0, 10, 20, 30, 50 μM concentrations) for 24 hours in 75 cm<sup>2</sup> flasks. Flasks were rinsed with 1X PBS and harvested using Trypsin-EDTA. From this point forward, the cells were kept at 4°C unless otherwise noted. Cells were transferred from flasks to 15 mL conical tubes and pelleted at 500 x g for 5 min. The supernatant was discarded and the pellet was washed with 1 mL of 1X PBS. Cells were pelleted at 500 x g for 10 min. The supernatant was discarded and the pellet was resuspended in ice cold 70% ethanol. Each sample was mixed well before being stored at -20° C overnight. Cells were pelleted at 1000 x g for 5 min. and the ethanol was discarded. Samples were resuspended in 990 μL of hypotonic buffer (0.5% Triton X-100 and 100 μg/mL RNase A (Sigma) prepared in 1X PBS) and incubated on ice for 30 min. 10 μL of a 500 μg/mL propidium iodide (Sigma) solution was then added and samples were allowed to incubate on ice for 30-60 min. DNA content was analyzed by fluorescence at 617 nm (excitation at 535 nm and cut-off at 565 nm) in a FACScan laser flow cytometer (Becton Dickenson).

**3.2.5 BrdU TUNEL Assay** *Neill*<sup>+/+</sup> and *Neill*<sup>-/-</sup> cells in the log phase of growth were exposed to chromate (0, 10, 20, 30, 50  $\mu$ M concentrations) for 24 hours. Flasks were rinsed with 1X PBS and harvested using Trypsin-EDTA. From this point forward, the cells were kept at 4° C unless otherwise noted. Cells were transferred from flasks to 15 mL conical tubes and pelleted at 500 x g for 5 min. The supernatant was discarded and the pellet was washed with 1 mL of 1X PBS. Cells were pelleted at 500 x g for 10 min. The supernatant was discarded and the pellet was resuspended in ice cold 70% ethanol. Each sample was mixed well before being stored at -20° C overnight. Cells were pelleted at 1000 x g for 5 min. and the ethanol was discarded. Pellets were resuspended in 0.5 mL of wash buffer provided in the APO-BrdU TUNEL Assay Kit (Invitrogen). Samples were stained with an Alexa Fluor 488 anti-BrdU antibody and propidium iodide as directed in the APO-BrdU TUNEL Assay Kit. Each sample had a final volume of ~600  $\mu$ L. Three 200  $\mu$ L aliquots of each sample were added to a 96-well plate and fluorescence was measured on a SpectraMax M2<sup>e</sup> Molecular Devices fluorescent plate reader at 519 nm (excitation at 495 nm and cut-off at 510 nm) for the Alexa Fluor 488 stain and at 617 nm (excitation at 535 nm and cut-off at 565 nm) for the propidium iodide stain.

**3.2.6 PARP-1 Assay** *Neill*<sup>+/+</sup> and *Neill*<sup>-/-</sup> cells were seeded at 1000 cells/ml in 96-well plates and allowed to incubate for 48 hours. Cells were exposed to chromate (0, 10, 20, 30, 50  $\mu$ M concentrations) or a known apoptosis inducing agent, etoposide (50  $\mu$ M concentration), for 24 hours. Cells were washed with 1X PBS before cell extracts were obtained and labeled with anti-PAR antibody using the method outlined in the HT Chemiluminescent PARP/Apoptosis Assay (Trevigen). PARP-1 activity in the form of PAR addition to histone proteins was then monitored as chemiluminescence at all wavelengths on a SpectraMax M2<sup>e</sup> Molecular Devices fluorescent plate reader.

**3.2.7 Statistical Analysis** Error bars in all of the graphs for chapters 3 and 4 represent the standard deviation in the average values shown. Figures 3.6 and 3.8 also have statistical data provided. Statistical calculations were done using the Student's two-

tailed T-test assuming equal variance. The number of observations gathered for the graphical representations is listed as “n” in the figure legends accompanying each graph.

### 3.3 Results

**3.3.1 Chromate Toxicity** *Neill*<sup>+/+</sup>, *Neill*<sup>+/-</sup>, and *Neill*<sup>-/-</sup> epithelial cells were exposed to Cr(VI) for 24 hours to observe their sensitivity to chromate. A toxicity curve was generated based on the percentage of cells that were still alive as compared to an untreated control sample following the 24 hour Cr(VI) exposure and a 22 hour incubation period in the CellTiter-Blue solution. CellTiter-Blue is a solution of resazurin dye which is taken up by and reduced to resorufin by live cells. Those cells that maintained an intact membrane were able to take up and reduce the resazurin dye to resorufin. The fluorescence of the resorufin was monitored for 24 hours at 585 nm to determine the optimal length of time for exposure of the epithelial cells to this stain. A maximal level of fluorescence was reached after 22 hours.

The epithelial cells were exposed to Cr(VI) concentrations ranging from 0 to 50  $\mu$ M. The *Neill*<sup>+/+</sup> and *Neill*<sup>+/-</sup> cell lines demonstrated similar responses to chromate exposure with an LD<sub>50</sub> occurring at a Cr(VI) concentration of approximately 40  $\mu$ M (Figure 3.4). In contrast, the *Neill*<sup>-/-</sup> cell line showed significantly greater tolerance to chromate than the *Neill*<sup>+/+</sup> and *Neill*<sup>+/-</sup> cell lines at all Cr(VI) exposure levels except 1 and 5  $\mu$ M (Figure 3.4). In a second trial, cells were dosed with chromate at concentrations between 50 and 100  $\mu$ M to determine the LD<sub>50</sub> for the *Neill*<sup>-/-</sup> cell line and to determine at what point the two cell lines would again have equivalent survival percentages. The LD<sub>50</sub> for the *Neill*<sup>-/-</sup> cell line was not reached until they had been exposed to a chromate concentration of nearly 70  $\mu$ M. Once the *Neill*<sup>+/+</sup> cells reached the 50  $\mu$ M exposure level, the amount of error in the data increased dramatically corresponding to a less than 50% cell survival rate. This same trend was observed for the *Neill*<sup>-/-</sup> cells except that the 50% cell survival rate was not reached until the 70  $\mu$ M exposure level. From that point forward, there is no longer any statistical difference in the cell survival percentages between the two cell lines. The data from this additional toxicity trial is presented in figure 3.5.

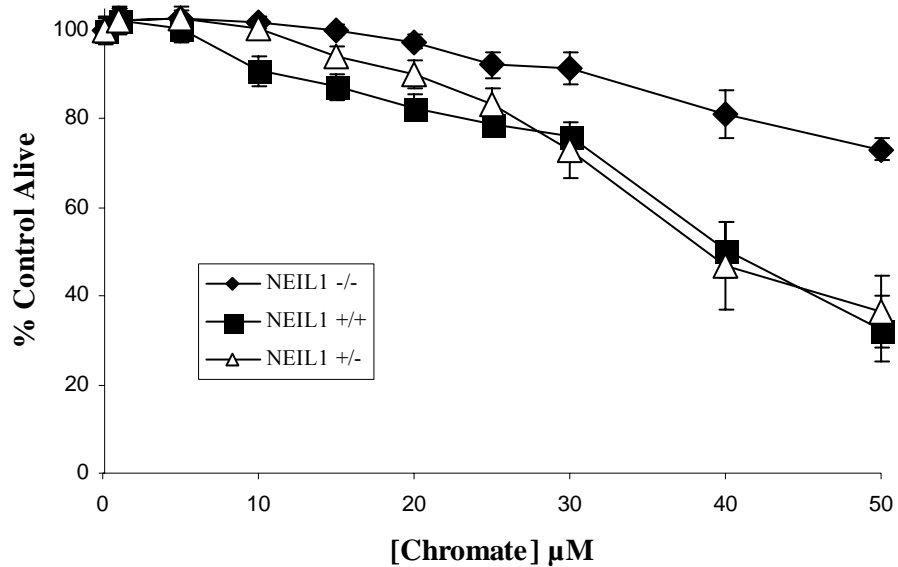


**Figure 3.4** – Toxicity curve for chromate exposure of the NEIL1 cell lines. The *Neil1*<sup>-/-</sup> cell line shows reduced sensitivity to Cr(VI) as compared to the *Neil1*<sup>+/+</sup> cell line. The *Neil1*<sup>+/+</sup> and *Neil1*<sup>+/-</sup> cell lines demonstrated similar responses to chromate exposure with the LD<sub>50</sub> occurring at a Cr(VI) concentration of approximately 40 µM. For each data point reported, n = 8 observations.

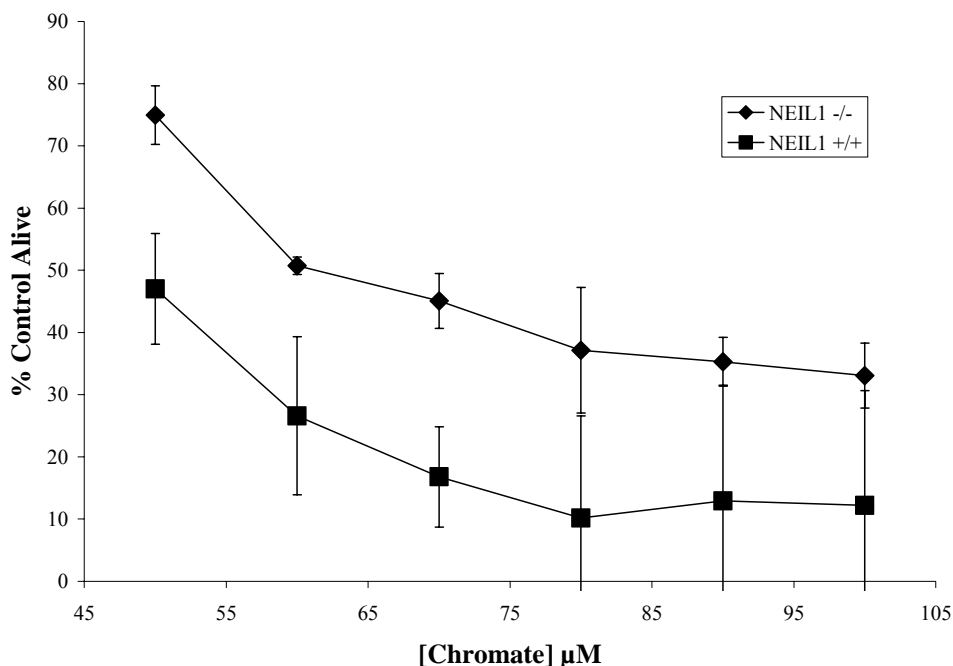


**Figure 3.5** – Extended toxicity curve for chromate exposure of the NEIL1 cell lines. The  $\text{LD}_{50}$  for the *Neil1*<sup>-/-</sup> cell line does not occur until a chromate concentration of nearly 70  $\mu\text{M}$  is reached. The *Neil1*<sup>-/-</sup> cell line maintains a decreased sensitivity to chromate as compared to the *Neil1*<sup>+/+</sup> cell line until an 80  $\mu\text{M}$  dosage is reached. From that point forward, there is no statistical difference in the sensitivity between the two cell lines. For each data point reported, n = 8 observations.

### 3.3.2 Chromium Uptake Analysis

NEIL1 deficient and proficient

epithelial cells were dosed with chromate and then analyzed for uptake. Harvested whole cells were digested and diluted so they could be analyzed by ICP-AES. It was important to monitor chromium uptake in each of the NEIL1 cell lines to ensure that one cell line was not being exposed to higher intracellular chromium concentrations than the other. Chromate is taken up by cells through non-selective anion channels that normally regulate uptake of phosphate and sulphate.<sup>17</sup> Cells that are actively growing will require a large amount of phosphate and sulphate for construction of proteins and nucleotides. Therefore, when chromate is present in the extracellular matrix, rapidly replicating cells will also inadvertently take in large amounts of chromate along with the influx of phosphate and sulphate. Our ICP-AES data revealed that chromate uptake was equivalent between the NEIL1 cell lines at 5 and 50  $\mu\text{M}$  extracellular exposure levels. However, at

the intermediate exposure levels (10, 20, and 30  $\mu\text{M}$ ) there was a significant difference in chromate uptake but it was not always the *Neil1*<sup>+/+</sup> cell line taking up larger amounts of chromate as we would have expected. The *Neil1*<sup>+/+</sup> cell line took up larger amounts of chromate than the *Neil1*<sup>-/-</sup> cell line at the 10 and 20  $\mu\text{M}$  exposure levels but the *Neil1*<sup>-/-</sup> cell line took up more chromate at the 30  $\mu\text{M}$  level as shown in figure 3.6.

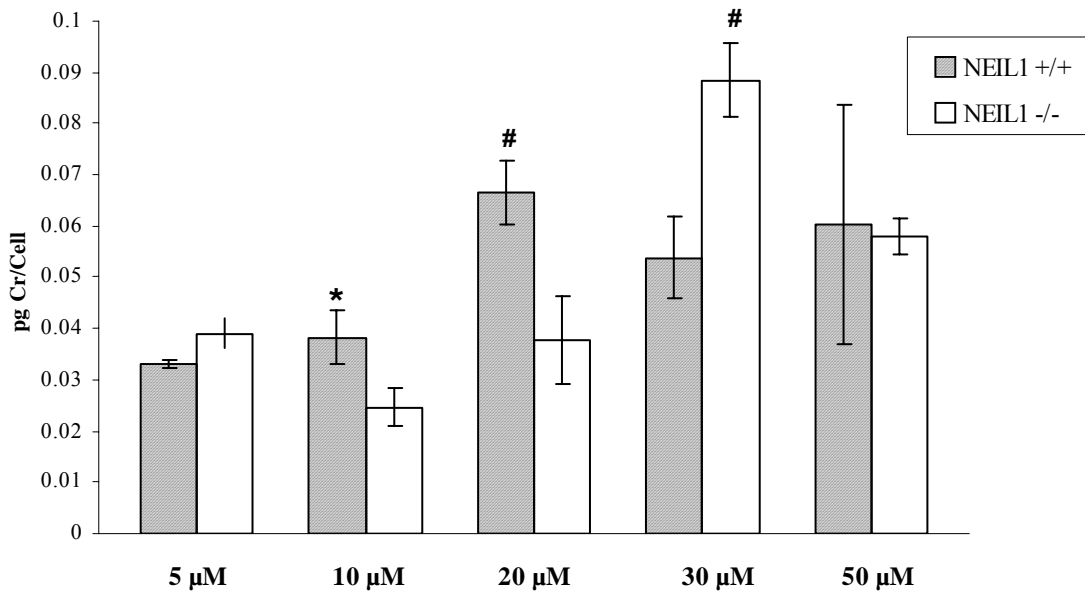


**Figure 3.6** – Chromium uptake was monitored on a pg of chromium/cell basis. A statistically significant difference was observed for chromium uptake at 10, 20, and 30  $\mu\text{M}$  chromate exposure levels (\* = 95% CL, # = 99% CL). *Neil1*<sup>+/+</sup> cells took up a greater amount of chromium at the 10 and 20  $\mu\text{M}$  exposure levels and *Neil1*<sup>-/-</sup> cells took up a greater amount of chromium at the 30  $\mu\text{M}$  level. All cell lines took up equivalent amounts of chromium at the 5 and 50  $\mu\text{M}$  exposure levels. For each data point reported, n = 3 observations.

### 3.3.3 Cell Cycle Progression Following Chromate Exposure

Induction of DNA damage can lead to cell cycle arrest allowing cells to repair the damage before progressing further along in the cell cycle. Chromate exposure induces DNA lesion formation and therefore exposure to chromate should cause cells to pause in the G0 or G2 arrest phases while the damage is assessed and/or repaired. Similar to the

differences observed in sensitivity to chromate, *Neil1*<sup>+/+</sup> and *Neil1*<sup>-/-</sup> cells also showed a difference in their progression through the cell cycle following chromate exposure. At chromate exposure concentrations between 10 and 30  $\mu$ M, the *Neil1*<sup>-/-</sup> cell line displayed elevated percentages of cells progressing into the S and G2/M phases of the cell cycle as compared to an untreated sample. The *Neil1*<sup>+/+</sup> cell line however, maintained similar percentages of its cells in the various phases of the cell cycle whether they had been exposed to chromate or not. The heterozygous NEIL1 cell line data fell between that of the *Neil1*<sup>+/+</sup> and *Neil1*<sup>-/-</sup> cell lines at each stage of the cell cycle analysis. Figure 3.7a shows the data from the G0/G1 phase analysis, figure 3.7b shows the S phase data, and figure 3.7c shows the G2/M phase data. Percentages of cells in each of the cell cycle phases were quantified based on propidium iodide (PI) fluorescence. PI is a DNA binding fluorescent stain. Cells were injected onto a FACScan laser flow cytometer and as they passed by the detector relative fluorescence was detected. Cells with a single copy of DNA (G0/G1 phase) gave half the fluorescence counts of cells with two copies (G2/M phase). Cells that were actively synthesizing DNA (S phase) gave fluorescence counts somewhere in between those of the G0/G1 and G2/M phase cells.

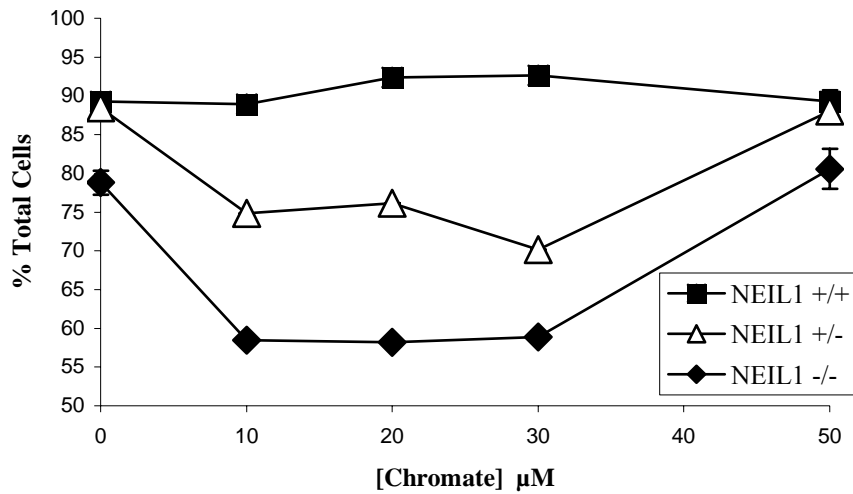


**Figure 3.7a** – All three NEIL1 cell lines have a similar percentage of cells in the G0/G1 phase of the cell cycle under chromate free growth conditions and following exposure to a 50  $\mu\text{M}$  chromate concentration (80-90%). The *Neil1*<sup>+/+</sup> cell line maintains that same level of ~90% of cells in the G0/G1 phase at all chromate exposure levels. The *Neil1*<sup>-/-</sup> cell line maintains only ~60% of its cells in the G0/G1 phase following exposure to 10, 20, and 30  $\mu\text{M}$  chromate concentrations.

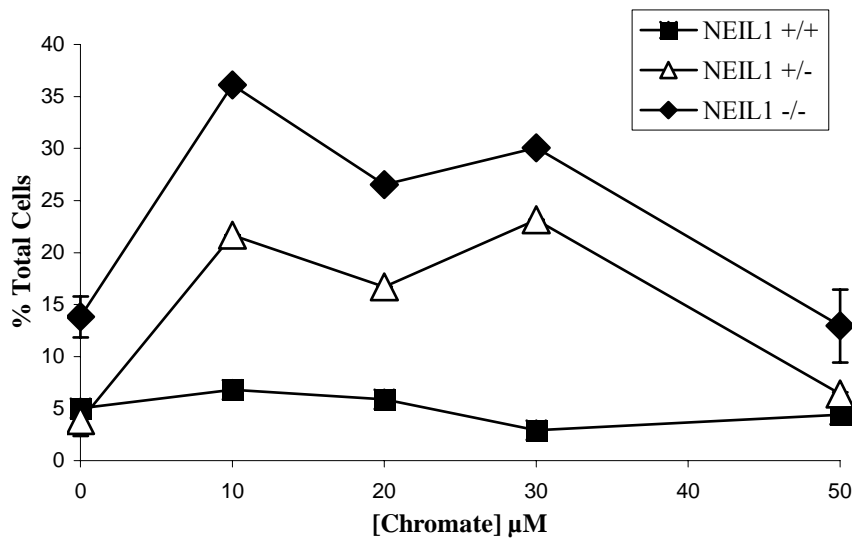


**Figure 3.7b** – All three NEIL1 cell lines have a similar percentage of cells in the S phase of the cell cycle under chromate free growth conditions and following exposure to a 50  $\mu\text{M}$  chromate concentration (5-14%). The *Neil1*<sup>+/+</sup> cell line maintains that same level of only 5% of cells in the S phase at all of the chromate exposure levels but the *Neil1*<sup>-/-</sup> cell line maintains between 27-37% of its cells in the S phase following exposure to 10, 20, and 30  $\mu\text{M}$  chromate concentrations.

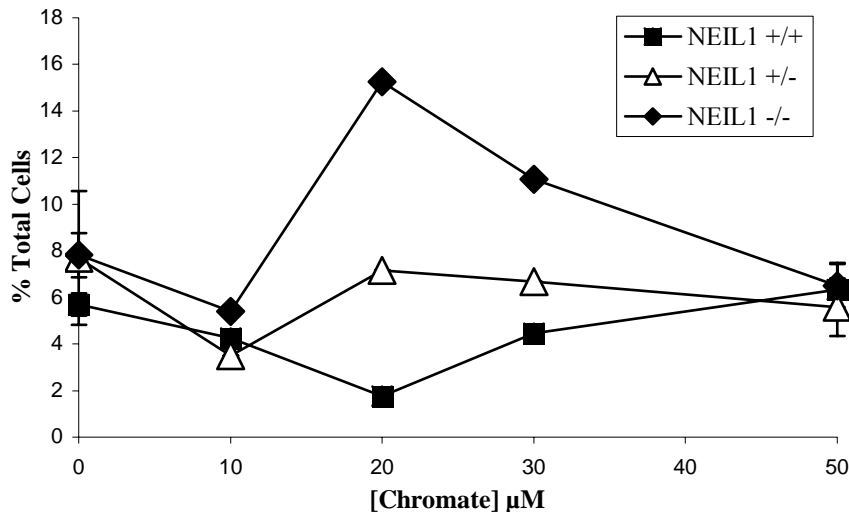


**Figure 3.7c** – All three NEIL1 cell lines have a similar percentage of cells in the G2/M phase of the cell cycle under chromate free growth conditions and following exposure to a 50  $\mu\text{M}$  chromate concentration (6-8%). The *Neil1*<sup>+/+</sup> cell line shows a reduced percentage of cells in the G2/M phase (2%) following exposure to a 20  $\mu\text{M}$  chromate concentration. However, the *Neil1*<sup>-/-</sup> cell line spikes to having as much as 12-16% of its cells in the S phase following exposure to 20 and 30  $\mu\text{M}$  chromate concentrations.

### 3.3.4 Quantification of Free 3'-OH Ends

The presence of high numbers of free 3'-hydroxyl ends in DNA can indicate that a cell is undergoing a large amount of excision repair<sup>18</sup> or that it has entered an apoptotic pathway which has lead to degradation of genomic DNA.<sup>19</sup> Terminal deoxynucleotidyl transferase (TdT) is an enzyme that will add any deoxyribonucleotide to free 3'-hydroxyl ends.<sup>20</sup> Using 5-bromo-2'-deoxyuridine 5'-phosphate (BrdUTP) – a deoxythymidine analog – and TdT, free 3'-hydroxyl groups in genomic DNA can be efficiently labeled. These groups can then be detected by further labeling the free 3'-hydroxyl groups with an anti-BrdU antibody coated with an Alexa Fluor 488 fluorescent tag. Epithelial cells from the NEIL1 proficient and deficient cell lines were analyzed for the presence of free 3'-hydroxyl ends using the above described transferase dUTP nick end labeling (TUNEL) technique. Cells were also labeled with propidium iodide (PI, an intercalating fluorescent DNA stain) as a way to quantify total DNA allowing us to compare the amount of free 3'-hydroxyl ends relative to total DNA per sample. All of the values were reported as a change in fluorescence from that of

untreated cell samples. A control cell sample provided in the APO-BrdU TUNEL assay kit was also analyzed in a similar fashion. The control cells were an HL60 cell line treated with camptothecin to induce apoptotic degradation of genomic DNA. At all chromate concentrations investigated, the *Neil1*<sup>+/+</sup> cell line showed an increase in the number of free 3'-hydroxyl ends over untreated *Neil1*<sup>+/+</sup> cell samples. There was no statistical difference observed in the number of free 3'-hydroxyl ends generated in the *Neil1*<sup>-/-</sup> cell samples for any of the chromate treatment concentrations versus those that were untreated. The relative number of free 3'-hydroxyl ends in the *Neil1*<sup>+/+</sup> cells exposed to 30 and 50  $\mu$ M chromate concentrations was statistically equivalent to the relative number observed in the control, HL60 cells.

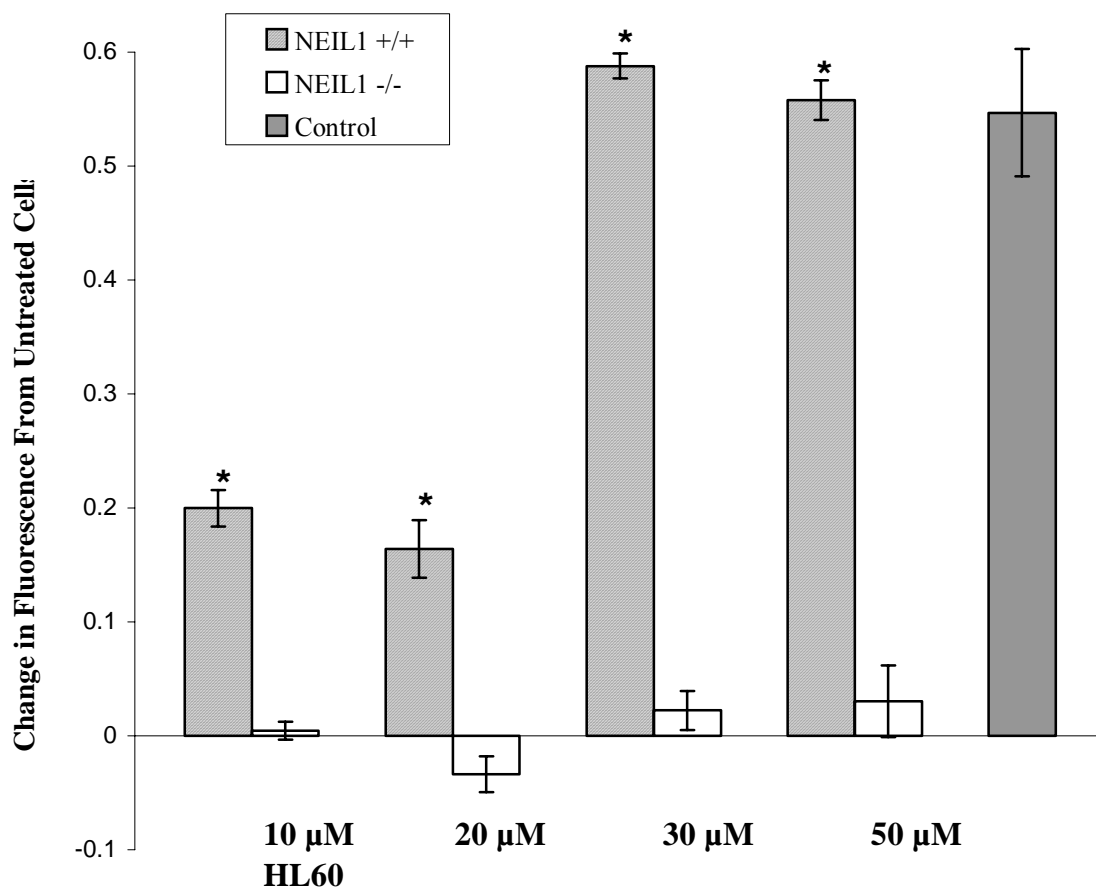


**Figure 3.8** – Graphical representation of the number of free 3'-hydroxyl ends in genomic DNA of NEIL1 cell lines following exposure to camptothecin. Values are reported as anti-Brd-UTP fluorescence counts (Alexa Fluor 488) per PI fluorescence count. All values represent difference in relative fluorescence from untreated NEIL1 proficient or deficient cell samples. The \* symbol indicates a statistical difference at the 99.9% confidence level. A positive apoptosis control sample of HL60 cells treated with camptothecin is also shown. For each data point reported, n = 6-9 observations.

**3.3.5 PARP-1 Activity** Poly (ADP-ribose) polymerase (PARP-1) is an enzyme that is involved in nuclear protein modification. It catalyzes the transfer of poly (ADP-ribose) at DNA strand breaks.<sup>21</sup> When apoptosis is initiated however, PARP-1 is cleaved from a 116 kDa to an 85 kDa protein by Yama/ CPP32β [caspase 3].<sup>21</sup> The cleaved PARP-1 enzyme then mediates the translocation of apoptosis inducing factor from the mitochondria to the nucleus.<sup>22</sup> Uncleaved PARP-1 activity can be monitored by

measuring poly (ADP-ribose) deposition onto an immobilized protein, in this case histone proteins. Based on the data from our BrdUTP TUNEL assay we knew that the NEIL1 proficient cell line was accumulating a significantly higher level of free 3'-hydroxyl ends than the NEIL1 deficient cell line. By monitoring PARP-1 activity in the two cell lines we were able to determine if that elevated level of free 3'-hydroxyl ends could be attributed DNA repair, as indicated by high levels of PARP-1 activity, or to apoptosis as indicated by depressed levels of PARP-1 activity. Values were reported as mU of poly (ADP-ribose) per  $\mu\text{g}$  of total protein. Total protein values for each cell sample were determined by BCA protein analysis using a Bicinchoninic Acid protein assay kit (Pierce). PARP-1 activity values represent a difference in activity from that of untreated cell samples. The NEIL1 proficient cells demonstrated an elevated PARP-1 activity level following exposure to a 10  $\mu\text{M}$  chromate concentration but very low levels of activity following exposure to 20, 30 and 50  $\mu\text{M}$  chromate concentrations. The NEIL1 deficient cells had an opposite trend. PARP-1 activity was reduced initially (10  $\mu\text{M}$  chromate exposure level) and then increased dramatically (20, 30, and 50  $\mu\text{M}$  chromate exposure levels). A positive apoptotic control was also used as a comparison for PARP-1 activity. Both *Neil1*<sup>+/+</sup> and *Neil1*<sup>-/-</sup> cells were exposed to a 50  $\mu\text{M}$  concentration of etoposide a well-documented apoptosis inducing agent.<sup>23</sup> Both cell lines showed similar trends in PARP-1 activity following treatment with etoposide as when they were treated with 20, 30, and 50  $\mu\text{M}$  concentrations of chromate in that PARP-1 activity was greatly reduced in the NEIL1 proficient cells relative to PARP-1 activity in the NEIL1 deficient cells.

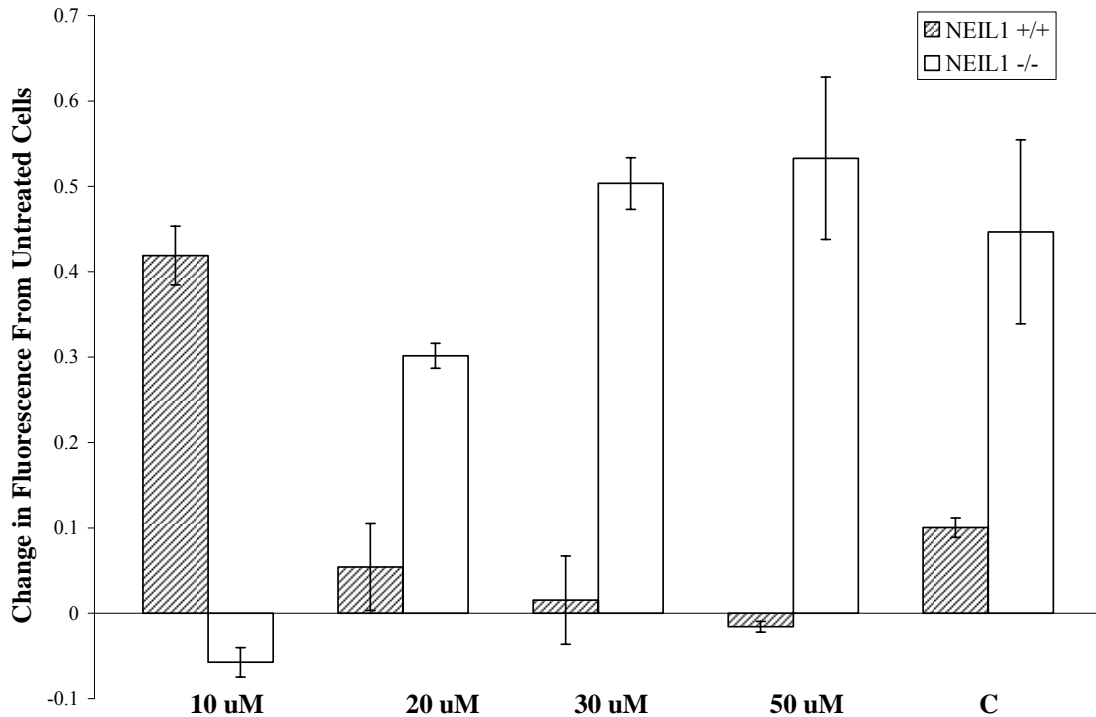


**Figure 3.9** – PARP-1 activity measured as poly (ADP-ribose) deposition on immobilized histones. *Neil1*<sup>+/+</sup> cells had elevated levels of PARP-1 activity at the 10  $\mu$ M chromate exposure level relative to the *Neil1*<sup>-/-</sup> cells but this activity was truncated at all other exposure levels and in the etoposide control sample. *Neil1*<sup>-/-</sup> cells showed an initial decrease in PARP-1 activity but elevated levels of activity relative to the *Neil1*<sup>+/+</sup> cells at all other exposure levels and in the etoposide (C) treated samples. For each data point reported, n = 3 observations.

### 3.4 Discussion

**3.4.1 Replication Coupled Base Excision Repair** BER glycosylases were once thought to all function in a similar, cell cycle independent manner. Further studies of these repair enzymes have shown that there are actually two distinct groups of BER glycosylases that carry out two slightly different forms of BER. The classical form of BER is now referred to as single nucleotide base excision repair (SN-BER).<sup>24</sup> The SN-BER pathway utilizes apurinic/apyrimidinic endonuclease 1 (APE-1) to process a  $\beta$ -elimination product or polynucleotide kinase (PNK) to process a  $\beta\delta$ -elimination product

formed by a BER glycosylase.<sup>25</sup> DNA polymerase  $\beta$  will then insert a new base using the complementary strand as a template and the gap in the phosphate backbone will be sealed by DNA ligase III $\alpha$ .<sup>26</sup> This type of BER occurs in DNA that is not being actively replicated and as such, does not utilize replication associated DNA polymerases or ligases. In fact, it has been reported that the BER glycosylases OGG1 and NTH1 are not even functional in single stranded DNA or replication bubble structures.<sup>27</sup> Therefore, it was of no surprise that although OGG1 and NTH1 function to remove oxidized nucleobase lesions (Table 1.3), their expression has been shown to be cell cycle independent. NEIL1 however, belongs to a second group of BER glycosylases that are cell cycle regulated and function as part of a modified BER pathway linked to DNA replication.

The second form of BER that has been identified is now defined as long patch base excision repair (LP-BER).<sup>28,29</sup> This second BER pathway functions in a very similar manner to SN-BER except that it is active only during DNA synthesis.<sup>24</sup> Since LP-BER is utilized during DNA synthesis, the accessory proteins involved in this repair pathway are proteins that are also involved in replication of undamaged DNA. SN-BER requires the use of DNA polymerase  $\beta$  as it contains intrinsic  $\beta$ -lyase activity that facilitates the removal of the 5'-terminal region formed by  $\beta$ - or  $\beta\delta$ -elimination prior to insertion of a new base.<sup>26</sup> This step is undertaken by flap endonuclease 1 (FEN1) in LP-BER<sup>30</sup> so that DNA polymerases  $\delta$  and  $\epsilon$ , which are already being employed for DNA replication, can fill in the AP site with a new base and then continue their progress along the DNA template being actively replicated.<sup>28,29</sup> The gap in the phosphate backbone will be sealed by DNA ligase I which is also part of the normal DNA replication machinery.<sup>31</sup>

A major difference between the two forms of BER is that SN-BER is carried out by individual proteins in relatively discrete steps whereas, LP-BER is carried out within a large protein complex in which repair and replication proteins may remain associated throughout the entire replication process. A DNA sliding clamp protein directs the assembly and functionality of the replication complex. Proliferating cell nuclear antigen (PCNA) is one DNA sliding clamp of particular interest to our research as it has been demonstrated that NEIL1 strongly associates with PCNA<sup>24</sup> as do several other BER glycosylases (MYH and UDG) that like NEIL1 are also cell cycle regulated.<sup>32</sup> Once

loaded onto the DNA by replication factor C (RFC), PCNA then recruits replication proteins such as DNA helicases, topoisomerases, polymerases, and glycosylases to assemble into a large replication complex, thus initiating DNA synthesis.<sup>33</sup>

DNA synthesis will come to a halt when a lesion is encountered in the template strand. Chromate may cause a variety of bulky lesions such as oxidatively induced protein-DNA crosslinks, and DNA-DNA crosslinks. These lesions will typically recruit nucleotide excision repair (NER) before synthesis has been initiated as they will extensively perturb the natural structure of B-form DNA acting as a beacon for repair systems. If these bulky lesions are still present when DNA replication is initiated, the replication complex will be unable to read through those points of damage.<sup>27</sup> Those bulky lesions would then have to be repaired before the replication complex could be reassembled and proceed with DNA synthesis. Small oxidative base lesions however, can easily go undetected in the genome prior to DNA replication as they do not greatly disturb the native DNA structure.<sup>27</sup> Therefore, it is very likely that a replication complex will encounter un-repaired oxidative base lesions such as Sp and Gh in genomic DNA from cells exposed to chromate. These lesions will cause the replication complex to stall long enough to either repair the lesion, or since the lesions are small, to read through the point of damage.

NEIL1, but not NEIL2, production is up-regulated during the S phase of the cell cycle.<sup>34,35</sup> NEIL1, but not NEIL2, has also been shown to be stimulated by PCNA<sup>24</sup> indicating that NEIL1 should be the glycosylase of choice to repair chromate induced oxidative lesions such as Sp and Gh that are encountered during DNA replication. Whether or not NEIL1 is part of the PCNA mediated replication complex from the initial point of assembly until the completion of DNA synthesis, or if it is only recruited when an oxidative lesion is encountered is still unknown. It has been demonstrated though that NEIL1 activity is stimulated by PCNA,<sup>24</sup> the DNA replication helicase Werner syndrome protein (WRN) that is associated with the PCNA complex,<sup>36,37</sup> and by the Rad9-Rad1-Hus1 (9-1-1 complex) another DNA sliding clamp protein that carries out functions similar to those of PCNA.<sup>38</sup> When an Sp or Gh lesion is encountered during replication, NEIL1 would be required to excise the lesion while the replication complex was temporarily stalled. If NEIL1 is not present to repair the lesion, PCNA has the ability to

recruit DNA polymerase  $\eta$  (a damage tolerant polymerase)<sup>39</sup> to simply insert any base across from the Sp or Gh lesion so that DNA synthesis can continue through the essentially non-disruptive damage point. It is beneficial for the PCNA complex to facilitate insertion of a single base mutation rather than to break apart because the replication fork can then collapse completely forming a double strand break. A double strand break requires recombination for repair<sup>40</sup> which can lead to the loss of critical genetic information when the template for recombination includes incomplete nascent DNA strands.

When an Sp or Gh lesion is encountered and NEIL1 is present, the replication complex would temporarily stall and the replication fork would partially collapse forming a “chicken foot” structure<sup>40</sup> in which the DNA template strands just down stream of the “chicken foot” would re-anneal.<sup>41</sup> NEIL1 would then bind to and excise the Sp or Gh lesion. PNK could then process the AP site, FEN1 could process the 5'-terminal region, polymerase  $\delta/\epsilon$  could insert a new base, and DNA ligase I could seal the nick in the phosphate backbone. A DNA helicase such as WRN would once again denature the DNA down stream of the “chicken foot” and PCNA would reinitiate DNA synthesis.<sup>41</sup>

**3.4.2 Implications of NEIL1 Deficient Epithelial Cell Data** Our initial hypothesis concerning the NEIL1 deficient murine epithelial cells was that they would show increased sensitivity to chromate relative to their wild type counterpart as was observed in Nei deficient *E. coli*.<sup>15</sup> However, this cell line actually showed reduced sensitivity to chromate with respect to the NEIL1 proficient cell line. This led us to believe that NEIL1 must play a more complex role in maintenance of cellular homeostasis than a classical mammalian BER glycosylase and or a BER glycosylase in a prokaryotic system. The recent work outlined above shows that NEIL1 does in fact play a different role in BER than OGG1 or NEIL2 in that NEIL1 functions to repair oxidized nucleobase lesions in actively replicating DNA whereas OGG1 and NEIL2 carry out this function in non-replicating DNA. Since NEIL1 is tied to replication, it is also inherently linked to the cell cycle. This proposal is supported by the findings that expression of NEIL1 is stimulated during the S phase of the cell cycle.<sup>34,35</sup>

Our data revealed that NEIL1 deficient cells not only display reduced sensitivity to chromate but that they also show aberrant cell cycle affects following chromate exposure. The DNA damage induced by chromate should cause a cell to pause and assess damage before moving along in the cell cycle, or in other words it should enter a period of cell cycle arrest. While we did not observe a large increase in the percentage of NEIL1 proficient cells stalling in the G0/G1 phases, we did see a decrease in the percentage of NEIL1 deficient cells in the G0/G1 phases following exposure to chromate. That decrease in cells in the G0/G1 phases correlated with an increase in the percentage of NEIL1 deficient cells found in the S and G2/M phases following exposure to chromate. This data suggests not only that chromate exposure does not hinder NEIL1 deficient cells from progressing through the S phase, it appears to stimulate cell cycle progression. This is occurring despite the fact that they would be accumulating significantly more oxidative DNA lesions than NEIL1 proficient cells. Thus, NEIL1 must play an essential role in oxidative DNA lesion detection, signaling the cell to postpone cell cycle progression while the damage is assessed and repaired. This proposal is supported by the fact that DNA replication complexes have the potential to read through small nucleobase lesions<sup>24</sup> if they are not repaired immediately following the encounter of a nucleobase lesion by the repair complex. By employing damage tolerant polymerase  $\eta$  that will simply insert any base across from the small nucleobase lesion, the replication complex can continue its processivity along the DNA template without risking replication fork collapse and double strand break formation.<sup>39</sup>

NEIL1 deficient cells not only display altered cell cycle characteristics following exposure to chromate, they also appear to be apoptosis resistant. When a large amount of DNA damage accumulates in a cell, p53 should signal the cell to switch from a survival pathway that would involve DNA repair, to an apoptotic pathway that will eventually end with the orderly degradation of genomic DNA.<sup>8</sup> The NEIL1 deficient cells, unlike the NEIL1 proficient cells do not appear to receive that apoptotic signal following exposure to levels of chromate that are ultimately toxic to the NEIL1 proficient cells. A large number of oxidative nucleobase lesions induced by reduced chromate in the cell would go undetected prior to DNA replication because lesions like Sp and Gh are relatively small, non-disruptive structures. During synthesis, DNA is progressively scanned by the

replication complex, so any lesions not repaired prior to replication will be encountered and will then be repaired or expressed as a mutation in the newly synthesized DNA. It would be the job of NEIL1 to repair any Sp or Gh lesions encountered during replication by utilizing the LP-BER pathway. However, if NEIL1 is absent from the replication complex, it is likely that a single base mutation would be inserted opposite the lesion by polymerase  $\eta$  allowing the replication process to continue.

Reading through nucleobase lesions would allow a large number of mutations to build up in the newly synthesized DNA. The actual repair of such lesions before they can be expressed as mutations, must then act as a signaling method. If too much repair is going on, a cell may receive signals that it is too badly damaged to salvage its DNA successfully so p53 would direct the cell into an apoptotic pathway. Without NEIL1 present, cells damaged by chromate exposure would not receive such a signal and would therefore continue to replicate as if nothing were amiss. Essentially, they would become apoptosis resistant. All the while, mutations would begin to accumulate in the newly synthesized DNA. Thus apoptosis resistance in the NEIL1 deficient cells would allow for accumulation of mutations that could eventually render the cells independent of cell cycle checkpoints or in other words a cancerous cell may be created. For this reason, apoptosis resistance is often referred to as a hallmark of cancer.

### **3.5 Conclusions**

NEIL1 deficient murine epithelial cells display an increased tolerance for chromate. They also did not enter cell cycle arrest following exposure to chromate and displayed characteristics of apoptosis resistance. Apoptosis resistance following chromate exposure would allow the NEIL1 deficient cells to accumulate mutations that can act as initiators for cancer. If these mutations accumulate in genes required for cell cycle control, gene transcripts would be altered and the cancer promotion stage would be reached. Studies have shown that deletions in the 15q chromosome arm – the location of the NEIL1 gene - are observed in more than 70% of human small cell lung carcinomas.<sup>16</sup> Lung cancers have been the major reported form of cancer caused by chromate exposure.<sup>42-45</sup> Therefore, people that carry mutations in their NEIL1 gene would stand a

higher risk of developing cancer from chromate exposure than those with two fully functional NEIL1 gene alleles. These conclusions are based on the assumption that the NEIL1 deficient cells accumulate oxidized base lesions following chromate exposure since they do not enter the apoptotic pathway even after they have been exposed to levels of chromate that lead to more than 50% toxicity in NEIL1 proficient cells. Accumulation of mutations in the NEIL1 deficient cell lines will be discussed in the Chapter 4.

## References

1. Murray, A., Hunt, T. (1993) *The Cell Cycle, an Introduction*. Oxford University Press. New York. pp. 7-9, 100-101,136.
2. Lewin, B. (2004) *Genes VIII*. Pearson Education Inc., Upper Saddle Rive, NJ. p. 843-845.
3. Potten, C., Wilson, J. (2004) *Apoptosis, the Life and Death of Cells*. Cambridge University Press. New York. pp. 18-24, 102.
4. Shall, S., de Murcia, G. (2000) Poly(ADP-ribose) polymerase-1: what have we learned from the deficient mouse model? *Mut. Res.* 460, 1-15.
5. Lee, S-M., Kleiboeker, S.B. (2007) Porcine reproductive and respiratory syndrome virus induces apoptosis through a mitochondria-mediated pathway. *Virology* 365, 419-434.
6. Budihardjo, I., Oliver, H., Lutter, M., Luo, X., Wang, X. (1999) Biochemical pathways of caspase activation during apoptosis. *Annu. Rev. Cell Dev. Biol.* 15, 269-290.
7. Kuida, K., Haydar, T.F., Kuan, C-Y., Gu, Y., Taya, C., Karasuyama, H., Su, M. S-S., Rakic, P., Flavell, R.A. (1998) Reduced apoptosis and cytochrome c-mediated caspase activation in mice lacking caspase 9. *Cell* 94, 325-337.
8. Kastan, M.B., Onyekwere, O., Sidransky, D., Vogelstein, B., Craig, R.W. (1991) Participation of p53 protein in the cellular response to DNA damage. *Cancer Res.* 51, 6304-6311.

9. Hockenbery, D.M., Nuñez, G., Milliman, C., Schreiber, R.D., Korsmeyer, S.J. (1990) Bcl-2 is an inner mitochondrial membrane protein that blocks programmed cell death. *Nature* 348, 334-336.
10. Hockenbery, D.M., Zutter, M., Hickey, W., Nahm, M., Korsmeyer, S.J. (1991) BCL2 protein is topographically restricted in tissues characterized by apoptotic cell death. *Proc. Natl. Acad. Sci. USA* 88, 6961-6965.
11. Vaux, D.L., Weissman, I.L., Kim, S.K. (1992) Prevention of programmed cell death in caenorhabditis elegans by human bcl-2. *Science* 258, 1955-1957.
12. Shi, Y. (2001) A structural view of mitochondria-mediated apoptosis. *Nat. Struct. Biol.* 8, 394-401.
13. Oltavi, Z.N., Milliman, C.L., Korsmeyer, S.J. (1993) Bcl-2 heterodimerizes in vivo with a conserved homolog, Bax, that accelerates programmed cell death. *Cell* 74, 609-619.
14. Chen, M., Wang, J. (2002) Initiator caspases in apoptosis signaling pathways. *Apoptosis* 7, 313-319.
15. Hailer, M.K., Slade, P.G., Martin, B.D., Sugden, K.D. (2005) Nei deficient *Escherichia coli* are sensitive to chromate and accumulate the oxidized guanine lesion spiroiminodihydantoin. *Chem. Res. Toxicol.* 18, 1378-1383.
16. Stanton, S.E., Shin, S.W., Johnson, B.E., Meyerson, M. (2000) Recurrent allelic deletion of chromosome arms 15q and 16q in human small cell lung carcinomas. *Genes Chromosomes Cancer* 27, 323-331.
17. Arslan, P., Beltrame, M., Tomasi, A. (1987) Intracellular chromium reduction. *Biochim. Biophys. Acta.* 931, 10-15.

18. Lewin, B. (2004) Genes VIII. Pearson Education, Inc. Upper Saddle River, NJ. pp. 449.
19. Bortner, C.D., Oldenburg, N.B.E., Cidlowski, J.A. (1995) The role of DNA fragmentation in apoptosis. *Trends Cell Biol.* 5, 21-26
20. Bollum, F.J. (1974) Terminal deoxynucleotidyl transferase. Boyer, R.D. (Ed.) *The Enzymes*. Vol. 10. Academic Press Inc., New York. pp. 145-171.
21. Tewari, M., Quan, L.T., O'Rourke, K., Desnoyers, S., Zeng, Z., Beidler, D.R., Poirier, G.G., Salvesen, G.S. (1995) Yama/ CPP32 $\beta$ , a mammalian homolog of CED-3, is a CrmA-inhibitable protease that cleaves the death substrate poly(ADP-ribose) polymerase. *Cell* 81, 801-809.
22. Yu, S.W., Wang, H., Poitras, M.F., Coombs, C., Bowers, W.J., Federoff, H.J., Poirier, G.G., Dawson, T.M., Dawson, V.L. (2002) Mediation of poly(ADP-ribose) polymerase-1-dependent cell death by apoptosis-inducing factor. *Science* 297, 259-263.
23. Baldwin, E.L., Osheroff, N. (2005) Etoposide, topoisomerase II and cancer. *Curr. Med. Chem. – Anti-Cancer Agents* 5, 363-372.
24. Dou, H., Theriot, C.A., Das, A., Hegde, M.L., Matsumoto, Y., Boldogh, I., Hazra, T.K., Bhakat, K.K., Mitra, S. (2008) Interaction of the human DNA glycosylase NEIL1 with proliferating cell nuclear antigen. *J. Biol. Chem.* 283, 3130-3140.
25. Wiederhold, L., Leppard, J.B., Kedar, P., Karimi-Busheri, F., Rasouli-Nia, A., Weinfeld, M., Tomkinson, A.E., Izumi, T., Prasad, R., Wilson, S.H., Mitra, S., Hazra, T.K. (2004) AP endonuclease-independent DNA base excision repair in human cells. *Mol. Cell.* 15, 209-220.

26. Krokan, H.E., Nilsen, H., Skorpen, F., Otterlei, M., Slupphaug, G. (2000) Base excision repair of DNA in mammalian cells. *FEBS Letters* 476, 73-77.
27. Dou, H., Mitra, S., Hazra, T.K. (2003) Repair of oxidized bases in DNA bubble structures by human DNA glycosylases NEIL1 and NEIL2. *J. Biol. Chem.* 278, 49679-49684.
28. Pascucci, B., Stucki, M., Jónsson, Z.O., Dogliotti, E., Hübscher, U. (1999) Long patch base excision repair with purified human proteins. *J. Biol. Chem.* 274, 33696-33702.
29. Matsumoto, Y., Kim, K., Hurwitz, J., Gary, R., Levin, D.S., Tomkinson, A.E., Park, M.S. (1999) Recognition of proliferating cell nuclear antigen-dependent repair of apurinic/apyrimidinic sites with purified human proteins. *J. Biol. Chem.* 274, 33703-33708.
30. Podlutzky, A.J., Dianova, I.I., Podust, V.N., Bohr, V.A., Dianov, G.L. (2001) Human DNA polymerase  $\beta$  initiates DNA synthesis during long-patch repair of reduced AP sites in DNA. *EMBO J.* 20, 1477-1482.
31. Waga, S., Bauer, G., Stillman, B. (1994) Reconstitution of complete SV40 DNA replication with purified replication factors. *J. Biol. Chem.* 269, 10923-10934.
32. Lu, A.L., Bai, H., Shi, G., Chang, G.Y. (2006) MutY and MutY homologs (MYH) in genome maintenance. *Front. Biosci.* 11, 3062-3080.
33. Warbrick, E. (2000) The puzzle of PCNA's many partners. *Bioessays* 22, 997-1006.

34. Hazra, T.K., Kow, Y.W., Hatahet, Z., Imhoff, B., Boldogh, I., Mokkalapati, S.K., Mitra, S., Izumi, T. (2002) Identification and characterization of a novel human DNA glycosylase for repair of cytosine-derived lesions. *J. Biol. Chem.* 277, 30417-30420.
35. Hazra, T.K., Izumi, T., Boldogh, I., Imhoff, B., Kow, Y.W., Jaruga, P., Dizdaroglu, M., Mitra, S. (2002) Identification and characterization of a human DNA glycosylase for repair of modified bases in oxidatively damaged DNA. *Proc. Natl. Acad. Sci. USA* 99, 3523-3528.
36. Das, A., Boldogh, I., Lee, J.W., Harrigan, J.A., Hegde, M.L., Piotrowski, J., Pinto, N. de S., Ramos, W., Greenberg, M.M., Hazra, T.K., Mitra, S., Bohr, V.A. (2007) The human Werner syndrome protein stimulates repair of oxidative DNA base damage by DNA glycosylase NEIL1. *J. Biol. Chem.* 282, 26591-26602.
37. Harrigan, J.A., Wilson III, D.M., Prasad, R., Opresko, P.L., Beck, G., May, A., Wilson, S.H., Bohr, V.A. (2006) The Werner syndrome protein operates in base excision repair and cooperates with DNA polymerase  $\beta$ . *Nucleic Acids Res.* 34, 745-754.
38. Guan, X., Bai, H., Shi, G., Theriot, C.A., Hazra, T.K., Mitra, S., Lu, A-L. (2007) The human checkpoint sensor Rad9-Rad1-Hus1 interacts with and stimulates NEIL1 glycosylase. *Nucleic Acids Res.* 35, 2463-2472.
39. Friedberg, E.C., Lehmann, A.R., Fuchs, R.P.P. (2005) Trading places: how do DNA polymerases switch during translesion DNA synthesis? *Mol. Cell* 18, 499-505.
40. Heller, R.C., Marians, K.J. (2006) Replisome assembly and the direct restart of stalled replication forks. *Nature Rev. Mol. Cell Biol.* 7, 932-943.

41. Sharma, S., Otterlei, M., Sommers, J.A., Driscoll, H.C., Dianov, G.L., Kao, H-I., Bambara, H.C., Brosh, R.M. Jr. (2004) WRN helicase and FEN-1 form a complex upon replication arrest and together process branch-migrating DNA structures associated with the replication fork. *Mol. Biol. Cell* 15, 734-750.
42. Baetjer, A.M. (1950) Pulmonary carcinoma in chromate workers II. Incidence on basis of hospital records. *Arch. Indust. Hyg. Occup. Med.* 2, 505-516.
43. Bidstrup, P.L. (1951) Carcinoma of the lung in chromate workers. *Br. J. Ind. Med.* 8, 302-305.
44. Bidstrup, P.L., Case, R.A.M. (1956) Carcinoma in the lung of workmen in the bichromate-producing industry in Great Britain. *Br. J. Ind. Med.* 13, 260-264.
45. Pfeil, R. (1935) Lungentumoren als Berufskrankung in Chromatbetrieben. *Dtsch. Med. Wochensh* 61, 1197-1202.

## CHAPTER 4

### Lesion and Mutation Accumulation in NEIL1 Cell Lines

#### 4.1 Introduction

The formation of oxidative DNA lesions in a cellular system may act as an initiator for mutation formation if the lesions are not repaired. Single oxidative nucleobase lesions can be potent sources for mutations as they do not typically cause a large disruption in the overall structure of B-form DNA<sup>1</sup> and can be overlooked prior to transcription or replication of DNA. For example, an 8-oxoG lesion maintains a planar ring structure similar to that of the four natural DNA bases G,C, T, and A. The N7 group is simply shifted from being a hydrogen bond acceptor to a hydrogen bond donor. Because the N7 group is not directly involved with the Watson-Crick hydrogen bonding between a normal guanine residue and a cytosine residue, an 8-oxoG lesion can still stably pair with a cytosine residue (Figure 4.1a). During a round of replication, the 8-oxoG lesion may be flipped into the *syn* conformation by DNA polymerases and will then be paired with an adenine residue (Figure 4.1b) leading to the formation of a G:C → T:A transversion mutation.<sup>2</sup>

While 8-oxoG has been shown to induce G:C → T:A transversion mutations,<sup>2,3</sup> the hydantoin lesions, Sp and Gh/Ia, have been shown to cause those same transversion mutations at frequencies at least one order of magnitude higher.<sup>4</sup> In addition to G:C → T:A transversion mutations, Sp and Gh/Ia have also been shown to induce G:C → C:G transversion mutations<sup>4-6</sup> and are >98% mutagenic whereas 8-oxoG is approximately 5% mutagenic.<sup>4,6,7</sup> The Sp and Gh/Ia lesions have a significantly altered structure relative to that of the parent guanine residue or an 8-oxoG lesion (Figure 4.2) making it more difficult for these lesions to form appropriate hydrogen bonding schemes that do not perturb the overall DNA structure. Since these lesions would create a more substantial alteration in the DNA structure, they should theoretically be easier for the SN-BER pathway to detect and repair prior to DNA replication. Sp lesions however, are identified and excised by the NEIL1 glycosylase.<sup>8</sup> NEIL1 expression is up-regulated during the S phase<sup>9,10</sup> and has been shown to associate with replication complex proteins indicating

that NEIL1 is involved in LP-BER rather than SN-BER.<sup>11-14</sup> Therefore, Sp lesions, despite their tendency to create a more dramatic kink in the DNA phosphate backbone than an 8-oxoG lesion, would typically not be repaired until a cell entered S phase increasing the odds that a point mutation could be generated opposite an Sp lesion.

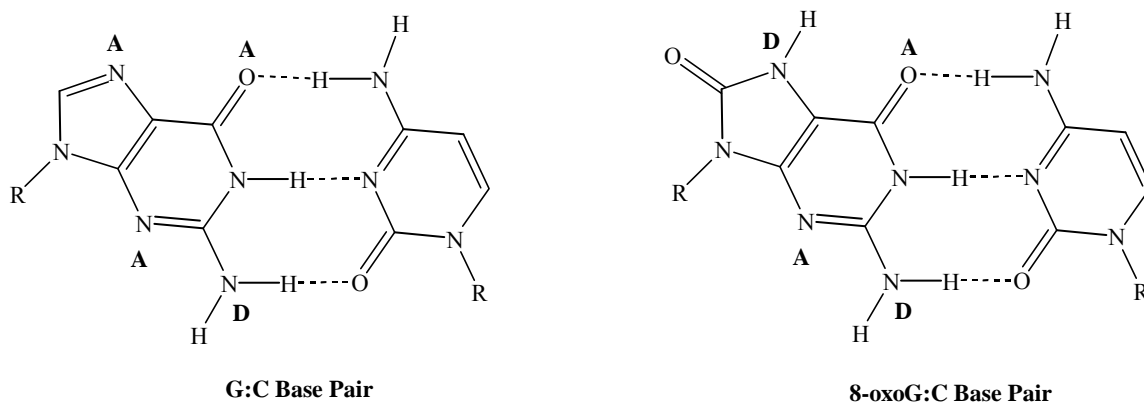


**Figure 4.1a** – Watson-Crick base pairing between guanine and cytosine and between 8-oxoG and cytosine. The N7 group of the 8-oxoG lesion is altered from a hydrogen bond acceptor (A) to a hydrogen bond donor (D) location. This alteration does not significantly alter the ability of 8-oxoG to pair with a cytosine residue.

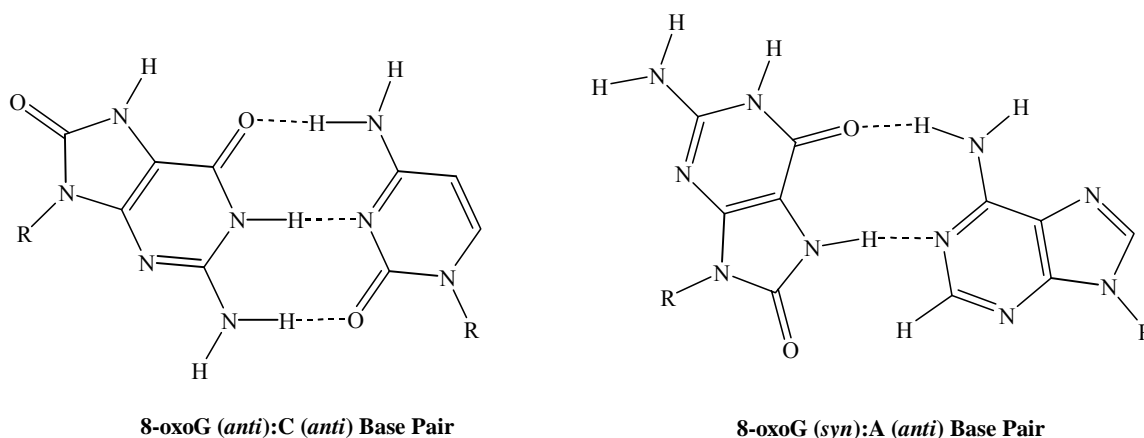


**Figure 4.1b** – An 8-oxoG lesion can be paired with a cytosine or an adenine residue during DNA replication. If the polymerases flip the 8-oxoG lesion into a *syn* conformation, it will be paired with an adenine initiating a G:C → T:A transversion mutation.

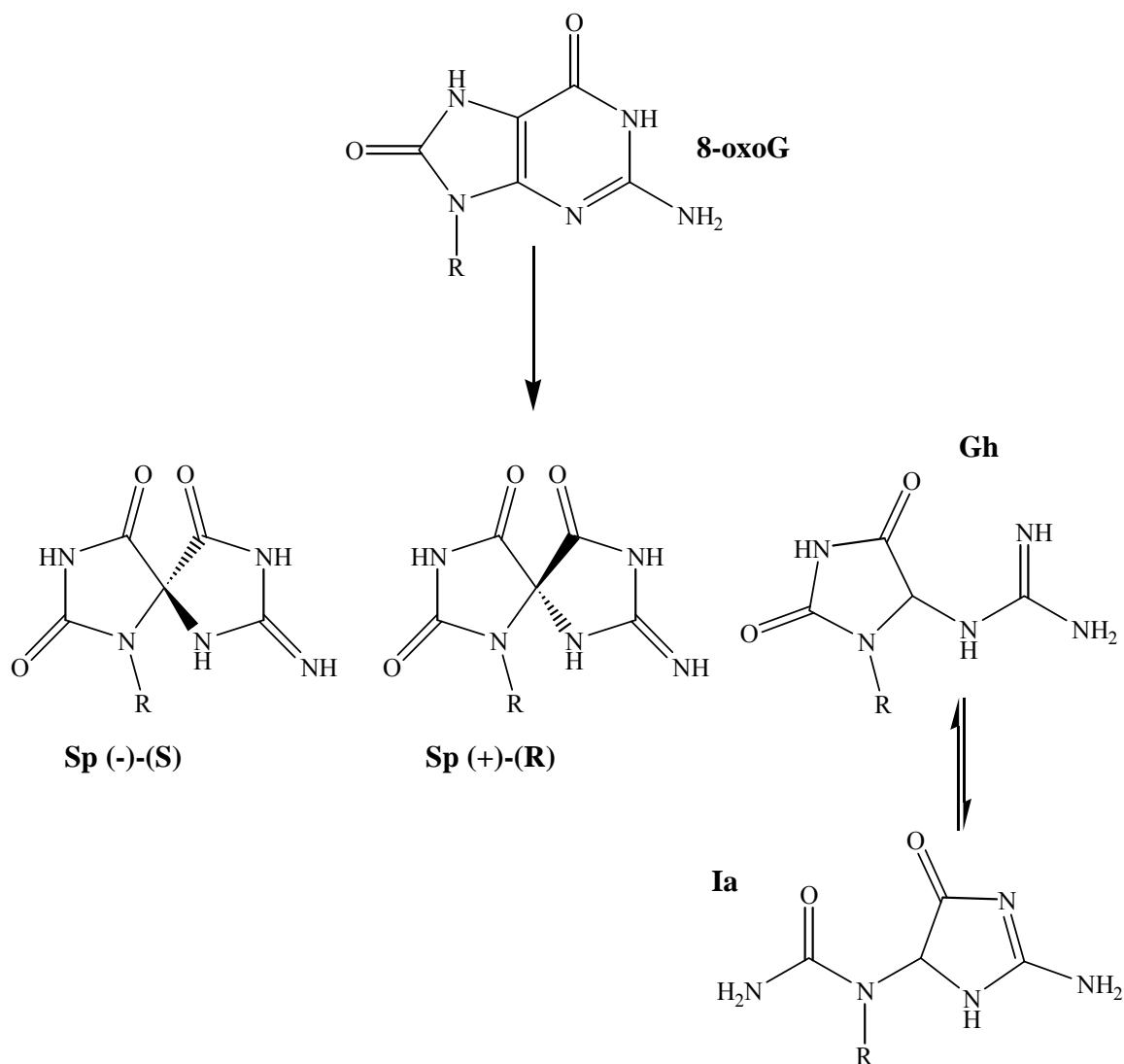


**Figure 4.2** – An 8-oxoG lesion maintains a planar, two-ring structure similar to that of the four natural DNA bases. The Sp lesion maintains a two-ring structure but the ring systems sit at a 90 degree angle to one another and thus disrupt the planar, stacked conformation of duplex DNA. During the formation of an Gh/Ia lesion, one ring opens.

Since repair of Sp is tied to the process of replication, DNA polymerase  $\delta/\epsilon$  will fill in the AP site once the lesion has been excised by NEIL1 and the termini have been processed by PNK<sup>15</sup> or FEN1.<sup>16</sup> Lesions such as 8-oxoG, will be replaced by DNA polymerase  $\beta$  following excision via the SN-BER pathway.<sup>17</sup> Studies have been

conducted with these different polymerases to determine their accuracy in inserting a specific base when the template nucleotide is an unrepaired lesion. It was reported that pol  $\beta$  (the non-replication associated DNA repair polymerase) favored insertion of the correct, dCMP residue across from an 8-oxoG lesion whereas pol  $\delta$  (the replication associated DNA polymerase) favored insertion of dAMP.<sup>18</sup> This study indicated that DNA replication polymerases would be more prone to insertion of point mutations than DNA repair polymerases suggesting that unrepaired lesions such as Sp, would be highly mutagenic when encountered during replication.

NEIL1 deficient murine epithelial cells show reduced sensitivity to chromate and cell cycle aberrations including apoptosis resistance. Without the NEIL1 glycosylase present to excise Sp lesions formed by oxidation of guanine residues by high valent chromium species, the NEIL1 deficient cell line should accumulate point mutations. The level of DNA repair in these cells should be attenuated possibly masking the extent of the damage which was shown to be extensive enough to initiate an apoptotic cascade in NEIL1 proficient cells. Instead of entering an apoptotic pathway, the NEIL1 deficient cells continued to grow and divide even following exposure to chromate concentrations that were far more than 50% lethal for the NEIL1 proficient murine epithelial cell line. We thus anticipated that we would see an accumulation of point mutations in correlation with an accumulation of Sp lesions in the NEIL1 deficient cells. To begin, we analyzed the cells for 8-oxoG levels following chromate exposure. We did not observe a significant difference in the maximal level of accumulated 8-oxoG lesions as expected since the mOGG1 glycosylase was functional in both cell lines. We also analyzed an MCF-7 (human breast cancer cell line) for 8-oxoG accumulation following chromate exposure. This was done as a way to compare the trends observed in our 8-oxoG data with another mammalian cell line with functional *Ogg1* and *Neil1* genes. Accumulation of point mutations was analyzed using an *Hprt* forward mutation assay.

## **4.2 Materials and Methods**

**4.2.1 MCF-7 Cell Line Growth Conditions** MCF-7 cells were purchased from ATCC. Cells were grown in DMEM containing 4.5 g/L D-glucose, L-glutamine,

and 110 mg/L sodium pyruvate (Gibco) which was supplemented with 10% fetal calf serum (HyClone), 1% 100X antibiotic-antimycotic (Gibco), 0.1 mM non-essential amino acids (Gibco), and 10 µg/mL insulin (Sigma, pH 8.2). Cells were maintained at 37° C under an atmosphere of 5% CO<sub>2</sub>.

**4.2.2 Cell Treatment** *Neil1*<sup>+/+</sup> and *Neil1*<sup>-/-</sup> murine kidney epithelial cells as well as MCF-7 cells were exposed to Cr(VI) for 4 hours. The concentrations used for the murine epithelial cell lines were 0, 10, 15, 25, 50 µM in correlation with the toxicity curve obtained for those cell lines. MCF-7 cells were exposed to Cr(VI) at levels of 0, 10, 25 and 50 µM and/or to 100 nM 17β-estradiol (Sigma, E2) levels either alone or in conjunction with Cr(VI) exposure. E2 exposure time was 48 hours with Cr(VI) being applied for the final 4 hours of the treatment period.

**4.2.3 Genomic DNA Extraction** *Neil1*<sup>+/+</sup>, *Neil1*<sup>-/-</sup> epithelial cells and MCF7 cells were washed with 1X PBS and harvested using Trypsin-EDTA as outlined previously. Cell samples were pelleted at 300 x g and the supernatant was discarded. Each 15 mL conical tube was placed on ice followed by the addition of 1 mL of 4° C DNA extraction buffer (0.1 M Tris-HCl, 0.1 M NH<sub>4</sub>Cl, pH 8.0). Cell pellets were mixed thoroughly but gently and were then sonicated for 5 min. in a Branson 3200 sonicating water bath. Cell samples were pelleted at 2400 x g (4° C) for 5 min. and the supernatant was discarded. Pellets were resuspended in 300 µL of DNA extraction buffer containing 33 U of RNase T1 (Sigma) and 200 µg of RNase A (Sigma) and incubated at 37° C for 1 hour. 300 µL of DNA extraction buffer containing 300 µg of Proteinase K (Invitrogen) and 1% SDS was then added. The samples were mixed thoroughly but gently and allowed to incubate for an additional 1 hour at 37° C. 750 µL of concentrated phenol (pH 7.9, Sigma) was then added and each sample was vigorously mixed before the organic and aqueous phases were separated by centrifugation at 2400 x g for 5 min. The supernatant was removed and placed into a fresh 1.5 mL tube, mixed vigorously with 250 µL of a 25:24:1 phenol : chloroform : isoamyl alcohol solution (pH 7.9, EMD), and separated by centrifugation at 12000 x g for 5 min. Again the supernatant was removed and placed into a fresh 1.5 mL tube, mixed vigorously with 250 µL of a 24:1 chloroform :

isoamyl alcohol solution (Sigma), and separated by centrifugation at 12000 x g for 5 min. The supernatant was mixed with 30  $\mu$ L of 10 M ammonium acetate (pH 5.0) and 1 mL of -20° C 100% ethanol in a fresh 1.5 mL tube. Samples were mixed and DNA was allowed to precipitate at -20° C overnight before being pelleted at 12000 x g (4° C) for 15 min. The 100% ethanol was discarded and pellets were washed with 1 mL of -20° C 70% ethanol. DNA was pelleted at 12000 x g (4° C) for 10 min. The 70% ethanol was discarded, residual liquid was dried and the pellet was resuspended in 100  $\mu$ L of deionized water. Absorbance at 260 nm ( $OD_{260}$ ) was obtained for each DNA sample in order to determine the DNA content of each sample.

**4.2.4 DNA Hydrolysis** DNA samples were denatured by heating to 95° C for 5 min. followed by flash cooling on ice for 3 min. Within one minute of being placed on ice, 0.1 U of phosphodiesterase II (Worthington Biochemicals) prepared in deionized water was added to each DNA sample. Samples were allowed to incubate at 37° C for 45 min. Addition of phosphodiesterase II and incubation at 37° C for 45 min. was repeated. 0.5 U of phosphodiesterase I (Worthington Biochemicals) buffered in 10 mM Tris-HCl, 10 mM  $NH_4Cl$ , 1.5 mM  $MgCl$ , pH 8.9 was added to each sample and they were allowed to incubate for 45 min. at 37° C. Addition of phosphodiesterase I followed by incubation at 37° C for 45 min. was repeated. 5 U of calf intestinal phosphatase (Promega) buffered in 50 mM Tris-HCl, 1 mM  $MgCl_2$ , 0.1 mM  $ZnCl_2$ , 1 mM spermidine, pH 9.3 was added to each sample and they were allowed to incubate for 45 min. at 37° C. Addition of calf intestinal phosphatase followed by incubation at 37° C for 45 min. was repeated. Samples were cleaned up in YM-30 centrifugal filters (Microcon) by centrifugation at 2500 x g for 25 min. Samples were stored at -80° C until analysis.

**4.2.5 8-oxoG Quantification** 8-oxoG lesions were quantified and reported as values relative to the amount of guanine present in each hydrolyzed DNA sample. Hydrolyzed DNA samples were analyzed using an Agilent 1200 series HPLC coupled with diode array detection for guanine quantification. Samples were separated using an Agilent C18 4.6 mm x 100 mm column, with an isocratic mobile phase of 100 mM ammonium acetate (pH 5.2) and 4% methanol at a flow rate of 1 mL/min. A calibration

curve for guanine was generated from standards of dG ranging from 125 ng to 2500 ng. The dG content of the hydrolyzed DNA samples was calculated by comparing dG peak areas from 25  $\mu$ L aliquots of hydrolyzed samples to the calibration curve. Separated DNA was then further analyzed using an ESA CoulArray electrochemical detector. Hydrolyzed DNA was subjected to four different voltages (50, 100, 150, 300 V) as it passed across a model 6210 ESA electrical cell. 8-oxoG was oxidized in the 300 V channel. A calibration curve for 8-oxoG was generated from standards of 8-oxoG ranging from 25 pg to 625 pg. The 8-oxoG content of the hydrolyzed DNA samples was calculated by comparing 8-oxoG peak areas from 25  $\mu$ L aliquots of hydrolyzed samples to the calibration curve.

**4.2.6 Hprt Mutation Analysis** Resistance to 6-thioguanine (Sigma, 6-TG) was assessed in both the *Neill*<sup>+/+</sup> and *Neill*<sup>-/-</sup> cell lines using a fluorescence 96-well plate assay. Cells were seeded in 96-well plates at a density of  $1 \times 10^4$  cells/mL and allowed to recover for 48 hours before being treated with 6-TG. Media was removed from the 96-well plates and 6-TG solutions were added with the final concentrations of 6-TG being 0, 5, 10, 20, 30, 40, 50, 60, 70 and 80  $\mu$ g/mL. Plates were allowed to incubate for 24 hours. 6-TG solutions were removed and each plate was then rinsed with 1X PBS. CellTiter-Blue (Promega) was mixed with complete media to form a 10% CellTiter-Blue solution. 200  $\mu$ L of this solution was added to each well in the 96-well plates. Plates were allowed to incubate in the CellTiter-Blue solution for 22 hours at which time fluorescence at 585 nm (excitation at 555 nm and cut-off at 570 nm) was measured using a SpectraMax M2<sup>e</sup> Molecular Devices fluorescent plate reader.

$1 \times 10^6$  of cells from each cell line were seeded in 75 cm<sup>2</sup> flasks and allowed to recover for 24 hours. Cells were dosed with chromate for 24 hours (0, 5, 10, 20, 30 and 50  $\mu$ M). Flasks were then washed with 1X PBS, refreshed with complete chromate-free media and allowed to recover for 5 days.  $1 \times 10^6$  cells from each cell line and treatment level were seeded in 25 cm<sup>2</sup> flasks. Complete media was supplemented with 20  $\mu$ g/mL 6-TG. Media, supplemented with 6-TG, was refreshed every 3-4 days. Cells were allowed to incubate for 7 days or until colonies had formed. Media was then aspirated and cells were incubated in a 2% methylene blue solution (100 mg methylene blue (Sigma)

prepared in 50 mL of 50% ethanol) for five minutes. The methylene blue solution was rinsed with deionized water and colonies were counted. Following recovery from chromate treatment, *NeiI*<sup>+/+</sup> and *NeiI*<sup>-/-</sup> cells were also seeded in 60 mm dishes at a density of 400 cells/plate to monitor plating efficiencies. These cells were also allowed to incubate for 7 days or until colonies had formed at which time they were stained with 2% methylene blue and counted.

### **4.3 Results**

**4.3.1 8-oxoG Quantification** Hydrolyzed DNA samples from both the *NeiI*<sup>+/+</sup> and the *NeiI*<sup>-/-</sup> cell lines were analyzed by diode array for guanine content (Figures 4.3 and 4.4) and electrochemical detection for 8-oxoG content (Figure 4.5) following exposure to chromate for 4 hours. Guanine and 8-oxoG content were quantified by measuring peak area and comparing those values to a standard curve. New guanine and 8-oxoG standards were analyzed prior to each analysis of the hydrolyzed DNA if all samples could not be run in a single session.

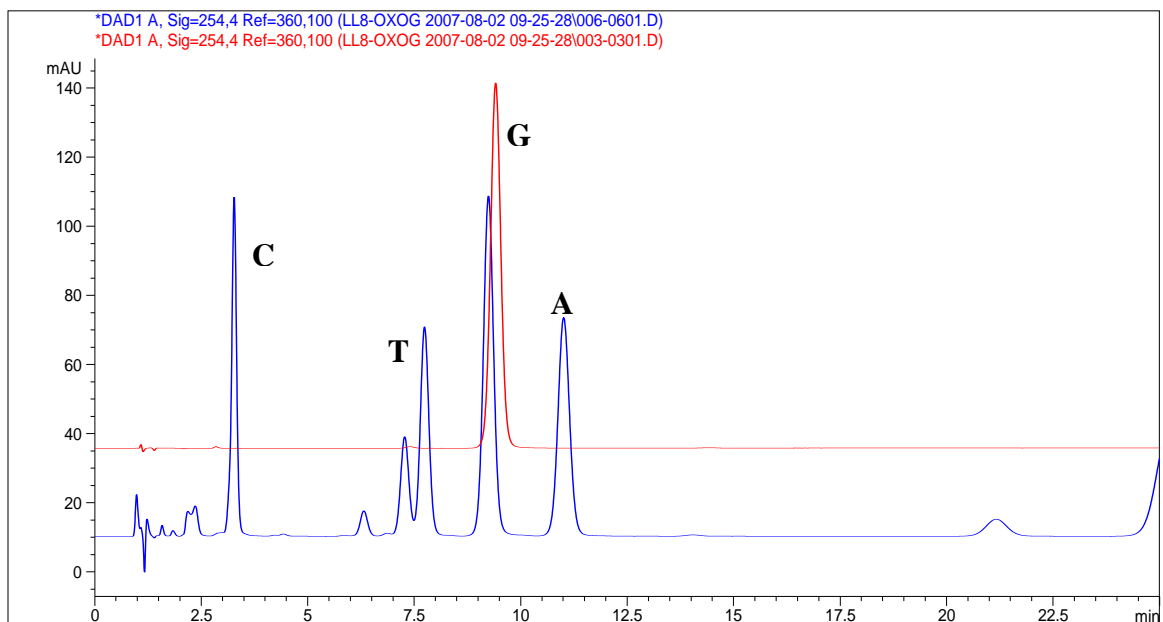


**Figure 4.3** – HPLC traces from a guanine standard (upper trace) and a digested DNA sample (lower trace). Guanine eluted at approximately 8.5 min. in both samples. All four DNA bases were visible in the digested DNA sample trace indicating that the DNA hydrolysis was effective.

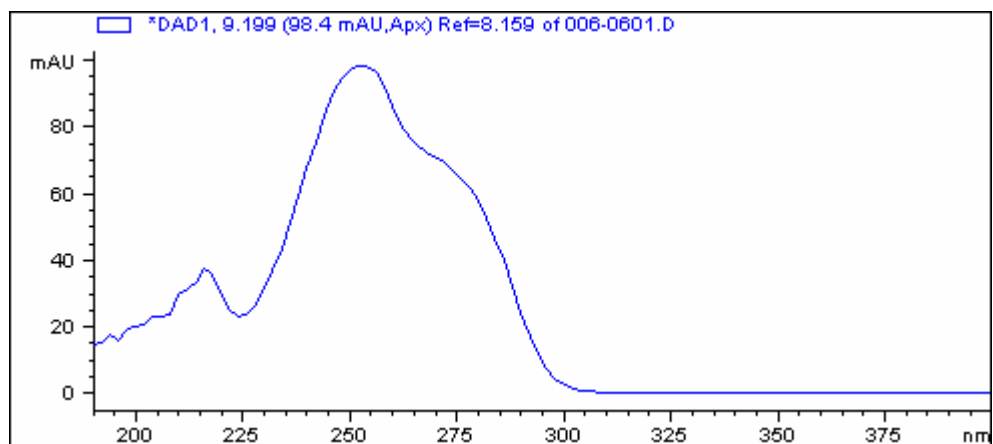


**Figure 4.4** – Guanine was identified by its characteristic ultraviolet absorbance spectrum.

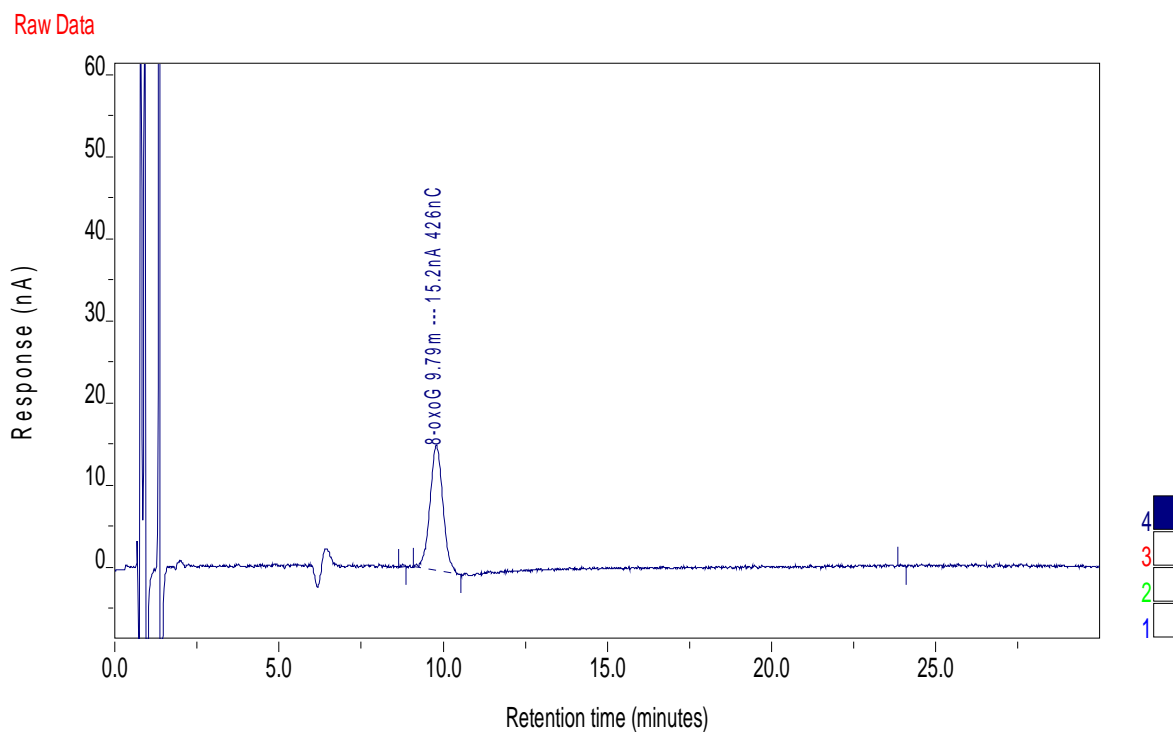


**Figure 4.5** – 8-oxoG elutes at 10 min. in channel 4. 8-oxoG is oxidized only in channel 4 of the electric cell at 300 V.

Both cell lines showed an initial increase in the number of 8-oxoG lesions present relative to the total number of guanine residues in each sample as compared to levels of 8-oxoG observed in the control samples. This increase was seen in the *Neil1*<sup>+/+</sup> cell line only between the untreated samples and the samples dosed with 10  $\mu$ M chromate. The levels of 8-oxoG in NEIL1 proficient cells dropped back to a level equivalent with that seen in the untreated samples following exposure to 15, 25, and 50  $\mu$ M chromate concentrations. The increase in the relative level of 8-oxoG lesions present in the *Neil1*<sup>-/-</sup> cell line increased in a dose dependent fashion over the untreated sample values following exposure to both 10 and 15  $\mu$ M chromate concentrations. After exposure to a 25  $\mu$ M chromate solution, the 8-oxoG levels in the NEIL1 deficient cell line fell from the level seen in the samples dosed with 15  $\mu$ M chromate. 8-oxoG levels in the NEIL1 deficient cell line also returned to a level equivalent to that observed in the untreated samples but only after being exposed to a 50  $\mu$ M chromate solution. There was no significant

difference observed in the maximum level of accumulated 8-oxoG lesions between the two epithelial cell lines. This data is presented in figure 4.6.

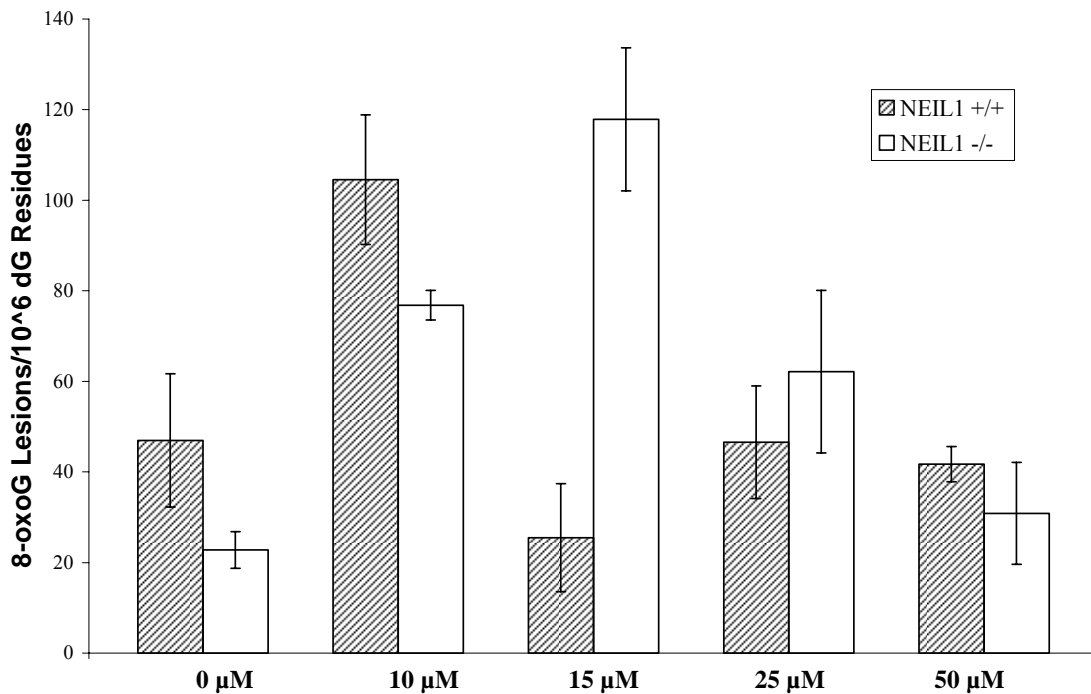


**Figure 4.6** – 8-oxoG lesions relative to the total number of guanine residues present in hydrolyzed DNA samples from NEIL1 epithelial cell lines exposed to chromate for 4 hours. Both cell lines show an initial, dose dependent increase in the level of 8-oxoG lesions present but that increase is followed by a decrease back to levels equivalent to those observed in the untreated samples. For each data point reported, n = 3-5 observations.

Hydrolyzed DNA from MCF-7 cells dosed with chromate and/or E2 were also analyzed by electrochemical detection. E2 is a female hormone that has been shown to induce ROS production in cells and to cause breast cancer development.<sup>19,20</sup> The MCF-7 DNA samples demonstrated a similar trend in 8-oxoG levels relative to total guanine residues as was seen in the NEIL1 DNA samples. Following exposure to chromate alone, 8-oxoG levels in the MCF-7 cells increased initially (10 μM chromate dose) relative to

the level seen in untreated samples. The 8-oxoG levels then decreased following exposure to 25 and 50  $\mu\text{M}$  chromate concentrations. Samples dosed with E2 alone developed higher 8-oxoG levels than untreated samples. The levels following E2 exposure were equivalent to those observed in samples dosed with 25 and 50  $\mu\text{M}$  chromate alone. Treating MCF-7 cells with both chromate and E2 caused a steep drop off in the level of 8-oxoG lesions present. 8-oxoG levels in samples dosed with 100 nM E2 and 15  $\mu\text{M}$  chromate fell below the level of 8-oxoG lesions observed in untreated samples. This data is shown in figure 4.7.

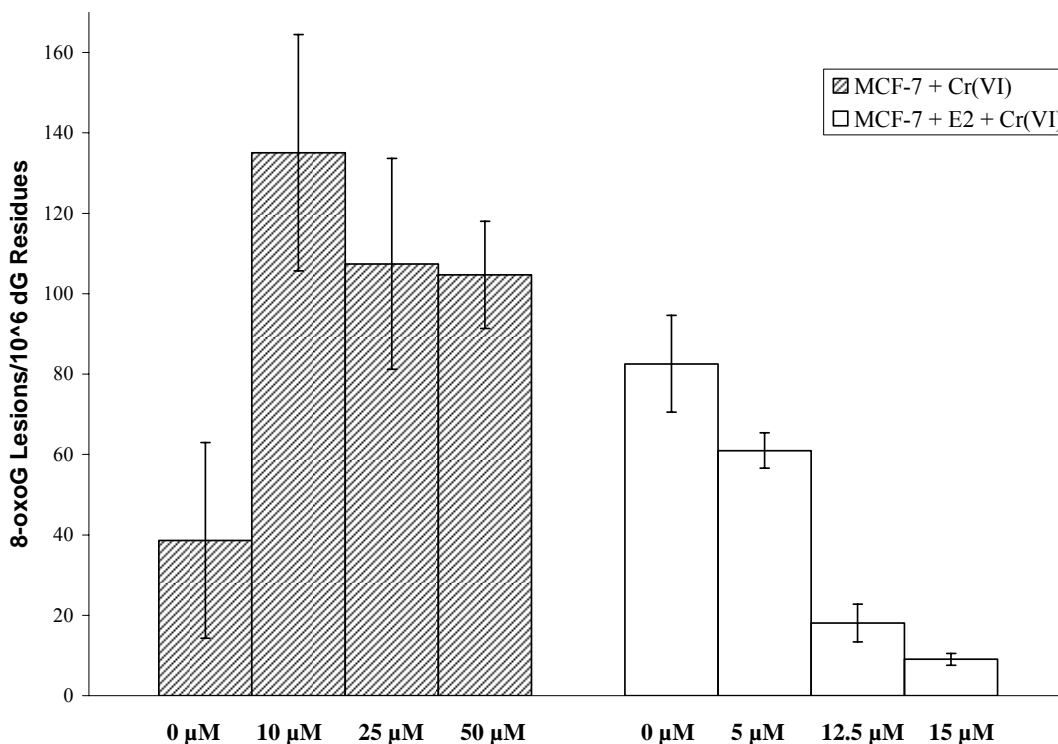


**Figure 4.7** – 8-oxoG lesions relative to the total number of guanine residues present in hydrolyzed DNA samples from MCF-7 cells exposed to chromate for 4 hours and/or E2 for 48 hours. 8-oxoG levels increase relative to those seen in untreated samples following exposure to a 10  $\mu\text{M}$  chromate solution and after exposure to E2 alone. The levels of 8-oxoG drop off dramatically following exposure to both chromate and E2 to levels lower than that observed in the untreated samples. For each data point reported,  $n = 3-4$  observations.

**4.3.2 *Hprt* Mutation Assay** Chromate treated cells from both the *Neil1*<sup>+/+</sup> and *Neil1*<sup>-/-</sup> cell lines were allowed to recover for 5 days in chromate-free complete media before being seeded in 60 mm dishes at a density of 400 cells per dish to assess plating efficiency. These cells were maintained in 6-TG-free media for 6 days at which time colonies had formed. Colonies were then stained and counted. The untreated cells from both the NEIL1 proficient and deficient cell lines formed equivalent numbers of colonies after 6 days (Figure 4.8a). This was followed by a slight increase in cell colony formation in both cell lines for cells exposed to 5  $\mu$ M chromate. The *Neil1*<sup>+/+</sup> dishes then showed a steady decrease in the number of colonies forming in conjunction with chromate treatment concentrations of 10, 20, 30, and 50  $\mu$ M. The *Neil1*<sup>-/-</sup> cell dishes showed a slight decrease in colony formation at the 10  $\mu$ M treatment level but then a significant increase in colony formation at the 20 and 30  $\mu$ M treatment levels. Colony numbers fell back to the level observed in the untreated *Neil1*<sup>-/-</sup> dishes for cells treated with 50  $\mu$ M chromate. The same trends presented themselves when colony formation was represented as a percentage of colonies in the control dishes (Figure 4.8b). Error in this data was quite high because of the small number of colonies that formed in the dishes.

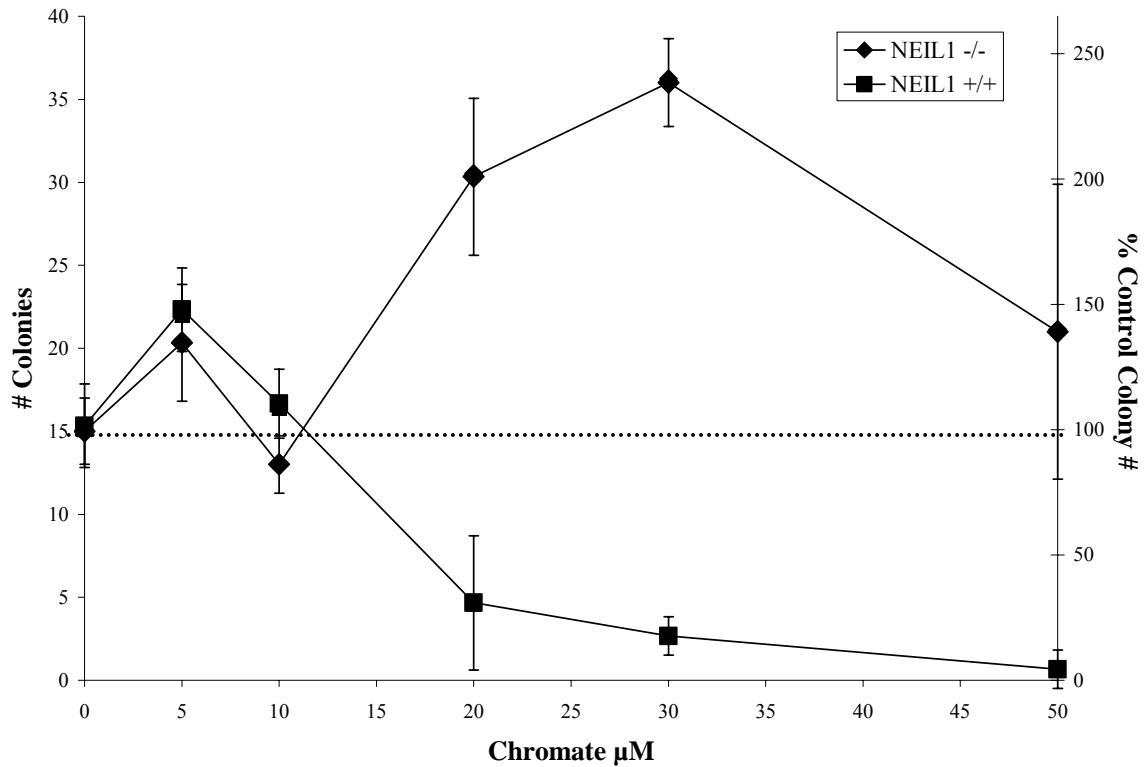


**Figure 4.8** – A similar number of colonies were counted in dishes containing untreated *NeilI*<sup>+/+</sup> and *NeilI*<sup>-/-</sup> cells. Cell growth was initially stimulated in both cell lines at the 5  $\mu\text{M}$  chromate treatment level but then steadily declined for the *NeilI*<sup>+/+</sup> cell line. Growth continued to be stimulated by chromate exposure in the *NeilI*<sup>-/-</sup> cell line through the 30  $\mu\text{M}$  chromate treatment level with colony formation dropping back to near control levels following exposure to 50  $\mu\text{M}$  chromate.

Mutation accumulation in the *Hprt* gene was assessed by seeding  $1 \times 10^6$  cells in 25  $\text{cm}^2$  culture flasks for both the *NeilI*<sup>+/+</sup> and *NeilI*<sup>-/-</sup> cell lines following chromate treatment and a 5 day recovery period. These cells were then maintained for 7 days in media supplemented with 20  $\mu\text{g}/\text{ml}$  6-TG. In order for cells to grow and form colonies in the presence of 6-TG, they must have first developed mutations in the *Hprt* gene. No quantitative data was able to be obtained for comparisons between the *NeilI*<sup>+/+</sup> and *NeilI*<sup>-/-</sup> cell lines in this assay but some qualitative observations could be made. No colonies formed in any of the *NeilI*<sup>+/+</sup> culture flasks (Figure 4.9a) indicating that 6-TG was toxic to these cells even following exposure to chromate. Colonies did form in flasks

seeded with *NeilI*<sup>-/-</sup> cells exposed to 0, 5, 10 and 20 μM chromate (Figure 4.9a-B). Colonies did not form in flasks seeded with *NeilI*<sup>-/-</sup> cells dosed with 30 and 50 μM chromate, instead the cells grew to confluence (Figure 4.9b). Since colonies did form in the *NeilI*<sup>-/-</sup> culture flasks dosed with 0, 5, 10, and 20 μM chromate, a quantitative trend in colony number could be presented graphically (Figure 4.10). Colony formation initially increased for flasks at the 5 μM chromate exposure level but then fell back to control values by the 20 μM chromate exposure level.

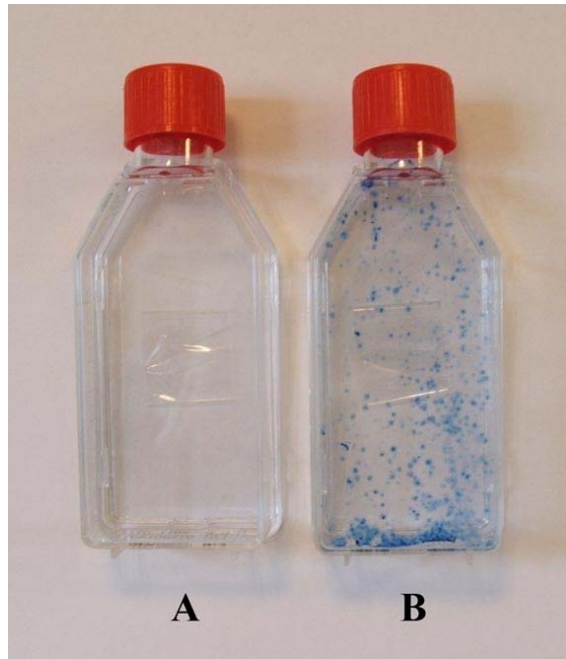


**Figure 4.9a** – Differences in colony formation between (A) *NeilI*<sup>+/+</sup> and (B) *NeilI*<sup>-/-</sup> cells. Both flasks were seeded with  $1 \times 10^6$  cells that had not been exposed to chromate and were then grown in media supplemented with 20 μg/ml 6-TG for 7 days. *NeilI*<sup>+/+</sup> culture flasks looked identical for all chromate exposure levels.

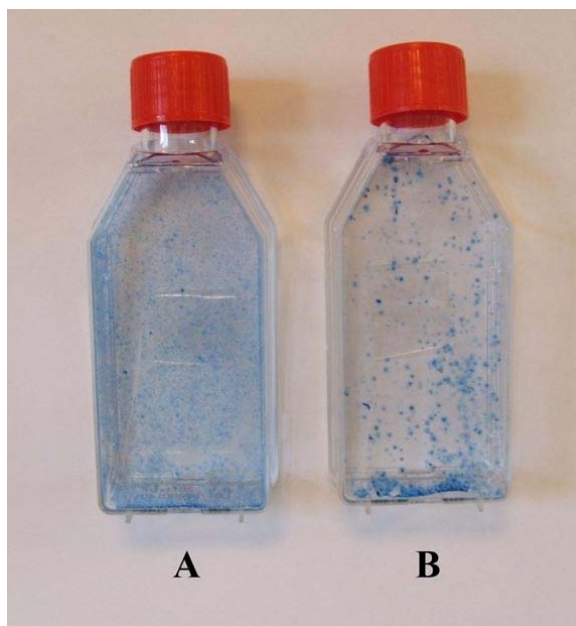


**Figure 4.9b** – Differences in colony formation between (A) *NeiI*<sup>-/-</sup> cells dosed with 30  $\mu$ M chromate and (B) *NeiI*<sup>-/-</sup> untreated cells. Both flasks were seeded with  $1 \times 10^6$  cells and grown in media supplemented with 20  $\mu$ g/ml 6-TG for 7 days. *NeiI*<sup>-/-</sup> culture flasks for the 0, 5, 10, and 20  $\mu$ M chromate exposure levels looked similar to (B) but with varying numbers of colonies present. *NeiI*<sup>-/-</sup> culture flasks for the 30 and 50  $\mu$ M chromate exposure levels looked identical to (A).

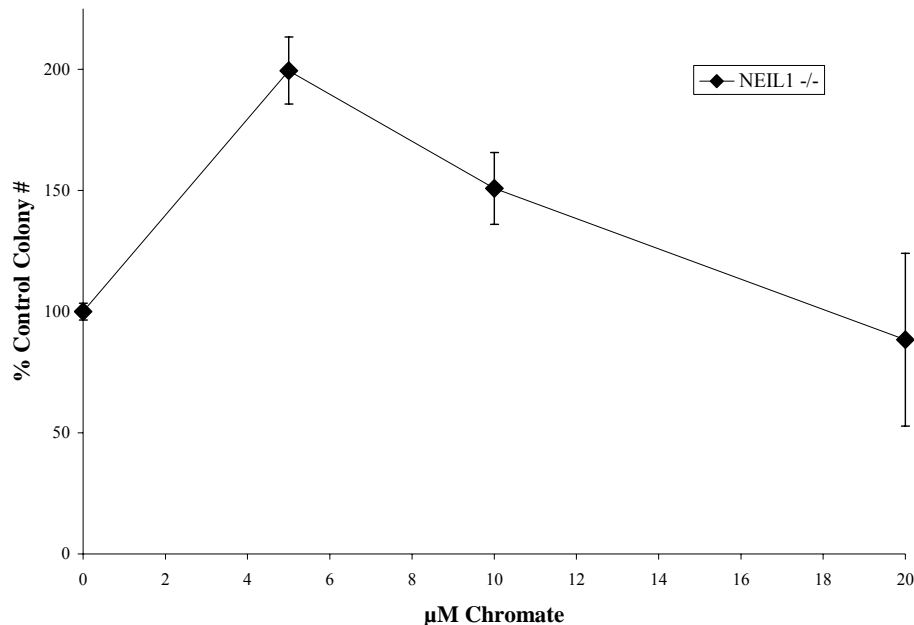


**Figure 4.10** – Colony formation trends for the *Neil1*<sup>-/-</sup> cell line maintained in media supplemented with 20 µg/ml 6-TG for 7 days following treatment with chromate. Colony numbers increase over control levels at the 5 µM chromate exposure level and then began to fall back to control values by the 20 µM chromate exposure level.

#### 4.4 Discussion

**4.4.1 Formation and Detection of Further Oxidized Lesions** In studies conducted in *E. coli*, Sp lesions, but not 8-oxoG lesion, were observed to accumulate in an *Nei* deficient *E. coli* strain.<sup>21</sup> Based on that information, we hypothesized that a NEIL1 deficient mammalian cell line would also accumulate large amounts of Sp following exposure to chromate. Mammalian cells however, unlike *E. coli* used in previous studies, have three variants of the *Nei* repair protein, NEIL1, NEIL2, and NEIL3.<sup>9,10,22</sup> A separate study has demonstrated that NEIL2 has the ability to excise Sp lesions *in vitro* as it was capable of cleaving Sp from single-stranded oligonucleotides.<sup>8</sup> Therefore, while we anticipated that NEIL1 deficient murine epithelial cells would accumulate Sp lesions, we also hypothesized that the accumulation may not occur at such pronounced levels as was seen in *Nei* deficient *E. coli*. as the NEIL1 deficient cell line maintains two functional *Neil2* alleles.

Sp lesions from *E. coli* DNA were quantified using a Waters 2790 HPLC coupled to a Micromass LCT mass spectrometer with electrospray ionization.<sup>21</sup> Unfortunately this analysis method was not effective for the NEIL1 epithelial cell lines. Several problems arose that prevented Sp quantification in these cell lines. The Waters mass spectrometer system was a core instrument and as such carried a wide variety of low level contaminants from polymers and buffers that had been run through the system. In order to detect Sp in DNA samples, a level of sensitivity in the 1 pmol range had to be reached. These low levels of Sp were essentially undetectable when contaminants such as high levels of salts were ionized along with the DNA samples. Another problem with this detection set-up was that a C18 reverse phase Microsorb 2.1 mm x 250 mm column was used for separation of the DNA bases prior to ionization in the mass spectrometer. Sp is a highly polar molecule and therefore does not interact strongly with a C18 matrix causing it to elute rapidly, often so quickly that it emerged in the buffer front. Another hurdle was obtaining large enough quantities of DNA from the epithelial cells for analysis. The ability to grow vast amounts of *E. coli* in just 24 hours makes it much easier to obtain large quantities of DNA than when one is working with mammalian cells that may take 5 days to reach confluence. Low amounts of DNA combined with the inherent problems with the mass spectrometer and the C18 column, prevented detection of Sp above background using the method previously employed for Sp detection.

Methods are being developed using a dedicated Agilent LC/MSD Trap XCT mass spectrometer coupled to an Agilent 1200 series HPLC to improve detection limits for Sp and Gh lesions in genomic DNA and decreased interference from contaminants within the system. The new methods being developed also use a Thermo Hypercarb 4.6 mm x 150 mm column for HPLC separation prior to analysis by ion trap mass spectrometry. Retention times for Sp on the C18 reverse phase Microsorb column were between 5 and 7 minutes but on the Thermo Hypercarb column, Sp does not elute until 15 minutes for the (-) isomer and 25 minutes for the (+) isomer (Figure 4.11a). A mobile phase gradient was employed over 21 minutes from 99% mobile phase A (deionized water + 0.1% acetic acid) and 1% mobile phase B (methanol) to 100% mobile phase B at a constant flow rate of 0.9 ml/min. We are also now able to conduct MS/MS analysis of the 300 molecular

weight ion associated with the Sp nucleoside in order to monitor the 184 molecular weight ion associated with the Sp free base (Figure 4.11b and 4.12).

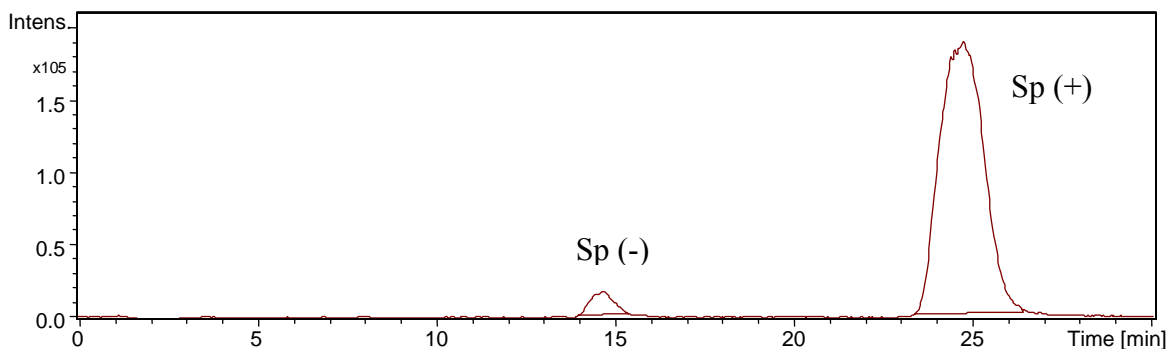


**Figure 4.11a** – Sp isomers from a single stranded oligonucleotide oxidized with Cr(V)-Salen. These isomers were separated and detected on an Agilent LC/MSD Trap XCT mass spectrometer. The Sp (+) appears to be the dominant species formed in single stranded oligonucleotides and in MCF-7 DNA digests.

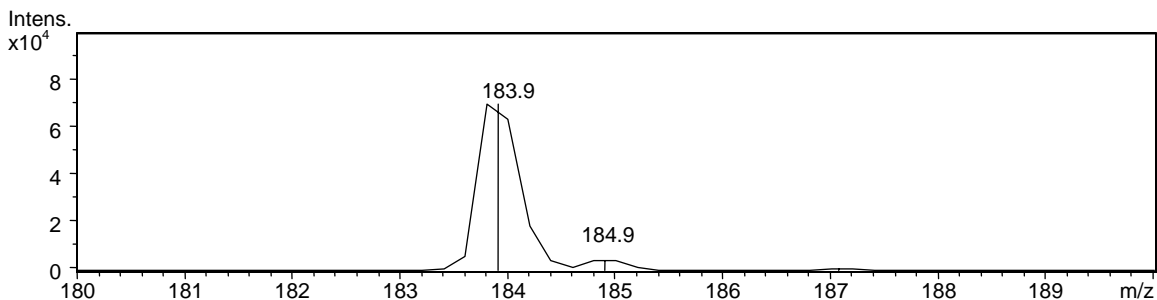


**Figure 4.11b** – The Sp isomer peaks from (a) both represent ions with a mass to charge ratio of 184. This 184 mass peak generated by free Sp base was obtained by splitting the 300 mass peak that is generated as the Sp nucleoside moves into the ion trap.

Some initial analysis have shown that Sp is present at levels above background in hydrolyzed DNA samples from MCF-7 cells exposed to chromate and E2. Hydrolyzed DNA samples from MCF-7 cells were used to look for Sp in our initial ion trap mass spectrometry trials for several reasons. First, these cells grow rapidly making it much easier to obtain large amounts of genomic DNA than from the much slower growing

NEIL1 epithelial cell lines. Secondly, a recent report looking at 8-oxoG metabolism in MCF-7 cells showed that further oxidized lesions may have been present in MCF-7 cells dosed with E2.<sup>23</sup> Following exposure to E2, hydrolyzed DNA samples from MCF-7 cells were analyzed using HPLC- accelerator mass spectrometry (AMS) and five peaks eluted that could not be attributed to 8-oxoG or any of the four natural DNA bases<sup>23</sup> indicating that further oxidized lesions such as Sp may have been forming. Of the Sp detected in our MCF-7 digests, the Sp(+) isomer appears to be the dominant species present. The Sp(+) isomer also appears to be the dominant species formed in oligonucleotides containing an 8-oxoG lesion that have been oxidized with Cr(V)-Salen or with Na<sub>2</sub>IrCl<sub>6</sub> (Figure 4.11a). This new system for Sp analysis has yet to be applied to DNA digests from the NEIL1 cell lines but we are hopeful that this system will be effective for detecting Sp at the 1 pmol level.

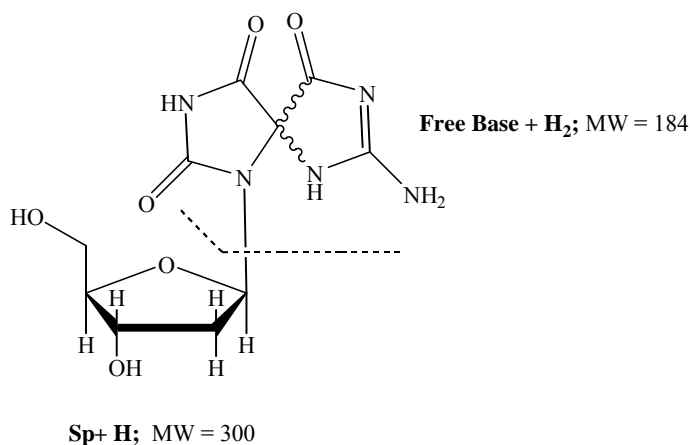


**Figure 4.12** – Mass profile of the Sp nucleoside and the free base.

**4.4.2 Implications of the *Hprt* Mutation Assay** The basis for detecting mutations in an *Hprt* mutation assay is resistance to the mutagen 6-TG. Under normal conditions, a cell that is exposed to 6-TG will produce functional copies of hypoxanthine-

guanine phosphoribosyl transferase (HPRT) which will metabolize 6-TG into a highly toxic mutagen.<sup>24</sup> As the number of mutations that a cell develops in the *Hprt* gene increases, so do the chances that a non-functional HPRT protein will be produced and resistance to 6-TG will ensue as 6-TG will not be metabolized. For this study, our hypothesis was that the *Neil1*<sup>-/-</sup> murine epithelial cells should accumulate mutations following exposure to chromate as compared to the *Neil1*<sup>+/+</sup> cell line because they have an attenuated ability to repair the oxidative lesion Sp. Therefore, we expected that *Neil1*<sup>-/-</sup> cells exposed to chromate and then allowed to undergo several rounds of replication would show an increased resistance to 6-TG as compared to their wild type counterpart.

In order to evaluate whether or not differences in colony formation for the *Neil1*<sup>+/+</sup> versus the *Neil1*<sup>-/-</sup> cell lines were caused solely by exposure to 6-TG, cells from both lines and at all chromate treatment levels needed to be plated in 6-TG-free media to simultaneously assess plating efficiencies. Figure 4.8a-b shows that untreated *Neil1*<sup>+/+</sup> and *Neil1*<sup>-/-</sup> cells both form similar numbers of colonies when seeded at a density of 400 cells per 60 mm culture dish and allowed to incubate in 6-TG-free media for 6 days. However, exposure to chromate appears to stimulate the growth of the *Neil1*<sup>-/-</sup> cells whereas it attenuates growth in the *Neil1*<sup>+/+</sup> cell line. A second control used in this experiment was the determination of 6-TG toxicity in both the NEIL1 cell lines. Using the same CellTiter-Blue fluorescence assay described in chapter 3, NEIL1 cells were dosed with 6-TG for 24 hours to determine a 50% toxicity level. Both cell lines reached a level of approximately 50% toxicity at a treatment level of 20 µg/ml 6-TG. One drawback to this toxicity assay however, was that it only assessed toxicity on a very short time scale. It did not show whether or not cells would be able to actively replicate following treatment with 6-TG but it provided a good starting point for this particular assay.

Figure 4.9a showed that untreated *Neil1*<sup>+/+</sup> cells were unable to survive over a longer time frame (7 days) when exposed to 6-TG at a level of 20 µg/ml. The untreated *Neil1*<sup>-/-</sup> cells however, appeared to thrive despite the addition of 6-TG to the media and despite the fact that they had a nearly identical plating efficiency as the *Neil1*<sup>+/+</sup> cells. This indicated that the *Neil1*<sup>-/-</sup> cells may accumulate mutations endogenously even in the absence chromate treatment. There are a large number of oxidants that routinely bombard

DNA but the resulting low level of oxidative lesions would be excised and repaired in a normal cellular system. The *NeiI*<sup>-/-</sup> cell line does not have a complete base excision repair system since the *NeiI* gene has been interrupted so it may accumulate some oxidative lesions even when not oxidatively stressed with chromate.

Figure 4.10 showed that colony formation actually increased over control levels for the *NeiI*<sup>-/-</sup> cells grown in 6-TG following exposure to increasing concentrations of chromate. It is difficult to say that this increased growth is solely due to increased 6-TG resistance because exposure to chromate actually stimulated cell growth as shown in figure 4.8a-b. Some of the increase in colony formation may be attributed to 6-TG though, based on the change in growth patterns observed for the 30 and 50  $\mu$ M chromate treatment levels as shown in figure 4.9b. The *NeiI*<sup>-/-</sup> culture flasks for the 0-20  $\mu$ M chromate treatment levels formed colonies in the presence of 6-TG as is typically observed when cells are plated at very low densities in mutagen-free media. Those flasks for the 30 and 50  $\mu$ M chromate treatment levels showed cells growing to confluence in the presence of 6-TG as is typically observed when cells are plated at much higher densities in mutagen-free media. This qualitative observation makes it appear as though the *NeiI*<sup>-/-</sup> cells dosed with the highest chromate concentrations are growing significantly better than those dosed with lower chromate concentrations. Plating efficiencies show that growth fell back to control levels after a 50  $\mu$ M chromate treatment but the 6-TG assay indicated that growth in flasks for the 50  $\mu$ M chromate treatment level were still growing better than those at the 20  $\mu$ M or lower chromate treatment levels.

The striking differences in 6-TG toxicity between the two NEIL1 cell lines will make it difficult to use a colony formation approach to compare mutation accumulation in the two cell lines. This assay could be repeated using lower 6-TG concentrations in order to allow colonies to form in the NEIL1 proficient flasks, but this approach will likely lead to overgrowth of the *NeiI*<sup>-/-</sup> cells. Another approach would be to treat the two cell lines with different 6-TG concentrations. However, the best way to move forward from this point would most likely be to sequence the *Hprt* gene in both cell lines and look for changes in mutation levels following exposure to chromate and selective growth in the presence of 6-TG. We would expect to see a high number of mutations at guanine residues following exposure to chromate. This approach would also determine whether or

not *Nei1*<sup>-/-</sup> cells accumulate mutations even under conditions that should not oxidatively stress the cells. However, we would anticipate that these mutations would not be concentrated specifically at guanine residues.

#### **4.5 Conclusions**

The *Nei1*<sup>-/-</sup> cell line has demonstrated a vastly different response to chromate than its wild type counterpart. Chromate is less toxic to the *Nei1*<sup>-/-</sup> cells despite the fact that they appear to retain some ability to excise Sp (potentially via a NEIL2 pathway). In addition, chromate also stimulates growth in the NEIL1 deficient cell line and can even induce apoptosis resistance. Levels of 8-oxoG are not significantly higher in the *Nei1*<sup>-/-</sup> cell line following chromate treatment so it stands to reason that the affects that we have observed may be linked to further oxidized products. More specifically, further oxidized base lesions since the only part of the genome that has been altered in the *Nei1*<sup>-/-</sup> cells is a single gene that codes for a BER glycosylase specifically designed for removal of oxidized nucleobase lesions. Mutation accumulation should also be assessed in a more specific manner. Sequencing the *Hprt* gene to quantify mutations at guanines would provide the most conclusive data on this point. In the big picture, developing a better understanding of the role that NEIL1 plays in protecting a cell from oxidative damage induced by chromate exposure has the potential to play an important part in preventing cancer formation in humans. We could use our knowledge about NEIL1 to develop biomarkers to identify people at high risk and advise them against working in a field where chromate exposure is unavoidable. A better understanding of how chromate can induce cancer will also be important as this information would aid in the search for better ways to treat those already affected by chromate induced lung carcinomas.

## References

1. Dou, H., Theriot, C.A., Das, A., Hegde, M.L., Matsumoto, Y., Boldogh, I., Hazra, T.K., Bhakat, K.K., Mitra, S. (2008) Interaction of the human DNA glycosylase NEIL1 with proliferating cell nuclear antigen. *J. Biol. Chem.* 283, 3130-3140.
2. Grollman, A.P., Moriya, M. (1993) Mutagenesis by 8-oxoguanine: an enemy within. *Trends Genet.* 9, 246-249.
3. Wood, M.L. Esteve, A., Morningstar, M.L., Kuziemko, G.M., Essigmann, J.M. (1992) Genetic effects of oxidative DNA damage: comparative mutagenesis of 7,8-dihydro-8-oxoguanine and 7,8-dihydro-8-oxoadenine in *Escherichia coli*. *Nucleic Acids Res.* 20, 6023-6032.
4. Henderson, P.T., Delaney, J.C., Muller, J.G., Neeley, W.L., Tannenbaum, S.R., Burrows, C.J., Essigmann, J.M. (2003) *Biochemistry.* 42, 9257-9262.
5. Duarte, V., Muller, J.G., Burrows, C.J. (1999) Insertion of dGMP and dAMP during *in vitro* DNA synthesis opposite an oxidized form of 7,8-dihydro-8-oxoguanine. *Nucleic Acids Res.* 27, 496-502.
6. Korniyushyna, O., Berges, A.M., Muller, J.G., Burrows, C.J. (2002) In vitro nucleotide misinsertion opposite the oxidized guanosine lesions spiroiminodihydantoin and guanidinohydantoin and DNA synthesis past the lesions using *Escherichia coli* DNA polymerase I (Klenow Fragment). *Biochemistry* 41, 15304-15314.
7. Korniyushyna, O., Burrows, C.J. (2003) Effect of the oxidized guanosine lesions spiroiminodihydantoin and guanidinohydantoin on proofreading by *Escherichia coli* DNA polymerase I (Klenow Fragment) in different sequence contexts. *Biochemistry* 42, 13008-13018.

8. Hailer, M.K., Slade, P.G., Martin, B.D., Rosenquist, T.A., Sugden, K.D. (2005) Recognition of the oxidized lesions spiroiminodihydroantoin and guanidinohydroantoin in DNA by the mammalian base excision repair glycosylases NEIL1 and NEIL2. *DNA Repair* 4, 41-50.
9. Hazra, T.K., Kow, Y.W., Hatahet, Z., Imhoff, B., Boldogh, I., Mokkalapati, S.K., Mitra, S., Izumi, T. (2002) Identification and characterization of a novel human DNA glycosylase for repair of cytosine-derived lesions. *J. Biol. Chem.* 277, 30417-30420.
10. Hazra, T.K., Izumi, T., Boldogh, I., Imhoff, B., Kow, Y.W., Jaruga, P., Dizdaroğlu, M., Mitra, S. (2002) Identification and characterization of a human DNA glycosylase for repair of modified bases in oxidatively damaged DNA. *Proc. Natl. Acad. Sci. USA* 99, 3523-3528.
11. Dou, H., Theriot, C.A., Das, A., Hegde, M.L., Matsumoto, Y., Boldogh, I., Hazra, T.K., Bhakat, K.K., Mitra, S. (2008) Interaction of the human DNA glycosylase NEIL1 with proliferating cell nuclear antigen. *J. Biol. Chem.* 283, 3130-3140.
12. Das, A., Boldogh, I., Lee, J.W., Harrigan, J.A., Hegde, M.L., Piotrowski, J., Pinto, N. de S., Ramos, W., Greenberg, M.M., Hazra, T.K., Mitra, S., Bohr, V.A. (2007) The human Werner syndrome protein stimulates repair of oxidative DNA base damage by DNA glycosylase NEIL1. *J. Biol. Chem.* 282, 26591-26602.
13. Harrigan, J.A., Wilson III, D.M., Prasad, R., Opresko, P.L., Beck, G., May, A., Wilson, S.H., Bohr, V.A. (2006) The Werner syndrome protein operates in base excision repair and cooperates with DNA polymerase  $\beta$ . *Nucleic Acids Res.* 34, 745-754.

14. Guan, X., Bai, H., Shi, G., Theriot, C.A., Hazra, T.K., Mitra, S., Lu, A-L. (2007) The human checkpoint sensor Rad9-Rad1-Hus1 interacts with and stimulates NEIL1 glycosylase. *Nucleic Acids Res.* 35, 2463-2472.
15. Wiederhold, L., Leppard, J.B., Kedar, P., Karimi-Busheri, F., Rasouli-Nia, A., Weinfeld, M., Tomkinson, A.E., Izumi, T., Prasad, R., Wilson, S.H., Mitra, S., Hazra, T.K. (2004) AP endonuclease-independent DNA base excision repair in human cells. *Mol. Cell.* 15, 209-220.
16. Podlutzky, A.J., Dianova, I.I., Podust, V.N., Bohr, V.A., Dianov, G.L. (2001) Human DNA polymerase  $\beta$  initiates DNA synthesis during long-patch repair of reduced AP sites in DNA. *EMBO J.* 20, 1477-1482.
17. Krokan, H.E., Nilsen, H., Skorpen, F., Otterlei, M., Slupphaug, G. (2000) Base excision repair of DNA in mammalian cells. *FEBS Letters* 476, 73-77.
18. Shibutani, S., Takeshita, M., Grollman, A.P. (1991) Insertion of specific bases during DNA synthesis past the oxidation-damaged base 8-oxodG. *Nature* 349, 431-434.
19. Li, K-M., Todorovic, R., Devanesan, P., Higginbotham, S., Köfeler, H., Ramanathan, R., Gross, M.L., Rogan, E.G., Cavalieri, E.L. (2004) Metabolism and DNA binding studies of 4-hydroxyestradiol and estradiol-3,4-quinone *in vitro* and in femal ACI rat mammary gland *in vivo*. *Carcinogenesis* 25, 289-297.
20. Tsuchiya, Y., Nakajima, M., Yokoi, T. (2005) Cytochrome p450-mediated metabolism of estrogens and its regulation in human. *Cancer Let.* 227, 115-124.
21. Hailer, M.K., Slade, P.G., Martin, B.D., Sugden, K.D. (2005) Nei deficient *Escherichia coli* are sensitive to chromate and accumulate the oxidized guanine lesion spiroiminodihydantoin. *Chem. Res. Toxicol.* 18, 1378-1383.

22. Bandaru, V., Sunkara, S., Wallace, S.S., Bond, J.P. (2002) A novel human DNA glycosylase that removes oxidative DNA damage and is homologous to *Escherichia coli* endonuclease VIII. *DNA Repair 1*, 517-529.
23. Hah, S.S., Mundt, J.M., Kim, H.M., Sumbad, R.A., Turteltaub, K.W., Henderson, P.T. (2007) Measurement of 7,8-dihydro-8-oxo-2'-deoxyguanosine metabolism in MCF-7 cells at low concentrations using accelerator mass spectrometry. *Proc. Natl. Acad. Sci. USA 104*, 11203-11208.
24. U.S. Congress, Office of Technology Assessment. (Sept. 1986) Technologies for detecting heritable mutations in human beings.